Abstract

In this thesis the relationship between grain properties and ethanol yield was investigated in the two varieties of wheat Warrior and Viscount. Protein content can indicate ethanol yield in some varieties but not in the case of Warrior. The biochemistry of Warrior starch breakdown was compared with that of Viscount. By doing so it was shown that the activity of the enzyme amyloglucosidase was strongly inhibited in Warrior. The inhibition occurred when only a fraction of Warrior starch was present in a mixture. Analysis of starch granule size and starch crystal structure by microscopy and x-ray diffraction revealed differences between Warrior starch and Viscount starch. Warrior starch was found to have an increased branch frequency that would yield more isomaltose, an inhibitor of amyloglucosidase. In light of this evidence it was concluded that the low ethanol yield in Warrior wheat is caused by competitive inhibition of amyloglucosidase, as a result of an increased amylopectin branch frequency. Amyloglucosidase is an industrially important enzyme that is used in blended whisky and biofuel manufacture; inhibition of this enzyme would reduce the amount of glucose available for fermentation. This trait can be used to screen wheat varieties during breeding to improve the wheat available for ethanol manufacture.

Acknowledgments

I would like to thank Professor Mike Burrell for his extraordinary support and insight throughout the course of the last three years. I am also very grateful to Richard Summers who provided all the experimental material and allowed me to spend so much time working at RAGT. I would also like to thank Professor Duncan Cameron for his encouragement and advice.

I'm also very thankful to have worked with all the members of D59 who made the last three and a half years so enjoyable. I would particularly like to thank, Bob Keen and Heather Walker who made the lab such a pleasant place to be and Amin Yaapar, whose friendship during my time in the lab is ineffable.

I would like to thank my parents and my family who have always been there for me, and Adeline Fluteau whose support and advice has been outstanding.

Finally, I'd like to thank Katie Colson who is missed by so many.

Table of Contents

1 Introduction

1.1 Overview

In 2009 Sir John Beddington gave a speech describing a “perfect storm” of events including the demand for food and energy rising by 50% (Beddington, 2009) (Godfray *et al.*, 2010). Food and energy availability needs to increase in order to prevent this “perfect storm” from happening. Although food crops can be used to produce liquid transportation fuels to alleviate the energy shortage, this would simultaneously increase the pressure on food supply. If the use of plants for fuel is to be sustainable then conversion to ethanol needs to be a very efficient process. Improving the conversion of wheat grain to ethanol would also benefit the Scottish whiskey industry, which is a major contributor to the economy.

1.2 Biofuel

Biofuel refers to any liquid transportation fuel (LTF) that is derived from organic material of recent origin, there are many different categories such as bio-ethanol, bio-diesel and plant extract oil. Sources of bio-ethanol include sugar cane, cassava and sorghum, all of which are grown in tropical countries (FAOSTAT, 2009). Bio-ethanol is by far the most commonly used biofuel since it can be produced from common food crops, is compatible with vehicle engines and requires no modification when mixed with petroleum.

The sources of bio-ethanol can be divided into conventional or advanced. Conventional bio-fuel is produced from the part of the plant that is also consumed as food, such as starch from wheat grain and simple sugars from sugar cane. On the other hand, advanced bio-ethanol can be made from lignocellulosic biomass such as straw, willow and grass. Advanced bio-ethanol is currently synthesised in relatively small quantities compared to conventional bio-ethanol because the yield is lower. This low yield renders the wide scale production of ethanol from lignocellulose uneconomical compared to conventional fuel.

In the 1970s the Brazilian government instituted widespread reforms to encourage the use of sugar cane as a bio-ethanol source. This initiative was a success, since 20% of total Brazilian LTE is now composed of bioethanol. As a tropical plant, sugar cane is well suited to the Brazilian climate so high yields of bioethanol can easily be achieved. Once harvested, sugar cane is transported to processing plants that are usually located near to the fields, the sugar cane juice is then extracted and fermented to produce ethanol. The residual biomass (bagasse) is burned to produce electricity that powers the refinery and can be sold to the electricity grid when there is a surplus energy supply. The high cane yield, bagasse surplus and electricity production combine to make the production of bioethanol from sugar cane economically viable (Macedo *et al.*, 2008). However Brazil is unique in that there is no requirement to irrigate the sugar cane fields. Countries such as the United States of America (USA) have a very different climate compared to Brazil, meaning that different crops need to be used for bio-ethanol production, maize being the crop of choice. Similarly to Brazil, the USA has also introduced legislation to stimulate the bio-ethanol market (United States Congress, 2008). However the difference between the two feedstocks is that the starch in maize needs to be broken down into glucose (saccharification) before fermentation can begin. Consequently the energy balance between renewable output and fossil input for maize is 1.4 compared to 10.2 for sugar cane

(Goldemberg, 2007). In other words, bio-ethanol produced from sugar cane consumes less fossil fuel during its production. Despite the higher fossil fuel input, maize is now very widely grown in the USA for bio-ethanol production. In fact, bio-ethanol production in the USA has increased from 1,622 million gallons in the year 2000 to 14,340 million gallons in 2014 ('Statistics | RFA: Renewable Fuels Association'). The result of this is that a 10% ethanol/90% petroleum blend has now been achieved across the USA. Since increasing the proportion of the blend further would render the fuel incompatible with current engines a so called "blend wall" has been reached (Peplow, 2014).

It is a point of some contention as to whether bio-ethanol is sustainable, in terms of both food security and greenhouse gas emissions. The utilization of maize as a source of bio-ethanol led to farmers in the USA switching from white maize to yellow maize. This switch caused a shortage of flour to produce tortillas, a staple food in Mexico. The previously stated energy balance of sugar cane and maize does not take into account the greenhouse emissions when land is converted to grow maize for bio-ethanol. When land use change is considered, bio-ethanol from maize would increase greenhouse gas emissions by 93% compared to petroleum (Searchinger *et al.*, 2008), instead of a reduction of 20% when land use change is excluded. Sugar cane on the other hand could be sustainable as long as rainforest is not cut down to grow sugar cane (Searchinger *et al.*, 2008). In the Searchinger study the source of ethanolic LTF that was found to be most sustainable was waste biomass, a source that would be classed as an advanced biofuel.

Advanced biofuels are produced from biomass that is not used for food. This includes agricultural waste, or biomass that is grown specifically for bio-ethanol production. Examples of

each include wheat straw or willow respectively (Mola-Yudego & Aronsson, 2008). With advanced biofuels, the lignocellulose from the plant cell walls is converted into ethanol. Using lignocellulose is an attractive option since it is very abundant and does not compromise food security. The main issue with lignocellulose-based fuel is that the conversion rate is very low and it is not an energy dense material. Building processing plants close to the source of the fuel and carefully controlling inputs can solve the latter issue, but increasing the conversion rate to a commercial level is far more difficult. This is because lignocellulose is complex and unordered and has evolved to be recalcitrant to degradation. Despite this, lignocellulose has great potential, with some sources suggesting that up to 20% of future energy needs could be met using lignocellulose (IEA, 2007). To achieve this, however, there need to be improvements in yield and efficiency. Current methods typically use a fungus called *Trichoderma reesei* (Martinez *et al.*, 2008) to degrade the lignocellulose. To improve the efficiency of the process thermostable cellulases have been transformed into *T. reesei* (Viikari *et al.*, 2007). To increase yield further the unique biology of certain organisms are being studied. For example, termites which consume lignocellulose as a food source are being studied in an effort to increase the rate of lignocellulose degradation (Brune, 2014). The potential of advanced biofuels is great but they are currently uneconomical due to low yield and low bio-ethanol prices. Further development of the technology and legislation is needed to support the transition from conventional to advanced bio-ethanol.

1.3 Wheat

Wheat (*Triticum aestivum*) is a cereal crop. It was domesticated at least 20,000 years ago in the Fertile Crescent at the advent of civilization (Piperno *et al.*, 2004). Since this period wheat has become a very important crop, in 2012 670 million tons of wheat grain were produced worldwide

Table 1.1 ***Reference values for five organic sources of ethanol.***

Type	Biomass conversion to sugar or starch (W/W%)	Conversion rate to ethanol (l/ton)
Sugar cane	12.5	70
Cassava	25	150
Sweet sorghum	14	80
Maize	69	410
Wheat	66	390

(FAOSTAT, 2012). Wheat is mainly grown to produce flour for bread making and as such comprises a substantial proportion of human calorific intake (Curtis *et al.*, 2002). In the UK wheat is the dominant cereal crop as the climate and latitude provide growing conditions which suit its commercial cultivation (Feldman, 1976). However wheat grain is also used in other contexts. For example wheat is used as a source of ethanol in the production of blended scotch whiskey, biofuel, sweeteners for soft drinks (BeMiller & Whistler, 2009) and also animal feed (Shewry, 2009). As the production of ethanol from wheat occurs on an industrial scale even small improvements in yield are extremely valuable. For example the Scottish whiskey industry contributes £4.27bn to the UK economy each year in exports alone (Scotch Whiskey Association, 2012).Therefore even a small improvement in ethanol yield during Whiskey or Biofuel production would be extremely valuable to the UK economy.

1.4 Ethanol production from Wheat for biofuel

In the UK wheat is used as a feedstock for fuel ethanol as it is already used by the beverage industry in the large-scale production of potable alcohol and because it is the most widely grown

cereal with a highly developed agricultural production process (FAOSTAT, 2009). The production of ethanol from wheat also yields valuable secondary products, which allow the process to be economically viable. These are high quality animal feed and carbon dioxide for the soft drinks industry (Ensus, 2014). Therefore wheat is key to satisfying the legislative requirement for biofuel to make up 5.75% of transportation fuel by December 2010 (Cutler & Von Lingen, 2003) which creates demand for biofuel in the energy market.

Ethanol production from wheat for use as a transportation fuel is highly contentious, because it reduces the amount of wheat available for food production. This increases the price of wheat grain and decreases availability to an ever increasing population (Graham-Rowe, 2011). Moreover yields could be threatened by climate change; in the long term climatic conditions for growing high yielding wheat varieties are expected to worsen across northern Europe (Kovats & Valentini, 2014) (Rötter *et al.*, 2011) as weather patterns become more variable (Olesen *et al.*, 2011). Given rising food demand and the impact of climate change the yield of ethanol from wheat needs to be as high as possible to replace fossil fuels. The typical ethanol yield from wheat is approximately 390 litres per tonne of wheat grain (Balat & Balat, 2009); a conversion efficiency of less than 50%. The conversion rate is relatively high compared to the other feedstocks (Table 1.1 (Balat & Balat, 2009)) and is only exceeded by maize. Ethanol yield is directly proportional to the conversion rate of sugar from starch (Balat & Balat, 2009). Increasing yield at harvest could be a solution to producing more ethanol by increasing the amount of biomass available. However the changing UK climate (Kovats & Valentini, 2014) mean that absolute yield cannot be relied upon to provide the quantity of ethanol required. To produce ethanol from wheat sustainably more ethanol from the same amount of grain needs to be produced. This is reliant upon the efficient conversion of the feedstock to sugars or starch, which can produce ethanol.

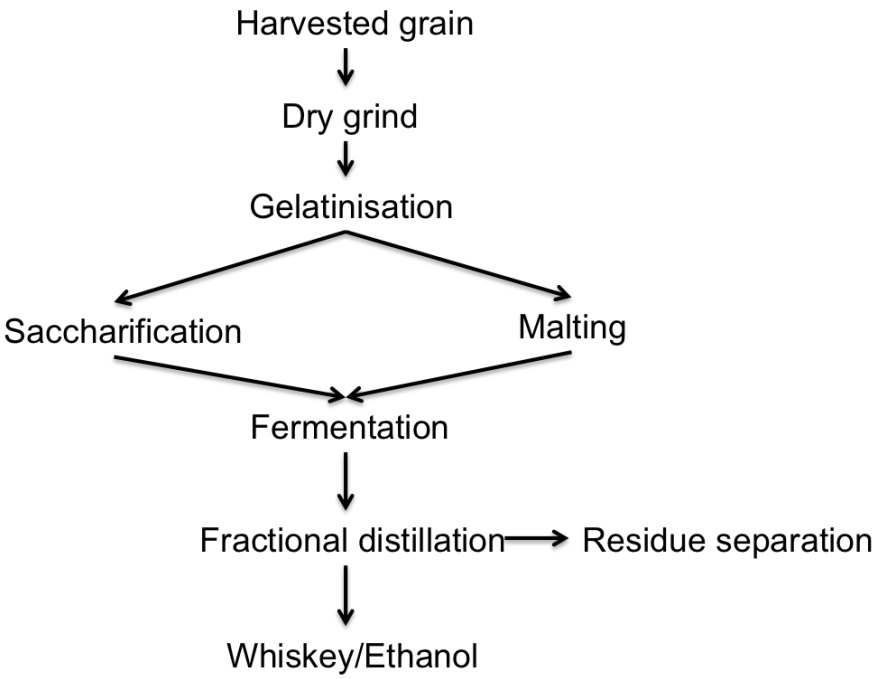

Figure 1.1 ***Major steps in the industrial production of ethanol from wheat****. Showing alternative methods to breakdown starch into sugars. Malting is the process used when single malt scotch whisky is produced and saccharification is when pure enzymes are added in the industrial production of alcohol.*

1.5 Making ethanol from wheat

Ethanol production requires the conversion of starch to glucose (Saccharification) and then glucose to ethanol (Fermentation) (Figure 1.1). The production of ethanol from wheat is a complex process. For both potable alcohol and fuel ethanol wheat grain is milled into flour without water (Figure 1.1) (Murphy & Power, 2008). To obtain the best ethanol yield milling must produce the smallest grains of flour possible. Flours that are finely milled have a higher ethanol yield (Song *et al.*, 2014) as they have a greater surface area. Water is added to the starch and it is 'cooked' at high temperature (120-150°C). This causes the starch granules to burst open and starch within is gelatinised (Murphy & Power, 2008). This step is needed as starch is a semi-crystalline structure arranged in granules (Buléon *et al.*, 1998). These complex structures need

to be disrupted in order to allow enzyme access. The third stage of processing in fuel ethanol production requires cooling of the mixture to 80°C at which point α-amylase and amyloglucosidase can be added to break the starch down into glucose. In whiskey production no enzymes are added, malting is relied upon to produce the enzymes required for starch degradation (Smith *et al.*, 2006). In malting, barley grain is germinated producing amylase enzymes; this mixture is then added to the wheat slurry (Evans *et al.*, 2010). The fourth stage is when ethanol is actually produced; under anaerobic conditions the yeast *Saccharomyces cerevisiae* produces ethanol via anaerobic respiration. Temperature, water content and dwell time are optimized for ethanol yield. After this stage the mash undergoes fractional distillation before residual mash is separated to recover co-products (Smith *et al.*, 2006).

1.5.1 Factors which affect ethanol yield from wheat

As wheat grain is the feedstock for ethanol production it is important to consider the constituents and their effect on ethanol production. Protein content is the most important constituent of the wheat grain when different varieties of wheat are classified. Commercial varieties of wheat typically contain 10-13% total protein content (HGCA, 2011). This is a value which is highly dependent on environmental conditions and crop management (Agu *et al.*, 2009). Wheat protein is very important for human nutrition, however high protein limits maximum ethanol yield. A 1% (w/w) reduction in total wheat protein will result in a 7.36 litre rise in ethanol yield per ton (Smith *et al.*, 2006). This negative correlation between increasing protein concentration and decreasing ethanol yield is very well established. This is because protein in the grain forms a matrix around the starch granules, and as total protein content increases the matrix becomes more extensive. Therefore the grain will be harder and larger flour particles will be produced after milling,

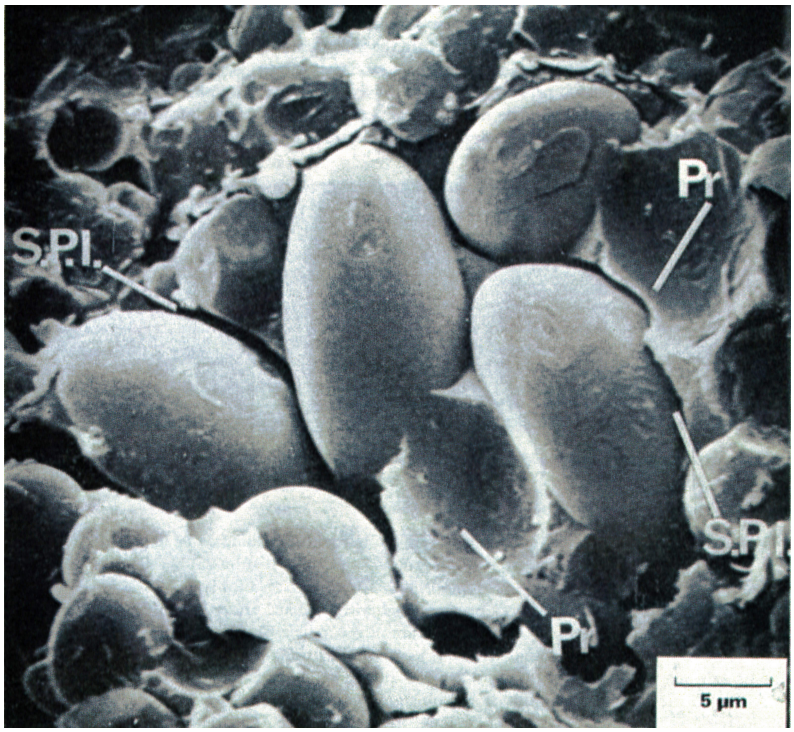

Figure 1.2. ***Scanning electron micrograph of starch granules in the protein matrix.*** *Pr is the label for the protein matrix and S.P.I labels the starch protein interface. The starch granules are the lenticular objects in the centre of the pictures. Image from Stenvert and Kingswood, 1977* (Stenvert & Kingswood, 1977).

reducing the surface area available for enzyme activity. However whether this is due to an effect of total protein or the presence of specific grain proteins remains unclear. Starch in the endosperm accounts for 75-85% of grain dry weight. This is less dependent on environmental conditions but it is directly affected by endosperm cell number (Brocklehurst, 1977). Starch needs to be broken down by enzymes into sugar before fermentation can take place. This is the second step in the production of ethanol from wheat and is the most inefficient. After this step 1/3 of the grain input remains of which a large proportion is starch which has not been degraded (Smith *et al.*, 2006).

1.6 Protein

Protein content is the most important determinant of wheat market value, the more protein there is the more valuable the grain will be. The protein in wheat also confers properties that are essential for good bread making; Not only does the protein provide high quality nutrition but the gluten proteins form a viscoelastic matrix when heated allowing bread to rise. In contrast, soft wheat has lower protein content this means the proteins present do not form a viscoelastic matrix. Wheat protein is classically divided into three groups; albumins, globulins and gluten (Osborne, 1909). The biological role of the gluten proteins in the wheat grain is to provide the developing wheat plant with carbon, nitrogen and other nutrients that are required to allow germination and the initial development of the seedling (Shewry *et al.*, 2002). The gluten fraction comprises 80% of total grain protein and 50% of total grain nitrogen (Dupont & Altenbach, 2003) and is therefore of most interest. Gluten is composed of two classes of protein, glutenins and gliadins and as such these proteins constitute the majority of protein in the endosperm. The gliadins are monomeric proteins soluble in 60-70% ethanol (Jones *et al.*, 1959) and comprise 10-20% of the total gluten composition in the endosperm. There are in turn four different classes of monomers, α-, β-, γ- and ω-gliadins (Ribeiro *et al.*, 2013), The genes encoding gliadin synthesis are located on homologous chromosome groups 1 and 6. The genes for gliadin synthesis are encoded at six loci; Gli-A1, Gli-B1, Gli-D1, Gli-A2, Gli-B2, and Gli-D2 (Payne *et al.*, 1982). The gliadin proteins contribute to different rheological properties of the dough specifically, viscosity and extensibility (Shewry *et al.*, 2003) (Ribeiro *et al.*, 2013). The more viscous dough is the more expensive it will be to process into bread or ethanol, therefore excessive viscosity is undesirable. This is because the more viscous the dough is the more energy it requires to be processed and it also increases maintenance costs. Gliadin is also attributed as being the main cause of the debilitating auto-immune condition celiac disease in

humans (Patey, 1980). In contrast the glutenins are large polymeric proteins that represent 80-90% of gluten in the endosperm. The glutenins can be further divided into two more classes the High Molecular Weight glutenin subunits (HMW-GS) and the low molecular weight glutenin subunits (LMW-GS) (Tosi, 2012), this nomenclature is based on their separation on Sodium dodecyl sulphate polyacrylamide gel electrophoresis (SDS-PAGE). The HMW-GS are encoded at the Glu-1, loci two genes are present at this loci, which encode the x-type and y-type subunits of the HMW-GS. The loci for the expression of the LMW-GS are located at Glu-A3, Glu-B3, and Glu-D3. The distribution of the gluten and gliadin fractions is not uniform throughout the endosperm, the lower molecular weight proteins are localised in the periphery of the endosperm and include gliadins and LMW-GS. The higher molecular weight glutenins (HMW-GS) are found more centrally in the grain (Tosi *et al.*, 2011). Protein in the wheat grain begins to accumulate after 10 days post anthesis (DPA), the total protein content then increases at a constant rate. Accumulation normally arrests at a late stage in grain development (~36 DPA) (Salgó & Gergely, 2012) (Shewry *et al.*, 2012) and the proportion of each protein fraction (Glutenins and Gliadins) remains constant throughout grain development (Shewry *et al.*, 2012). Albumins and Globulins comprise the smallest protein fraction of all the wheat grain proteins, Albumins were originally defined as being water soluble and the globulins were salt soluble (Osborne, 1909). As they contribute little to grain protein and to dough rheology they have been studied less. Protein within the wheat endosperm forms a matrix that surrounds starch granules. This protein matrix affects the hardness of the grain endosperm. More extensive grain protein matrices can increase the hardness of the grain (Stenvert & Kingswood, 1977). This can affect the yield of glucose from starch as the granules are more deeply embedded within a protein matrix and as such the starch is harder to extract in order for it to be digested (Agu *et al.*, 2009). This reduces ethanol yield. The proteins described above form the matrix and as such need to be quantified in order to assess the effect of protein content in this experimental paradigm.

1.7 Starch

The organization and structure of wheat starch presents some problems when ethanol needs to be produced. The starch polymer is organised within granules. During the development of the grain, granules develop within individual endosperm cells. This occurs after the endosperm cells have formed cells walls after the coencytic expansion of the endosperm (Bennett *et al.*, 1975). The amount of starch in a single wheat grain is dependent on the number of granules in each cell and since a single cell can only hold a finite amount of granules the number of endosperm cells directly affects the yield of starch (Brocklehurst, 1977). Starch granules in wheat can be catergorised into two size classes; A and B (Dengate & Meredith, 1984) (Peng *et al.*, 1999). The tribes Triticeae and Brachypodium are the only members of the Pooideae, which have a bi-modal size distribution of starch granules; other tribes exhibit compound starch granule size distribution (Shapter *et al.*, 2008). The A-type granules form first at 4 days post anthesis (DPA) and then grow in size to between 25μm and 50μm, they are also lenticular in shape. In contrast to this B-type granules are spherical and are of a smaller size with a diameter usually between 1-10μm (Salman *et al.*, 2009). Growth initiation of the granules is different; A-type granules begin to grow and accumulate at four days post anthesis and continue to grow for twenty days. In comparison the B type granules will begin to grow at 10 days post anthesis and stop growing after only ten days (Salman *et al.*, 2009). It is possible that B-type granules are just smaller A-type granules but the synthesis of B-type granules could be fundamentally different. This is an important difference as a separate synthesis mechanism could result in a different supramolecular structure. A-type granules are large but relatively rare accounting for only 4.8% of the total number of granules but 51.6% of total weight (Bechtel *et al.*, 1990). The smaller B-type granules are therefore far more numerous but contribute a similar quantity of starch to the overall starch content total.

Starch granules are complex structures; they have alternating semi-crystalline and amorphous rings, which are composed of the two glucan polymers amylose and amylopectin. There is evidence that the supramolecular structure of A-and B-starch granules is not different but few varieties have been tested (Li *et al.*, 2013). The crystalline rings are composed of amylopectin and the amorphous rings are composed of amylose. Amylose does not form a stable crystal structure because it is in the form of a single coil, which does not have the required hydrogen bonding to produce a crystal (Mikus *et al.*, 1946). More complex coils can be formed with lipids (Morrison *et al.*, 1993) but these are not crystalline and will not affect amylose packing. The single amylose coil and the amylose complexes have six glucose residues per repeat unit which has a pitch height between 7.92-8.04Å (Godet *et al.*, 1993) and produce a 'V' type X-ray powder diffraction pattern (Mikus *et al.*, 1946). The Amylopectin polymer produces the semi-crystalline structure as it is able to form a parallel stranded double helix with six glucose units per turn which is 10.5 Å long (Imberty *et al.*, 1988) (Imberty *et al.*, 1991). Wheat starch which contains the parallel double stranded helix produces an 'A type' X-ray powder diffraction pattern, with maltotriosyl as the repeating unit. The two helices are able to form complexes with lipids because hydrogen bonds stabilize the structure and therefore allow the formation of a crystal matrix when it is organized with other strands (Imberty *et al.*, 1988). The alternating crystalline/amorphous ring structure of the starch granule makes the conversion of starch to glucose and ethanol difficult. This is because unless the structure is exposed for enzyme attack the digestion is inefficient. Solubilisation involves adding water and heating the mixture to a high temperature, the 'cooking' stage (Murphy & Power, 2008) requires a large amount of energy, as a large volume of water and flour needs to be heated to high temperature. Therefore the structure and properties of the starch granules is of great interest to brewers and ethanol producers as reducing the temperature of the cooking stage would be of great economic benefit.

The constituents of the two rings are amylose and amylopectin. Both polymers have glucose as the single molecule moiety. The two types of polymer differ by relative proportions of α-D-1, 4 glycosidic and α-D-1, 6 glycosidic bonds. α-D -1, 4 glycosidic bonds form linear linkages between adjacent glucose monomers in both amylose and amylopectin. α-D-1, 6 glycosidic bonds form branches in polyglucan chains to produce a branched structure from the original linear backbone (Taiz, Lincoln. Zeiger, 2010). It is this subtle difference in the molecular structure, which produces the difference between the two polymers. In wheat, amylose has a branch frequency of 0.2-1.0 branch points for every 100 glucose subunits and an average chain length of 1220-1239 monomers within a range of amylose polymers with chain lengths between 190-3130 monomers (Hanashiro & Takeda, 1998). Its single coil structure is a result of the linear α-D-1, 4 glycosidic bonds and the glucose molecules being in the chair configuration (Nakamura, 1996). Amylopectin, in contrast, is a far more complex molecule. Amylopectin has a branch percentage of 4.0-5.5 branch points for every 100 glucose subunits with an average chain length of 18-25 units (Nakamura, 1996). It has an exceptionally high molecular weight varying between 10^{7}-10^{8} Daltons which is an order of magnitude higher than amylose (Aberle *et al.*, 1994). Starch accumulation in the wheat endosperm begins ~9 DPA and continues for around twenty days until 30-34 DPA at which point the sugars which donate the glucosyl moiety reduce in availability and starch content stabilizes (Verspreet *et al.*, 2013). There are three classes of glucose chains within the amylopectin molecule, they are labeled A,B and C (Peat *et al.*, 1956). For each amylopectin molecule there is a single glucan chain in the middle, which has the single reducing unit at the end (Figure 1.3). It is from this single glucan chain that the rest of the molecule originates. This is the C chain and in wheat it has been found to be around 40 residues long, which is similar to other cereals (Hanashiro *et al.*, 2002). The C chain is positioned in the center of the amylopectin molecule. The B chain has no reducing end and

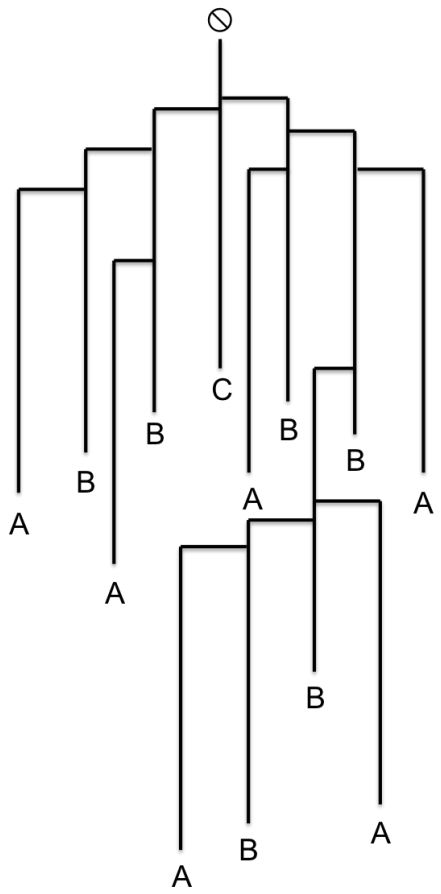

Figure 1.3 ***Amylopectin schematic with the three classes of chains labeled A, B and C****. The non-reducing end is also shown (⦸).*

originates on another chain but also has a chain attached to it (Peat *et al.*, 1956). B chains have been subdivided into several categories based on size (Hanashiro *et al.*, 1996); B_1 = chains 13 and 24 units long, B_2 = chains 25 and 36 units long and B_3 chains which are >36 units long (Hanashiro *et al.*, 1996). B chains are located in the interior of the granule. In wheat only the B_1 chains are present in a great quantity accounting for 27 or 28% of the total molar content of amylopectin. B chains more than 24 units long account for less that 8% total molar content of amylopectin (Hanashiro *et al.*, 2002). The A chains lie of the exterior of the amylopectin molecule, they have no reducing end, originate from another chain and have no other chains originating from them (Peat *et al.*, 1956). A chains in wheat have been shown to be 12-13 units

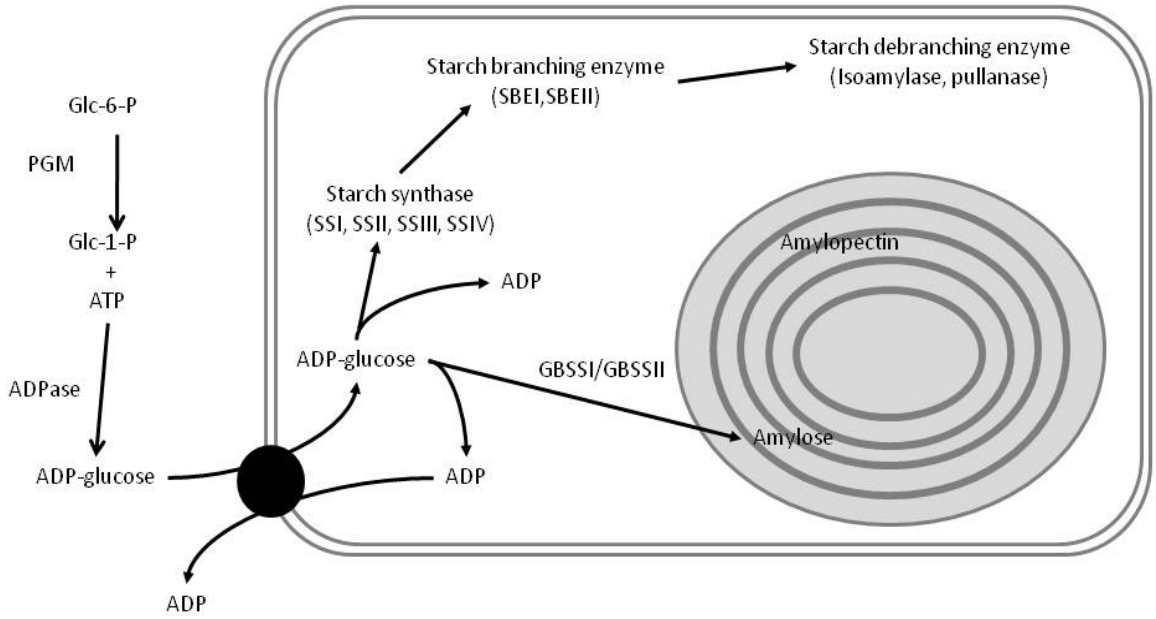

Figure 1.4 ***Starch biosynthetic pathway in wheat****. ADP-glucose is transported into the amyloplast where it is used as the substrate in starch synthesis. GBSSI in conjunction with GBSSII synthesises amylose using ADP-glucose as the substrate. Starch synthases produce unbranched starch that is subsequently branched to make amylopectin by starch branching enzymes. Starch debranching enzymes are responsible for modifying the starch structure to produce the starch granule structure.*

long (Hanashiro *et al.*, 2002). In wheat the A chains are the most abundant, they comprise between 64 and 65% of the total molar content of amylopectin (Hanashiro *et al.*, 2002). Other cereals such as oat, barley and rye have a smaller percentage (49-52%) of A-chains representing the total molar content of amylopectin. The B_1 chain range in lengths of these species is between (42 and 46%). With larger B_2 and B_3 chains comprising the remainder (Bertoft *et al.*, 2008). Therefore wheat can be placed with other members of the subfamily Pooidae based on the amylopectin chain length profile, with a higher proportion of shorter chain lengths in amylopectin than longer ones. Phosphorus can also be detected in wheat starch, a very small proportion of which is as a phosphate monoester. The phosphate group is donated to starch from adenosine triphosphate and the phosphate monoester is attached at the sixth carbon on a glucose monomer (Lim *et al.*, 1994). The majority of the phosphate present in wheat starch is within the phospholipids bound to the amylose molecule; 0.053% of dry starch is phosphorus within phospholipids (Lim *et al.*, 1994). Phosphate content is unlikely to affect

ethanol yield as the phosphate monoester is present in exceedingly small quantities (0.001% of grain weight (Lim *et al.*, 1994)). Starch synthesis is complex and requires multiple stages and enzymes to produce the highly ordered polymer (Figure 1.4). The initial precursor for starch production is glucose-1-phosphate. In the pathway shown in figure 1.4 glucose-1-phosphate can be imported directly into the amyloplast (Hill & Smith, 1991) or it can be synthesised in the plastid from glucose-6-phosphate by the activity of phosphoglucomutase (PGM) (Tyson & ap Rees, 1988). ATP (adenosine triphosphate) is added to glucose-1-phosphate by ADP-glucose pyrophosphorylase, the products of this reaction are ADP-Glucose (adenosine di-phosphate glucose) and pryrophosphate (Greenberg & Preiss, 1964). In wheat the ADP-glucose is then transported across the membrane into the amyloplast in exchange for ADP (adenosine di-phosphate) around 70% of ADP-glucose is supplied this way with around 30% being synthesised by ADP-glucose pyrophosphorylase in the amyloplast (Tetlow *et al.*, 2003). Once transported into the amyloplast ADP-glucose provides the glucosyl moiety for the synthesis of the starch polymer. This precursor is utilised by starch synthases to elongate the linear glucan chains by catalysing the transfer of the glucosyl unit of ADP-glucose to the non-reducing end of the glucan chain (Jeon *et al.*, 2010) (Leloir *et al.*, 1961) to produce an α-D -1, 4 linkage. Starch synthases can use amylose or amylopectin as a substrate in this reaction (Martin & Smith, 1995). There are two groups of starch synthases involved in starch synthesis. Firstly, granule bound starch synthases, of which there are two forms: GBSSI and GBSSII. GBSSI is encoded by the waxy locus (Nelson & Rines, 1962), waxy mutants produce starch with a low amylose content and as such are responsible for the production of amylose in the endosperm (Nelson & Rines, 1962). GBSSII in wheat has previously been shown to not be expressed in the endosperm, and therefore it does not play a significant role in amylose synthesis in wheat (Vrinten, 2000). GBSSI is expressed at a high level throughout grain development, until later stages around 20 days post anthesis where expression reduces (Cao *et al.*, 2012).

Starch synthases (SSI-SSIV) produce the amylopectin polymer component of starch. Each of these four enzymes have different functional effects that act in concert to produce the amylopectin molecule. The function of starch synthase I is the initial synthesis of the short amylopectin chains. It is located on the surface of the wheat starch granules and is gradually incorporated as the granule grows. This means that as time goes on the detectable amount of SSI decreases (Peng *et al.*, 2001). Starch synthase II has been shown to be crucial for the elongation of these short polymers (Kosar-Hashemi *et al.*, 2007). This enzyme is critical, if it is not present in the endosperm then amylopectin synthesis is severely compromised with only 20% of the normal amount of amylopectin present at grain maturity (Morell *et al.*, 2003) (Clarke *et al.*, 2008). Both SSI and SSII are expressed throughout grain development at a consistent level which eventually declines as development passes 20 DPA (Cao *et al.*, 2012). Starch synthase III in rice functions to produce the long B_3 amylopectin chains, starch that does not contain this protein affected the physiochemical properties of the starch and the expression of other starch synthases (Fujita *et al.*, 2007). A SSIII has been identified in wheat and is homologous to rice and maize SSIII (Li *et al.*, 2000). However if SSIII serves to produce the long B_3 amylopectin chains then it is very unlikely that there is much expression or enzyme activity in wheat as observed molar values for amylopectin chains over 24 units long are very low in wheat with the shorter amylopectin chains dominating (Hanashiro *et al.*, 2002). This is reflected in its expression profile, SSIII transcript is only expressed at a high level for around three days commencing ten days post anthesis (Cao *et al.*, 2012). In wheat SSIV is expressed in the embryo and leaf tissues but not in the endosperm. This means that it does not function to produce amylopectin or amylose in the starch granules in the endosperm. It has also been shown to be homologous to SSIII and could therefore have a similar mechanism of action (Leterrier *et al.*, 2008). It has been shown that SSIV is involved in plastid initiation in *Arabidopsis*

thaliana however its specific role in starch synthesis has not been defined in wheat (Roldán *et al.*, 2007). As outlined above starch synthase enzymes are crucial for the synthesis of the amylopectin molecule however the starch synthases will only elongate the amylopectin molecule. A different family of enzymes is required to introduce the branching structure of the amylopectin molecule.

Starch branching enzymes (SBEs) cleave the α-D-1, 4 glycosidic bond to produce an oligosaccharide fragment which is repositioned by the enzyme in a different orientation allowing the formation of a α-D-1, 6 glycosidic bond between the two polymers. This results in the formation of a branch point and the amylopectin polymer. The starch branching enzymes fall into two classes, SBEI and SBEII which have distinct functions (Hannah & James, 2008). SBEI transfers relatively long chains whereas SBEII transfers shorter amylopectin chains (Takeda *et al.*, 1993). SBEII can be further divided into two more classes; SBEIIa and SBEIIb based on sequence (Morell, 1997). By controlling the activity of these enzymes the structure of the amylopectin can produce the classic clustered structure. SBEI is expressed at a low level in the early stages of endosperm development 0-12 DPA after which point expression of the enzyme increases to its highest level around 20 DPA (Morell, 1997) (Cao *et al.*, 2012).

Unlike granule bound starch synthases, starch synthases and starch branching enzymes the de-branching enzymes have a less clear role. There are two types of starch de-branching enzymes: pullanase and isoamylase (ISA). Both will hydrolyse the α-D-1, 6 glycosidic bond between two polyglucans which includes amylopectin and amylose. The functional effect of these enzymes is to modify the starch structure. For example ISA in barley reduces the branching of excessively branched chains or to maintain the cluster structure of amylopectin

during starch biosynthesis (Jeon *et al.*, 2010), however ISA function has not been studied in wheat. Using these enzymes wheat is able to produce semi-crystalline starch granules, which are contained within the amyloplast of the endosperm cells. As starch structure is dependent on not only the specific enzymes expressed (as each enzyme has a specific function) it is also dependent on the time of expression. Therefore changes in the timing of gene expression in any of the diverse enzymes in the biosynthetic pathway of starch could have a dramatic effect on the starch structure at maturity.

The industrial conversion of starch to glucose requires the addition of two enzymes α-amylase and glucan 1,4-alpha-glucosidase (Godfrey & West, 1996). The enzyme α-amylase is an endo-hydrolase (EC 3.2.1.1, (ExPASy)), it will cleave the α-D-1,4 glycosidic bond in a glucan chain containing more than three residues. Glucan 1,4-alpha-glucosidase (amyloglucosidase, EC 3.2.1.3 (ExPASy)) acts as an exo-amylase cleaving α-D-1,4 glycosidic bonds in succession from the end of a glucan chain producing β-D-glucose. These two enzymes act in concert, α-amylase will break down the large amylose and amylopectin molecule into smaller chains (it will also produce β -D-glucose), amyloglucosidase will then act on the smaller chains to yield β -D-glucose. As these are the enzymes used in the industrial conversion of starch to glucose (and therefore ethanol) it is important to understand if the source of starch can affect how each enzyme performs in the reaction. Enzymes such as α-amylase that are active during the fermentation of starch into ethanol require access to the starch structure in order to complete the digestion of the starch. Upon boiling, the starch granules can be broken open but the helices remain intact (Gaillard & Bowler, 1987). The unbroken double helices have a pitch of 2.13 nm and no central cavity. Similarly, the single helices have a pitch of 0.805nm and a central cavity (Buléon *et al.*, 1998). This compact structure inhibits the access of the 55.4 kDa α-amylase protein which requires four available glucose molecules for amylose/amylopectin hydrolysis

(Qian *et al.*, 1997). If the degree of amylopectin branching increases there will be a large proportion of the starch in the inaccessible helical form. As a consequence of this ethanol will be produced less efficiently from a variety with a highly branched amylopectin structure.

1.8 Research approach

Commercial wheat varieties have very diverse phenotypes and are bred to suit the needs of farmers and millers. The national association of British and Irish millers (NABIM) classify commercial wheat varieties into four groups based on their milling and baking performance. This allows farmers to make an informed choice as to which wheat varieties they grow. Group 1 wheat will produce flour that has a consistent milling and baking performance, group 2 wheat has consistent baking but not milling performance, group 3 wheat is soft and is suitable for biscuit or cake making and group 4 wheat is only suitable for growing as fodder. Hard wheat which has high protein content is inherently poor at making ethanol (NABIM group 1/2) as they will not produce a fine flour. Hence, softer milling wheat is preferred (NABIM group 3). NABIM group three varieties have soft milling characteristics and low protein concentration, which should typically be suitable for the production of ethanol. However the group 3 variety "Warrior" is an exception. It has a soft endosperm texture with a protein content (11.3%) representative of other NABIM group 3 varieties (NABIM, 2012). But it is rated 'poor' for distilling, the Home Grown Cereals Authority (HGCA) advise that the inclusion of this variety in the distillation procedure could lead to problems in processing and a reduction in the efficiency of the distillation procedure (HGCA, 2011). It is important to note that this is true even if ground Warrior is in a mixture with other flours. It is of interest to breeders and farmers because it has a high disease resistance and a high untreated yield. It is resistant to mildew, yellow rust, brown rust, orange wheat blossom midge, *Septoria nodorum* and *Septoria tritici* and it is not vulnerable to any other major disease (HGCA, 2011). Warrior is a result of crossing the parental lines Robigus (a commercial variety) and CM-8228, which has not been commercialized (Figure 1.5). Another variety of variety of wheat with similar properties to Warrior is Viscount. Viscount has a soft endosperm texture with a protein content of 10.8%, which is within the range of NABIM

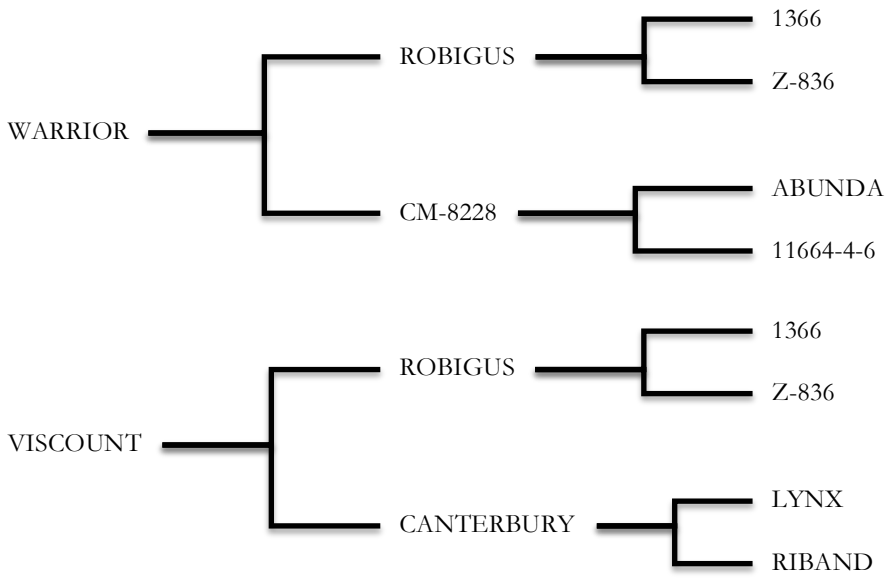

Figure 1.5 ***Pedigree diagram for Warrior and Viscount****. Warrior is a product of crossing Robigus with CM-8228 and Viscount is a product of crossing Robigus with Canterbury, which are two commercial wheat varieties.*

group 3 varieties. It is rated 'good' for distilling and as such allows it to be rated as export quality. Viscount is actually a group 4 variety and this is because of its poor baking performance. Viscount is of interest as it is a high yielding variety which is suitable for distilling. These two varieties have been selected as they exhibit ethanol yields, which are the highest and lowest of the soft milling wheat varieties (Weightman *et al.*, 2011). By comparing different biological properties of these two varieties I hope to define the underlying cause of the ethanol yield disparity. This information can then be used to identify varieties of wheat unsuitable for ethanol production. Warrior and Viscount share a parental variety, Robigus (Figure 1.5). It is therefore important to understand the segregation of the low ethanol yield genotype in order to prevent the lesion from being propagated in subsequent crosses.

1.9 Aims

1. To identify trait(s) associated with low ethanol yield in Warrior wheat
2. To understand the cause of low ethanol yield in wheat

1.10 Hypotheses

1. Protein content/composition explain the disparity in ethanol yield in Warrior and Viscount wheat.
2. Starch degradation properties explain the difference in ethanol yield.
3. The supramolecular organization of starch affects ethanol yield

2 Methods

2.1.1 Field samples

Plants were grown by RAGT seeds Ltd (Cambridge) and harvested in August 2013 (Adam's right, 52°05'10.8"N 0°09'31.7"E). The field plot consisted of 13 blocks of wheat; each block comprising 48 individual rows, each row being a single breeding line or variety. Five ears were harvested from three positions in each row, 2m from the beginning, middle and end. Collected ears were threshed for 5-10 seconds using a LD180 stationary thresher (Wintersteiger AG, Ried im Innkreis). Harvested seeds were kept dry and stored at -20°C.

2.1.2 Sample preparation

For the field grown samples forty seeds were collected and ground in a Mega-grinder© (Monsanto, St Louis). All samples not grown in the field were ground to a fine powder using a pestle and mortar before starch was extracted. Finished samples were stored at -20°C.

2.2 Protein analysis

2.2.1 Wheat protein extraction methods

Proteins were either extracted from powdered wheat grain with 2%-β-mercaptoethanol (v/v) in 50% propan-1-ol (v/v), as described by Shewry (Shewry ***et al.***, 2009). Or with

70% ethanol (v/v) followed by 100% dimethyl sulphoxide (v/v) (DMSO), as described by Graybosch (Graybosch & Morris, 1990). After extraction samples were stored at -20°C.

2.2.2 Protein quantification

Protein concentration was quantified according to Bradford (Bradford, 1976). 1-10µg of bovine serum albumin (BSA) was solubilised in 100µl of buffer and added to 900µl of Bradford reagent. The optical density measured at 595nm was measured using a Lambda 40 spectrophotometer (Perkin Elmer, Waltham) and used to calculate a standard curve.

2.2.3 SDS-PAGE of wheat protein

Protein was solubilised in SDS protein extraction buffer and boiled with sample loading buffer (New England BioLabs, P7709V). Extracted wheat protein was visualized by SDS-PAGE (Laemelli, 1970) using a 12% Mini-PROTEAN® TGX™ Precast Gel (Bio-Rad®, Hercules). Samples were loaded onto the gels and run using a BIO-RAD, Mini PROTEAN® 3 System. 180 volts of power was then applied constantly until adequate separation was observed. Proteins were stained with Coomassie (Diezel *et al.*, 1972). Once destained the gel was imaged by scanning on a Canon LIDE scanner.

2.2.4 Protein extraction and identification by peptide fragment fingerprinting

Protein was extracted by the Shewry method (Shewry *et al.*, 1995) as described previously and solubilised in Tris-HCl protein extraction buffer before quantification by Bradford assay. The protocol for SDS-PAGE was as above except samples were separated on a NuPAGE® Novex® 4-12% Bis-Tris gel (Life Technologies®, Waltham), stained with SimplyBlue™ SafeStain (Invitrogen®, Waltham). Within a laminar flowhood the bands were excised. In gel trypsin digest was then carried out and peptides were extracted for mass spectrometric analysis following the method of Shevchenko (Shevchenko *et al.*, 2007). The extract was injected, using a Dionex Ultimate 3000 uHPLC, onto a PepMap100 C18 2cm x75µm I.D. trap column (ThermoFisher Scientific, Waltham) in a 0.1% formic acid (v/v), 2% acetonitrile solution (v/v) at 35°C in the column oven and 6°C in the autosampler. The sample was separated, over a 35 minute gradient of increasing acetonitrile, using a 15cm PepMap100 C18 analytical column (2µm particle size, 100Å pore size 75µm I.D, (ThermoFisher Scientific, Waltham)) at 300nL/min and 35°C. The mass spectrometer analyser used was an electron transfer dissociation (ETD) enabled ThermoFisher-Scientific Orbitrap Elite, equipped with a NanoSpray Flex Ion ESI source (ThermoFisher Scientific, Waltham). Nanospray ionization was carried out at 2.1kV, with the ion transfer capillary at 250°C, and S-lens setting of 60%. MS1 spectra were acquired at a resolving power of 60,000 with an automatic gain control (AGC) target value of $1x10^6$ ions by the Orbitrap detector, with a range of 350-2000m/z. Following MS1 analysis the top 20 most abundant precursors were selected for data dependant activation (MS2 analysis) using collision induced dissociation (CID), with a 10ms activation time, and an AGC setting of 10,000 ions in the dual cell linear ion trap on normal scan rate resolution. Precursor ions of single charge were rejected, and a 30

second dynamic exclusion window setting was used after a single occurrence of an ion. The resulting spectra were searched with OMSSA (Wenger *et al.*, 2011) against the NCBInr database (restricted to *Triticum aestivum*), and a decoy database, within the SearchGUI 1.19.5 software package (Vaudel *et al.*, 2011). Full trypsin enzymatic specificity was required with up to 2 missed cleavages permitted. The instrument was set to ESI-TRAP. A mass tolerance of 10ppm was used for precursors and 0.5 Da for fragment ions. Acetylation of the protein n-terminus was specified as a variable modification. Peptide-spectral match validation was carried out using peptide shaker (Barsnes *et al.*, 2011). Proteins required a single unique peptide with a 95% confidence interval or above in order to be reported.

2.3 Starch analysis

2.3.1 Isolation and solubilisation of starch from wheat grain

Pure starch was isolated by adding 1% sodium bisulphite (v/v) (1 ml/grain) to the requisite amount of flour before the mixture was filtered through muslin. After 20 min on ice the supernatant was removed and the flour was washed twice with distilled water (1ml per grain). The resulting starch pellet was resuspended in acetone (500µl per grain), left to stand on ice for 20min and the supernatant removed. This was repeated and the pellet left to dry overnight in a fume cupboard. Starch was solubilised by heating at 105°C (25mg starch /0.35ml of distilled water) for ten minutes with agitation at 108g.

2.3.2 Chemical hydrolysis of starch

Starch was hydrolysed with hydrochloric acid (0.56N HCl, 0.15M $CaCl_2$) (Kunlan *et al.*, 2001). Samples were incubated at 105°C for 10 minutes followed by 80°C for 12 hours and dried under vacuum. The amount of glucose after hydrolysis was assayed in a 96 well microtitre plate, the method was adapted from Bergmeyer (Bergmeyer, 1984) by changing the assay buffer from 100mM HEPES to 100mM Citrate buffer. This change was made, as the HEPES buffer was found to inhibit the glucose-6-phosphate dehydrogenase. The generation of NADH at 340nm (McComb *et al.*, 1976) was followed using a FLUOstar optima (BMG Labtech, Aylesbury) multi well plate reader.

2.3.3 Enzymatic hydrolysis of starch

Starch was boiled for ten minutes in water before acetate buffer (0.2M, pH4.6) was added and samples homogenised. Starch hydrolysis was achieved by digestion at 24°C for 12 hours with α-amylase (EC 3.2.1.1, 1 units/10mg of starch), α-glucosidase (EC 3.2.1.1, 40 units/10 mg starch) and isoamylase (EC 3.2.1.68, 0.8 units/10mg of starch). The reaction was stopped by boiling for three minutes and glucose was then measured spectrophotometrically as previously described (section 2.3.2).

2.3.4 Starch polymer branch chain analysis

β-amylase (EC 3.2.1.2, 10 units/mg of starch) was added to solubilised starch and incubated at 37°C for 2.5 hours with agitation. The reaction was stopped by boiling and centrifuged. An aliquot of sample was removed, had citrate buffer (pH 6.6) added (2:1 ratio) and was then digested with α-glucosidase (EC 3.2.1.20, 15.6 units/mg) at 37°C for

8 hours with agitation, this sample was labeled “β-limit digest”. A second aliquot of sample was removed and digested completely according to the previous method, this sample was labeled “Isoamylase digest”. The amount of glucose in each sample was measured using the spectrophotometric assay method described previously.

2.3.5 Measurement of enzyme kinetics

Based on the method described in Bergmeyer (Bergmeyer, 1984) the production of glucose over time was measured. Citrate buffer (0.1M citrate, pH 6.6) was added to the sample with 0.001M adenosine triphosphate (ATP) and 0.005M nicotinamide adenine dinucleotide (NAD). hexokinase (EC 2.7.1.1, 1.1 Units) and glucose-6-phosphate dehydrogenase (EC 1.1.1.49, 1.5 Units) were then added in order before the enzyme of interest was added. The enzyme of interest was either amyloglucosidase (EC 3.2.1.3, 5.6 Units), α-amylase (EC 3.2.1.1, 40 units) or β-amylase (EC 3.2.1.2, 10 units). The absorbance change at 340nm was followed to measure NADH generation (McComb *et al.*, 1976).

2.3.6 Dialysis of LMW soluble molecules from starch

Dialysis was used to separate soluble molecules from solubilised starch. Purified starch was solubilised in distilled water (4mg/ml) and placed in dialysis tubing with a molecular weight cut off of 12-14 kDa. The filled dialysis tube was placed in distilled water and left to dialyse for 18 hours.

2.3.7 Analysis of starch digests by matrix assisted laser desorbtion ionisation mass spectrometry (MALDI-MS)

Each sample was diluted in α-cyano-4-hydroxycinnamic acid (25mg/ml) and spotted onto a MALDI target plate. The ionisation was carried out in positive mode with a laser power of 200 and a laser pulse rate of 1kHz. The resolution of the mass spectrometer (Waters, Manchester) was set at 10000 and each spot was acquired for three minutes with 1 scan/second. The mass range used was 50-1000m/z.

2.3.8 Starch granule size measurement

The size of starch granules was measured by microscopy (Leica, Wetzler) after staining with Lugol's solution (2% w/v KI, 1% w/v I_2, 10mg/0.5ml). The Feret diameter frequency was determined from 15 representative fields of view with ImageJ (Schneider *et al.*, 2012).

2.3.9 X-ray diffraction analysis of A-type starch granules

The crystal properties of A-type starch granules were analysed by X-ray diffraction based on the method of Zhang (Zhang *et al.*, 2013b). Starch was purified as previously described from samples harvested in the field. Starch granules were separated by size based on the method of Peng (Peng *et al.*, 1999). Small starch granules were separated from larger granules by centrifugation at 469g through two sucessive 80% sucrose (v/v) solutions. Once small starch granules were isolated they were dried in acetone. Dried samples were wax mounted and exposed for 15 minutes on an X-ray diffractometer (Marrresearch GmbH, Norderstedt). The diffractometer was operated at 40 mA and 40

kV; the X-ray source was Cu Ka radiation with a wavelength of 0.154182 nm. Data were obtained at 2θ (θ being the angle of diffraction) at angles between 4-40 degrees by scanning at a speed of 10 degrees/min with a scanning step of 0.033 degrees/min. Acquired images were analysed using marView (Marrresearch GmbH).

2.3.10 Starch debranching

Starch was debranched according to the method of Morrell (O'Shea & Morell, 1996). Starch was boiled in 0.5M NaOH for 10 minutes. Once cooled glacial acetic acid and 0.01M sodium acetate buffer (pH4.0) was added. Isoamylase (EC 3.2.1.68, 5 units/10mg of starch) was then added and the solution was left to digest for 2.5 hours at 37°C. Once complete the reaction was stopped by boiling for 3 minutes.

2.3.11 Starch depolymerisation

Debranched starch was suspended in 0.01M acetate buffer (pH 4.8) and β-amylase (EC 3.2.1.2, 1 unit) was added. The solution was incubated for 2.5 hours at 37°C. Once complete the reaction was stopped by boiling for 3 minutes.

2.3.12 Nelson-Somogyi reducing sugars assay

Reducing sugars were measured using the method outlined by Nelson-Somogyi (Smogyi, 1952). Samples were heated with 0.12M alkaline copper tartrate at 105°C for 10min. Once cooled the arsenomolybdate reagent (18mM) was added to the sample solution. After 10 minutes the absorbance of each sample at 620nm was measured.

2.3.13 Analysis of starch digests by electrospray ionization mass spectrometry (ESI-MS)

Each starch digest was centrifuged for 1 minute at 18187g before being diluted in a solution of 50% dH_2O/ 49% methanol (v/v) and 1% formic acid (v/v). The diluted sample was then injected via electrospray into a time-of-flight mass spectrometer (AB-Sciex, Framingham) using a syringe pump. The flow of the syringe pump was set to 50µl per minute and each sample was run for three minutes. Ionization was carried out in positive mode at 4kV, the ion transfer capillary was set at 200°C, curtain gas set at 20 $L.h^{-1}$, the declustering potential/declustering potential 2 was 80/15, focusing potential was 265, with a mass range of 700-2500m/z or 50-2500m/z.

3 Does protein content and composition affect ethanol yield?

The aims of the work presented in this chapter were to determine whether the content or composition of protein differed between Warrior and Viscount.

3.1 Introduction

The first aim was to accurately determine the total grain protein content in each variety. This aim was chosen as it has been widely documented that increasing protein content in wheat is correlated with a decrease in ethanol yield (Agu *et al.*, 2009), (Awole *et al.*, 2011), (Kindred *et al.*, 2008). A 1% (w/w) reduction in total wheat protein will result in a 7.36 litre rise in ethanol yield per ton (Smith *et al.*, 2006) and soft wheat varieties have a higher ethanol yield than hard wheat varieties (Kindred *et al.*, 2008). This effect has been attributed to the formation of a protein matrix which has been observed by SEM (Scanning electron microscopy) surrounding (Stenvert & Kingswood, 1977) and binding to the starch granules (Barlow *et al.*, 1972), (Giroux & Morris, 1998). A more extensive protein matrix has been shown to be resistant to milling, resulting in larger flour particles after milling has taken place (Song *et al.*, 2014). Larger flour particles reduce the surface area for enzymatic attack and consequently ethanol yield decreases. Therefore to examine whether the ethanol yield difference between Warrior and Viscount can be explained by the amount of protein they contain, protein content was measured in extracts of whole grain with the Bradford assay (Bradford, 1976). The application of nitrogen to wheat can greatly influence the final protein content of the grain (Godfrey *et*

al., 2010). Therefore it was essential to use grain grown with the same fertiliser regime and in the same years (2010, 2011 and 2012).

The measurement of protein content using this method had two main issues. These issues arose from the nature of protein in the granule, in that it is tightly bound to starch granules (Stenvert & Kingswood, 1977). Firstly, all the protein had to be extracted from the grain in order for it to be accurately measured. Secondly, the extraction method needed to be compatible with the Bradford assay if calculation of protein concentration was to be accurate. It has been shown that a variety of compounds will interfere with the Bradford assay including detergents, flavonoids and basic protein buffers (Bradford, 1976), (Compton & Jones, 1985). Each compound will shift the dye equilibrium in favour of the dye anion, which will absorb at 595nm creating a false positive. With proper controls the first problem has been resolved rather simply; once the protein extraction was complete the residual material was then tested using the Bradford assay. Any residual protein would react with the Bradford reagent and be detected. The second issue required more attention to ensure protein measurement was accurate. This was achieved by testing and validating both the extraction method and the buffers used.

The second aim of the chapter was to identify differences in the protein composition of the two varieties. The protein matrix formed by the proteins within the endosperm packs starch granules together. As the protein content of the grain increases the amount of protein in the matrix and therefore its ability to bind the starch granules together increases (Stenvert & Kingswood, 1977). If the protein matrix is more extensive or its constituents are different (which could change the properties of the matrix) then more

energy is required to grind the endosperm in order to release the starch granules (Song *et al.*, 2014).

Individual proteins that have been associated with changes in grain properties include high molecular weight glutenin (HMW-glutenin) and friabilin (Feiz *et al.*, 2009; Burešová & Hřivna, 2011). In a study limited to two lines it was shown that increasing HMW-glutenin content by introducing selected chromosome segments (1R.1D $_{5+10}$-2) was negatively correlated with ethanol yield compared to commercial varieties (Burešová & Hřivna, 2011). However it was not clear if this really was due the protein matrix becoming more extensive as only two lines were used. The protein friabilin has been shown to bind polar lipids on starch granules via their tryptophan rich domains (Feiz *et al.*, 2009), this has been observed via immunolocalisation of friabilin's two constituent subunits. This binding will prevent the breakdown of these polar lipids during seed maturation (Kim *et al.*, 2012) and will result in a softer endosperm texture, indeed when the puroindoline proteins are mutated the hardness of the endosperm increases (Giroux & Morris, 1998), (Hogg *et al.*, 2004). Thus a small difference in protein composition can profoundly affect grain properties. It is therefore possible that individual proteins are responsible for the difference in ethanol yield between Warrior and Viscount.

The protein composition of the two wheat varieties was assessed using SDS-PAGE (Laemelli, 1970), allowing visualisation and assessment of the protein. Extraction and visualisation of proteins using this method was repeated in order to ensure the initial observations were consistent and differences in the protein composition were true. To

identify specific differences in protein composition peptide fragment fingerprinting (PFF) was used to identify the proteins of interest in the two varieties.

Since the purpose of this experiment was to compare the two varieties it was very important to use homogenous material. Warrior and Viscount are nationally listed commercial wheat varieties and as such are genetically uniform and stable as certified by the HGCA. To remove yearly variation all samples were kindly provided by RAGT (Cambridge) from plots grown in three different years (2010) with the same fertiliser regime. The limitation in using a one-dimensional SDS-PAGE was its relatively low resolution compared to techniques such as western blotting. This limitation hinders the accurate identification of proteins, particularly low molecular weight proteins. This problem was surmounted by separating the protein fractions (ethanol soluble and insoluble) and accounting for the difference by sorting proteins by their peptide abundance in the PFF analysis.

3.2 Hypotheses

1. Protein content is higher in Warrior than Viscount causing a reduced ethanol yield due to a more extensive protein matrix

3.3 Results

3.3.1 Reliability of the Bradford assay

To ensure the accuracy of measurements, the Bradford assay was optimised. Many chemicals interfere with the Bradford assay (Compton & Jones, 1985) therefore it was critical to make sure that the reagents used in the extracts did not compromise the accuracy of the assays. When dH_2O was used in the generation of a standard curve (Figure 3.1) the resulting line exhibited a very good correlation between protein concentration and absorbance at 595nm (R^2=0.9968). However distilled water alone was unlikely to solubilise much wheat grain protein as it is a weak polar molecule. Detergents are often used in protein solubilisation buffers to improve protein recovery; they increase the solubility of protein aggregations by reducing their surface tension (Shewry *et al.*, 1995). However when a solution containing 2% SDS was used in the Bradford assay buffer, the protein calibration curve was a horizontal line and failed to increase in absorbance in proportion with increasing protein content (Figure 3.1). For protein to be accurately quantified three alternative protein solubilisation buffers were tested. The zwitterion Bicine in a 200mM solution, PBS-TWEEN and a Tris-HCl buffer were individually tested, the latter was trialled with and without TRITON X-100 detergent. The Bicine buffer produced a good fit but the quantification of larger amounts of protein was less accurate, as the slope value was much lower than that of dH_2O (Figure 3.1). The PBS-TWEEN buffer showed a strong interaction of the detergent with the Bradford reagent (Figure 3.1); the lowest protein concentration had a much higher OD value than had been observed in the other graphs. The TRIS-HCl buffered solution was able to produce an accurate calibration curve. When the detergent Triton X-100 was present in the mixture the baseline OD increased and sensitivity was lost at the higher protein

concentrations. From these data it was concluded that all the new buffers tested produced a calibration curve that was able to measure protein concentrations accurately. It has also been shown that Triton X-100 can be used in extracting proteins, as it is compatible with the Bradford assay. Of all the buffers tested TRIS-HCl interfered the least with the Bradford assay.

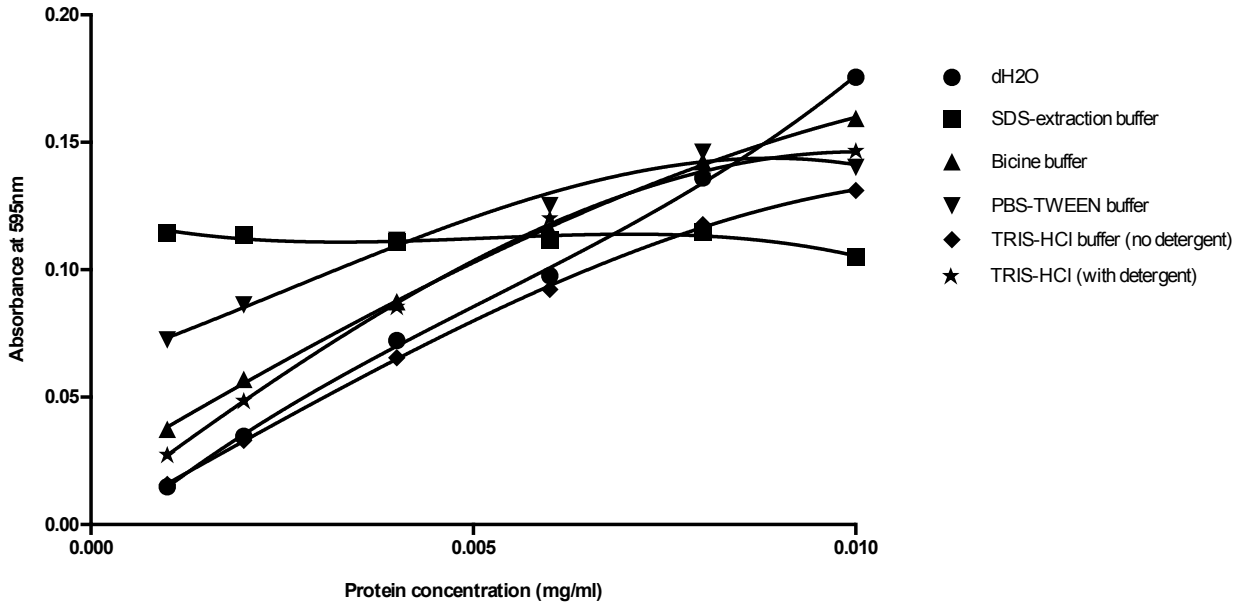

Figure 3.1 ***The effect of buffers on the Bradford assay****. A standard curve of 1-10 µg of BSA was prepared as a solution in one of six different solvent solutions. Each solution was then added to Bradford reagent and the absorbance at 595nm was measured according to the method outlined in chapter 2. Curves were fitted with a third order polynomial, n=3.*

3.3.2 Buffer validation

The efficacy of each buffer needed to be tested to ensure that it would dissolve all the protein present in the sample. This was essential for the accurate measurement of protein content in the two varieties. In order to ensure that all proteins present in the wheat grain were represented a known amount of protein was solubilised by each buffer. 1.0mg of α-amylase (Sigma, Porcine pancreas) enzyme was weighed into a centrifuge tube and suspended in 1ml of buffer. Therefore the protein concentration calculated by the Bradford assay was expected to be 1mg/ml. Figure 3.2 shows the protein content of the solution measured by Bradford assay. According to the graph, dH_2O reliably yielded around 0.6mg/ml of protein. In comparison to dH_2O the Bicine buffer extracted less protein and was therefore not used further. Both the PBS-TWEEN buffer and the TRIS-HCl recovered around 1.0 mg/ml so these were tested further for their ability to solubilise wheat protein. It is important to note that the standard deviation for the TRIS-HCl was high. Protein yield was also slightly higher than is to be expected because the detergent was interacting with the Bradford reagent. In this experiment the protein calibration curve was prepared using dH_2O to accurately compare samples. Therefore the baseline reading with the buffer in combination with detergent was slightly higher. In later experiments the solubilisation buffer was used to produce the calibration curve and not dH_2O.

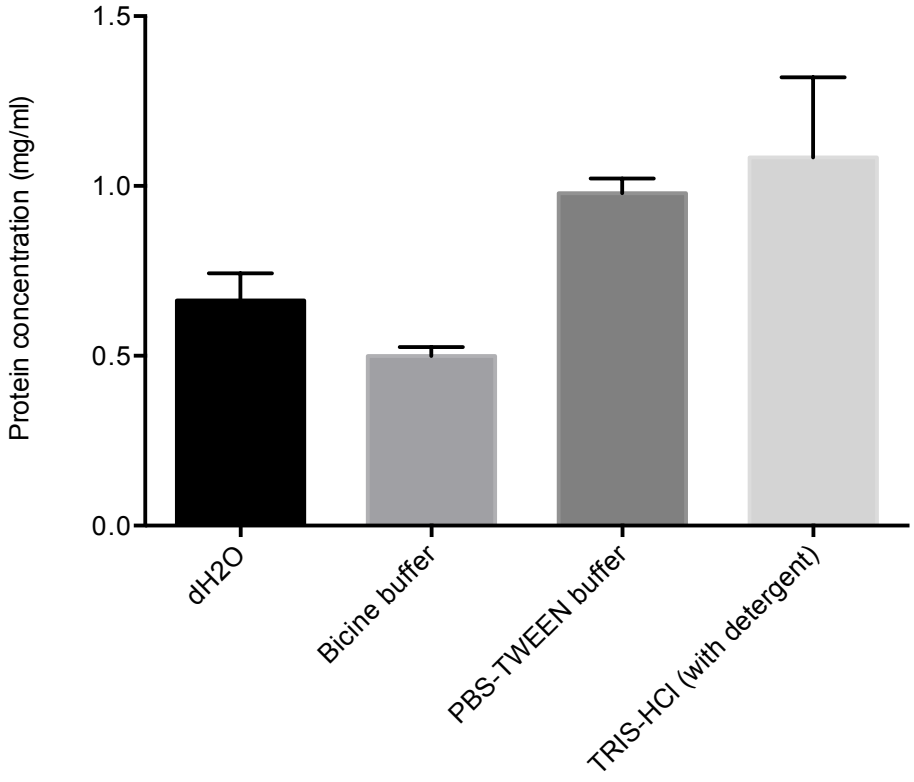

Figure 3.2 ***Solubilisation of protein by different buffers.*** *1mg of α-amylase (1mg) was dissolved in each buffer and the resulting solution assayed with Bradford reagent. Each bar represents the mean of three solutions and the error bars show standard deviation, n=3.*

3.3.3 Protein extraction method validation

Many different methods exist for extracting wheat protein from wheat endosperm. Commonly used methods include those of Graybosch (Graybosch & Morris, 1990) and Shewry (Shewry *et al.*, 2009). Both of these methods exploit the properties of gluten in alcohols. Gliadin, which is alcohol soluble is the lower molecular weight component of the granule protein whereas glutenin is the high molecular weight component and is not alcohol soluble (Cook & Rose, 1934). The Shewry method uses 50% propanon-1-ol to solubilise the gliadin fraction. To allow the glutenin proteins to be solubilised in alcohol the Shewry method uses β-mercaptoethanol to reduce di-sulphide bonds between glutenin subunits. The Graybosch method extracts alcohol soluble protein using alcohol and DMSO. The glutenin protein fraction is collected as the insoluble fraction. The two fractions of protein produced after the method was complete had to be combined before the Bradford assay calculated protein content. The separation of the two fractions was desirable for observing protein composition but not for calculating total protein content. Figure 3.3 shows the protein yield from each extraction method after resolubilisation with the selected buffers. The Shewry method produced the highest yield after the extraction procedure, whereas the Graybosch method resulted in a poor estimate of the total protein content. Therefore determining the total protein content was carried out with the Shewry method. In both cases Tris-HCl with TRITON X-100 improved protein concentration over PBS-TWEEN and was therfore used for all subsequent protein extractions.

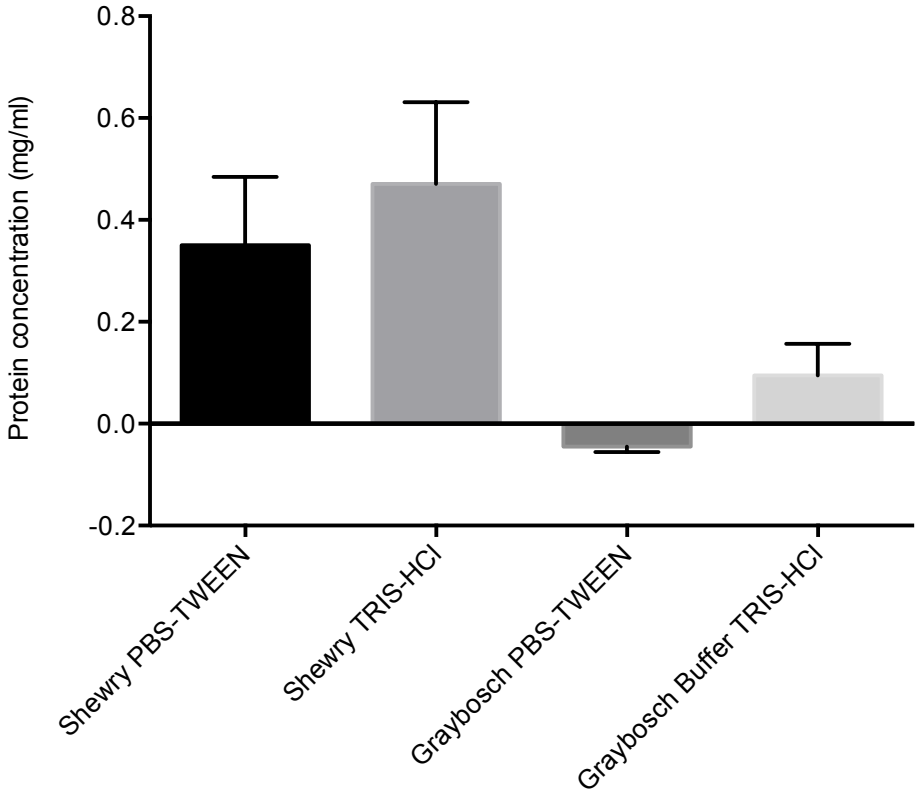

Figure 3.3 ***The amount of protein recovered after two different wheat protein extraction procedures****. Wheat protein was extracted from ground grain according to either the Shewry method or the Graybosch method (Chapter 2). Extracted protein was then dissolved either with protein extraction buffer 4 or 5 and assayed according to the method of Bradford (Chapter 2). Protein yield has been calculated using a standard curve of BSA dissolved in the buffer used in the extraction, yield has also been normalised against the initial extraction weight. Error bars show standard deviation, n=3.*

3.3.4 Protein content recovery experiment

To confirm the protein content measurement of Warrior and Viscount (Table 3.1) was accurate a recovery experiment was carried out. In this experiment 1mg of α-amylase protein was extracted along with wheat grain protein. A third sample was prepared where wheat grain protein had 1mg of α-amylase protein added. The efficiency protein recovery was calculated to be 94% using this method.

Table 3.1. Efficiency of protein recovery. *Three protein samples were prepared and measured using the Bradford assay; Protein extracted from wheat, a known amount of α-amylase and protein extracted from wheat with a known amount of α-amylase. The efficiency of protein recovery was calculated by dividing extracted wheat protein with α-amylase by the sum of extracted wheat protein and α-amylase, n=3.*

	Protein content (mg/ml)	Standard error of mean (+/-)
Wheat protein	2.27	0.175
Wheat protein with α-amylase	2.96	0.0889
α-amylase	0.877	0.187

3.3.5 Protein content of Warrior and Viscount

The protein concentration of the two wheat varieties was determined by extracting protein from a known amount of ground grain (~20mg). The amount of protein extracted from Viscount was just over 2mg (Figure 3.4). Therefore the extracted protein represented 9.9% of grain weight in Viscount. In contrast the protein content of Warrior grain was 9.1%. The difference between the total amounts of protein between the two varieties was significant (unpaired t-test, $P<0.05$).

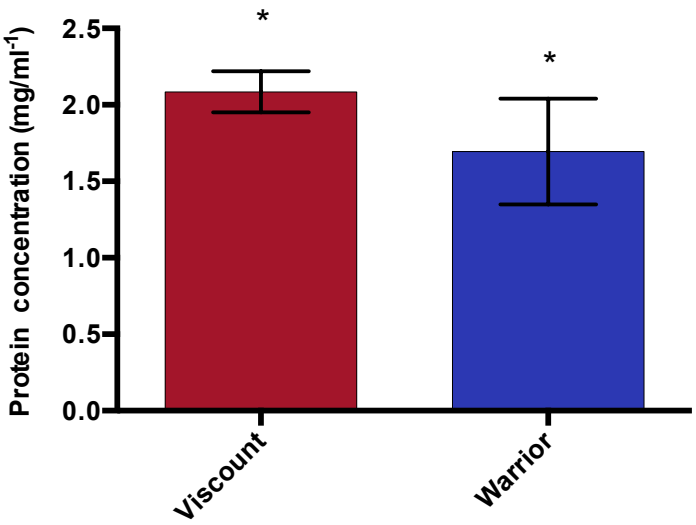

Figure 3.4 ***Protein content of Warrior and Viscount wheat.*** *Protein was extracted according to the method of Shewry (Chapter 2) and suspended in protein extraction buffer 5. The amount of protein in the buffer was then measured using the Bradford assay (Chapter 2). Protein yield was calculated using a standard curve of BSA suspended in buffer 5. The error bars represent the 95% confidence interval of each mean. The difference between the two means is significant when P<0.05 (unpaired t-test, n=9).*

3.3.6 Protein composition of Warrior and Viscount

SDS-PAGE was used to observe any variation in protein composition in the two varieties. The protein extracts from the Shewry method were used. In Figure 3.5 two replicate SDS-PAGE gels are shown. The separation pattern of each sample was very consistent, as observed by comparing replicate lanes on each gel and between the gels. However there were differences in the protein present in the high molecular weight fraction between the two varieties. Viscount seemed to have an extra band between 32 and 46kDa compared to Warrior (Figure 3.5, box A). Which was conserved in all gels and all four Viscount sample lanes. In addition differences in protein composition could be observed at around 80kDa. In the Viscount lanes there was a band, which was not present at the same weight at the corresponding Warrior weight (Figure 3.5, box B). In the Warrior ethanol insoluble lane there was two bands not present in Viscount, they had a weight <80kDa (Figure 3.5, box C).

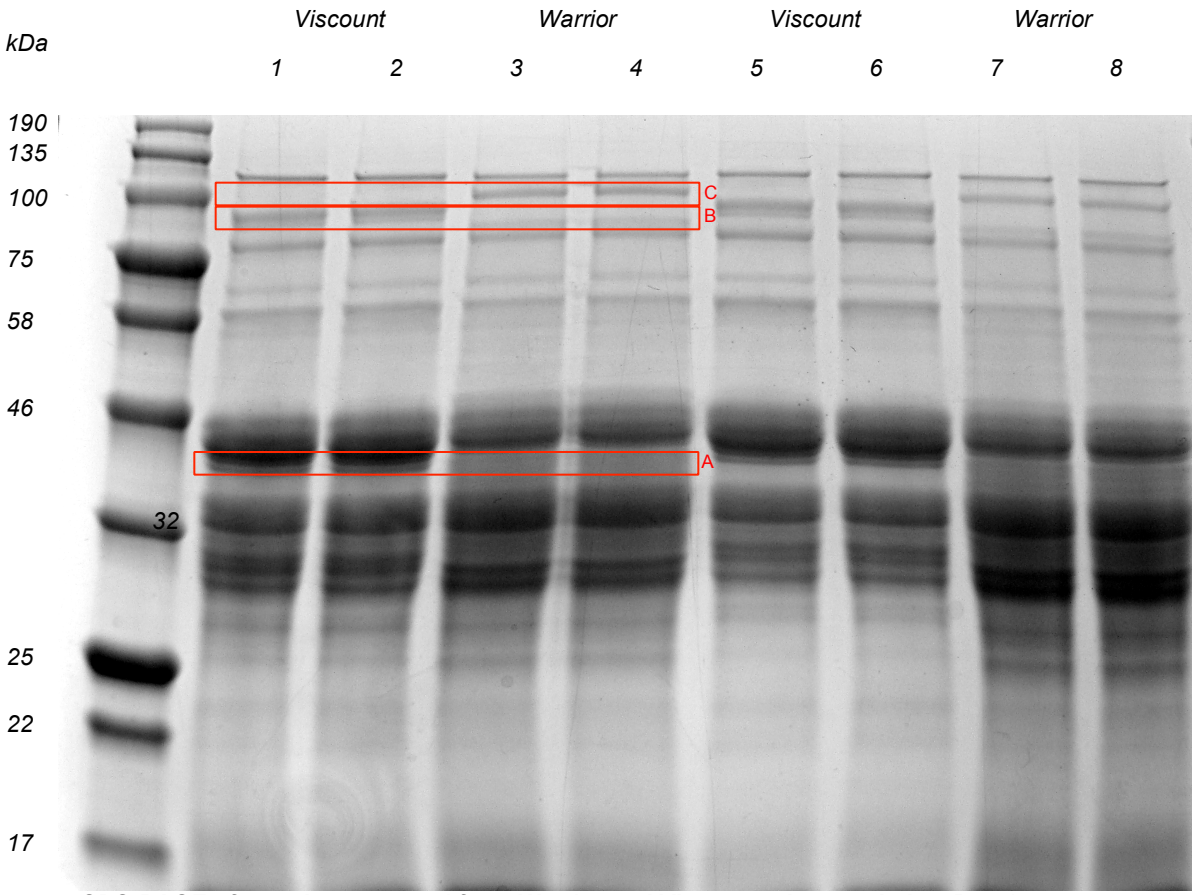

Figure 3.5 ***SDS-PAGE of proteins extracted from Warrior and Viscount wheat varieties.*** *Protein was extracted from ground grain using the method of Shewry (Chapter 2). The extracted protein was suspended in the SDS containing protein extraction buffer. 5µg of protein was loaded per lane and was then separated by SDS-PAGE using the method outlined in Chapter 2. Each lane represents an individual extraction procedure. Lanes 1 and 2 are replicate Viscount protein separations from a single extraction, Lanes 3 and 4 are replicate Warrior separations from a single extraction. Lanes 5 and 6 are replicate Viscount protein separations from a separate, single extraction. Lanes 7 and 8 are replicate Warrior protein separations from a separate, single extraction.*

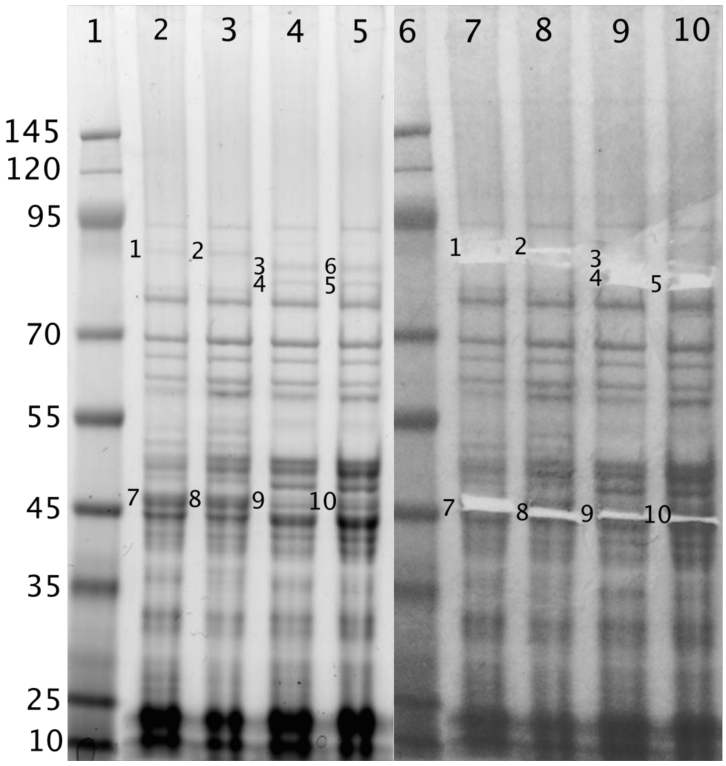

Figure 3.6 ***SDS-PAGE of proteins extracted from Warrior and Viscount wheat varieties for peptide fragment fingerprinting.*** *Protein was extracted from ground grain using the method of Shewry (Chapter 2). The extracted protein was suspended in protein extraction buffer 5 and quantified by Bradford assay (Chapter 2). 5µg of protein was loaded per lane and separated by SDS-PAGE. Once the SDS-PAGE was complete bands of interest were excised. Bands in the gel labelled 1-10 were excised for peptide fragment fingerprinting. Lanes 1-5 show the gel before band excision and lane 6-10 show the gel after band excision. Each lane represents duplicate samples from a single extraction procedure. Lane 1,6, Prestained protein marker (kDa); Lanes 2,3, Viscount protein before excision; Lanes 4,5, Warrior protein before excision; Lanes 7,8, Viscount protein after band excision; Lanes 9,10, Warrior protein after band excision.*

3.3.7 Identification of the differences in protein composition

To identify the proteins that differed between the two varieties the corresponding bands were excised from the gels (Figure 3.6). Identity of constituent proteins in each band was then established by peptide fragment fingerprinting (PFF). The purified protein was digested with trypsin, which cleaves amino acids at the carboxyl side of the amino acid lysine. The peptide fragments were then subjected to tandem mass-spectrometry. In tandem mass spectrometry peptides of a single molecular weight are fragmented and the pattern of fragmentation is used to derive the sequence of the peptide. The derived sequence is then matched to a protein(s) in the Uniprot *Triticum aestivum* pepetide database.

Proteins identified by peptide fragment fingerprinting are listed in Table 3.2. As could be expected the higher molecular weight bands are high molecular weight glutenins. However this name only refers to a range of proteins that are not soluble in ethanol. By comparing the observed peptide fragment fingerprint with the UniProt *Triticum aestivum* protein database a precise identification was made. As can be seen in Table 3.2 bands 1/2 in the Viscount fraction were identified as being an HMW-glutenin subunit, specifically subunit 14 of the protein expressed from the 1Bx gene. The molecular weight of this protein accurately corresponded to its position on the gel. These bands are absent in the Warrior Lanes at the same position, so it was deduced that this protein is not present in Warrior at detectable levels. Similarly bands 4/5 shown in Figure 3.6 have been identified by peptide fragment fingerprinting as being a HMW-glutenin. This is a different subunit compared to bands 1/2 (Figure 3.6), identified as HMW-glutenin subunit 1By15. This protein is expressed at the same locus as 1Bx14 but not the same gene

(Table 3.2). These bands cannot be detected in the Viscount lanes in the same position therefore this protein was unique to Warrior at detectable levels. When the observed peptide fragment fingerprints for bands 7-10 were compared with the UniProt *Triticum aestivum* protein database they were identified as being Alpha/Beta-gliadin. This identification encompasses a class of protein, as individual identification was not possible. The reason for this is that the low molecular weight gluten proteins are poorly covered in the wheat peptide database, therefore a more specific identification could not be made (Mamone *et al.*, 2009). However a more general observation was reached in that the alpha/beta-gliadins from this band were more abundant in the Viscount variety than in Warrior, based on the higher intensity of the relevant bands in the Viscount lanes of the SDS-PAGE gel.

Table 3.2 ***Protein identification by peptide fragment fingerprinting****. Bands excised from the SDS-PAGE gel (fig 6) were subjected to in gel tryptic digestion (Chapter 2). Once the tryptic digest was complete peptides were removed from the gel slice and purified. The purified peptides were subjected to Tandem mass spectrometry using an Orbitrap Elite (Thermo Fisher) mass spectrometer. Collected spectra were searched against a peptide database restricted to aTriticum aestivum using OMSSA* [95]*. Final analysis was completed using peptide shaker* [96]*. Equivalent bands in replicate lanes were used as replicates in the post-processing analyais.*

Variety	Band	Name	Locus	Gene	Molecular weight (kDa)
Viscount	1/2	HMW-Glutenin 1Bx14	*Glu-B1*	*1Bx*	85.18
Warrior	4/5	HMW-Glutenin 1By15	*Glu-B1*	*1By*	76.69
Viscount	7/8	Alpha/beta-gliadin	N/A	N/A	30.61
Warrior	9/10	Alpha/beta-gliadin	N/A	N/A	32.65

3.4 Discussion

The evidence presented in this chapter does not support canonical understanding of the production of ethanol from wheat. The hypothesis stated, “Protein content is higher in Warrior than Viscount causing a reduced ethanol yield”, which must be rejected as protein content was found to be higher in Viscount than Warrior (Figure 3.4). However, differences in protein composition have been identified (Table 3.2).

The inverse correlation between ethanol yield and protein content has been widely reported (Agu *et al.*, 2009), (Awole *et al.*, 2011), (Kindred *et al.*, 2008), (Swanston *et al.*, 2007) and is one of the most important determinants of ethanol yield from wheat. However this paradigm does not apply to Warrior, which had a lower protein content than Viscount. When the calculations of Smith (Smith *et al.*, 2006) are applied where a 1% (w/w) reduction in total wheat protein will result in a 7.36 litre rise in ethanol yield per tonne then Warrior should yield 5.8% more ethanol per tonne of grain. However this is not the case, as depending on location and nitrogen application Warrior has been shown to actually yield 5% less than Viscount on average (Weightman *et al.*, 2011).

Proteomic analyses of wheat proteins has mostly been focused on understanding the genetic diversity of different wheat crops around the world (Ribeiro *et al.*, 2013) and the effect of grain protein composition on the performance of dough in the production of bread (Liu *et al.*, 2009, 2012; Dupont *et al.*, 2011; Guo *et al.*, 2012). In contrast very few studies have examined protein composition and ethanol yield (Burešová & Hřivna, 2011). In this chapter differences in the protein composition of the two varieties tested

have been identified, a role for these proteins in affecting ethanol yield has not been previously identified in the literature.

3.4.1 Measurement of protein content in Warrior and Viscount Wheat

The protein content of the two varieties was accurately measured using the optimised method, accuracy was guaranteed by the high R^2 value of the standard curve (9.522) and the reliable recovery of a known amount of protein. The results showed that Warrior had a lower protein content than the Viscount variety, with a protein content of 9.1% and 9.9% respectively. This result shows that the disparity in ethanol yield between Warrior and Viscount cannot be explained by the amount of protein present in the wheat grain.

3.4.2 Protein quantification method optimisation

To ensure the results of the protein quantification were reliable the method was optimised extensively. The Bradford assay was used as it is a fast and, once optimised was an accurate method to measure the concentration of protein in a sample. The presence of the detergent SDS in the original protein extraction buffer prevented the accurate detection of protein concentration. The SDS will indeed change the point of equilibrium between the Bradford reagent cation (red) and the anion (blue) to favour the anion (Compton & Jones, 1985) causing an increase in absorbance at 595nm irrespective of protein content. This also holds true for many other detergents (Bradford, 1976). Due to this it was necessary to use a protein extraction buffer, which did not contain detergent or had detergent below detectable levels. Three different buffers were selected based on their reported ability to extract proteins from biological samples.

Bicine was selected as it is one of Good's buffers (Good *et al.*, 1966) and is commonly used in protein solubilisation. Secondly phosphate buffered saline (PBS) with TWEEN® 20 has also been tested, commonly used to solubilise proteins from cell culture. PBS is a water-based buffer composed of sodium chloride and sodium phosphate, whereas TWEEN is a detergent and as such some interference is expected in the Bradford assay. The final buffer used was 50mM TRIS-HCl (pH7.0), 10mM $MgCl_2$, 1mM EDTA, 5mM DTT, 5% (w/v) polyvinylpolypyrolidone (PVP) and 10% Glycerol. This buffer was tested with and without a detergent Triton X-100 (0.1% v/v). The $MgCl_2$ was added to bind proteins and to prevent protein aggregation, EDTA chelated metal ions, DTT was used as a reducing agent and prevented oxidation damage to proteins, PVP bound phenolics (Loomis & Battaile, 1966) and Triton X-100 is a detergent, which was key to solubilise the protein. TRITON X-100 interfered with the Bradford assay; however as it was already dilute in the extraction buffer, further dilution in the course of the Bradford assay reduced its effect. The final concentration is 0.01%, this has the same effect as adding 0.099µg of BSA which did not affect the outcome of the assay. Measuring the total protein content required that all the protein present in the sample was recovered. To ensure that this was the case each buffer was used to solubilise a known amount of protein. The protein concentration was then measured by Bradford assay to determine the yield of each buffer (Figure 3.2). The TRIS-HCl buffer with TRITON X-100 solubilised the most protein (α-amylase) albeit with a large amount of variation. The PBS-TWEEN buffer recovered slightly less protein but had a much smaller standard deviation than the TRIS-HCl buffer as it contained no detergent. The Bicine buffer performed very poorly, it solubilised less protein than water and as such it was not used any further.

The results show that the TRIS-HCl based buffer with detergent and the PBS-TWEEN buffer produced accurate standard curves and solubilised known amounts of protein accurately. TRIS-HCl is commonly used for solubilising extracted proteins (Bancel *et al.*, 2010) from wheat grains as it is considered to be the most compatible buffer with mass spectrometry (Heick *et al.*, 2012). Other buffers such as urea are also commonly used (Branlard & Bancel, 2007), (Guo *et al.*, 2012) but are considered to be less compatible with mass spectrometry (Heick *et al.*, 2012).

However α-amylase is very different to the gluten proteins of wheat. Because of this the two buffers were tested with purified wheat protein. To ensure the amount of protein measured in the Bradford assay was representative of actual protein content of the grain the extraction method also needed to be validated. Two commonly used protein extraction methods of Shewry and Graybosch were used to do this. Unlike the Shewry method the Graybosch method separates the alcohol soluble proteins. When the two extraction procedures were tested with both buffers the Shewry method recovered the most protein, this was true for both extraction buffers. The disparity in the yield of protein from the two extraction methods is likely due to the inclusion of β-mercapoethanol which reduced the extensive disulphide bonds in the wheat protein, particularly in the higher molecular weight glutenins (Shewry *et al.*, 2002). More protein was then solubilised and detected in the Bradford assay. The TRIS-HCl buffer solubilised much more protein than the PBS-TWEEN (Figure 3.3) buffer, the standard deviation of the two extraction buffers was very similar, allaying previous concerns over the variability of the TRIS-HCL measurements (Figure 3.2). The protein content of the wheat grains was not known at that point so the TRIS-HCl buffer was chosen as it produced a greater protein yield than

PBS-TWEEN. Thus the method for measuring protein content from wheat was optimised and validated to ensure the results were reliable.

3.4.3 Identification of differences in protein composition

The finding that total protein is not responsible for the disparity in ethanol yield between the two varieties does not mean that individual proteins in the grain could not affect ethanol yield. Therefore the protein composition of the two varieties was investigated. A few differences in proteins present were observed (Figure 3.5, Figure 3.6). The main difference in composition observed consisted of two proteins of molecular weight 80-90KDa which would correspond to high molecular weight glutenin subunits (Dupont *et al.*, 2011). In Figure 3.5 and Figure 3.6 where protein loading onto the gel was controlled there appeared to be some differences in abundance of band that are typically identified as being low molecular weight glutenins (Shewry *et al.*, 2003).

The first difference identified by SDS-PAGE and PFF was the presence of HMW-Glutenin 1Bx14 in Viscount but not Warrior (Table 3.2) and the presence of HMW-Glutenin 1By15 in Warrior but not Viscount. These x and y glutenin subunits are expressed from the Glu locus, they are classified based on their electrophoretic mobility and have been shown to affect the properties of bread flour (Rogers *et al.*, 1991). No role for either of these proteins in affecting ethanol yield has yet been identified. Their properties seem to lie primarily in their ability to form extensible dough during baking (Peggy Tao *et al.*, 1992) (Xu *et al.*, 2006), (Zheng *et al.*, 2011).

The second difference identified by SDS-PAGE and PFF was the higher abundance of the alpha/beta gliadins in Viscount compared to Warrior. Due to the lack of sequence coverage of the Alpha/beta gliadins in the wheat proteome database a more accurate identification was not possible. This was further limited by the complexity of the protein band itself. The bands excised from the gel could not be considered as a single protein but rather as multiple proteins of the same molecular weight. Though differences in protein abundance have been accounted for in the PFF analysis only the use of two-dimensional SDS-PAGE could have truly reduced noise to an acceptable level.

Having a lower proportion of these alpha/beta gliadins to HMW-glutenins in flour increases viscosity (Uthayakumaran *et al.*, 2000). As Warrior has a higher proportion of this gliadin subset it could contribute to relatively high viscosity compared to Viscount. Though viscosity can hinder processing of flour for alcohol production it does not lower the overall ethanol yield (Agu *et al.*, 2006) and as such is unlikely to contribute to the observed disparity in ethanol yield.

3.4.4 Conclusion

In conclusion, the protein content cannot explain the difference in ethanol yield between the two varieties. Higher protein content does not correlate with lower ethanol yield in these two varieties. This conclusion indicates that Warrior is a unique case, which cannot be explained alone by canonical understanding of the relationship between wheat grain properties and ethanol yield. Differences in the HMW glutenin subunits have been observed; the HMW-glutenin subunit 1By15 is present in Warrior and not Viscount. This subunit is only correlated with low ethanol yield; a causal relationship cannot be

deduced from this experiment. Thus, further work is necessary if this correlation is to be proven. However protein only accounts for 9-10% of total grain weight. The major component of the wheat grain is starch which accounts for 75-85% of grain weight (Brocklehurst, 1977). Since ethanol yield is also limited by the conversion of starch to glucose it is this component of the wheat grain that will be of further interest

4 Does the molecular structure of starch prevent efficient conversion into glucose?

4.1 Introduction

The aim of the research in this chapter was to determine if the difference in ethanol yield of Warrior and Viscount could be explained by a property of the starch present in the grain.

To achieve a good ethanol yield from wheat grain it must be extensively milled (Song *et al.*, 2014). This suggests that the difference between Warrior and Viscount could be due to starch structure or the structure of the granule itself, which alters the access of amylase enzymes (Li *et al.*, 2014).

However it was first necessary to establish that the starch of both varieties had the potential to yield the same amount of glucose. This was done by acid hydrolysis and enzymatic hydrolysis. This approach was taken as the procedure with amylase enzymes (McCleary *et al.*, 1997) could result in a difference due to the structure of the starch. Thus any difference in yield of glucose between the two varieties could be unequivocally ascribed to either a difference in amylase enzyme activity or glucose content. The starch was hydrolysed to glucose using hydrochloric acid and then the total released glucose was measured spectrophotometrically (Bergmeyer, 1984; Kunlan *et al.*, 2001). This ensured that the entire starch molecule was broken down to its constituent glucose

monomers irrespective of structure. The amount of glucose yielded was then compared with the result obtained by hydrolysis with amylase enzymes. The combination of α-amylase (3.2.1.1), α-glucosidase (3.2.1.20) and isoamylase (3.2.1.68) was used to release the glucose from the starch. The quantification of glucose, as in both cases was achieved by using a modified enzyme linked spectrophotometric assay method described in Bergmeyer (Bergmeyer, 1984) which is a rapid and sensitive method for determining glucose concentration.

The main issue with this experiment was to maintain accuracy when using a high-throughput procedure. This problem was resolved by greatly increasing the repetition of glucose measurements. A secondary issue was the presence of soluble hexose sugars such as sucrose and fructan (Verspreet *et al.*, 2013) which would be detected in the acid hydrolysis experiment. To prevent this from occurring the starch sample had to be purified. This was achieved by using a purification procedure that precipitates the insoluble starch and removes other contaminants such as soluble carbohydrates and lipids.

The second aim was to investigate the properties of the starch during enzymatic breakdown in each variety. In brewing malted barley is used to provide enzymes to degrade starch whereas with industrial ethanol production is permitted to use exogenous enzymes to degrade the starch (Smith *et al.*, 2006). Despite this difference the main enzymes that degrade starch are the same; α-amylase (3.2.1.1), β-amylase (3.2.1.2) and amyloglucosidase (3.2.1.3), these enzymes mediate the step in alcohol production

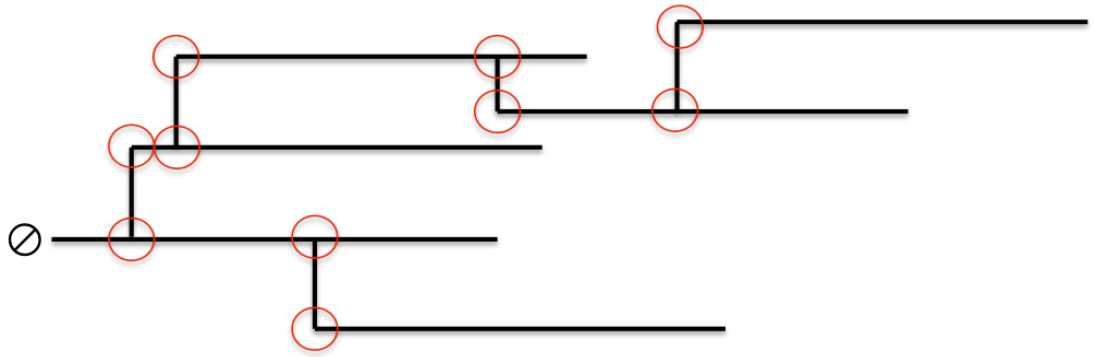

Figure 4.1. Schematic of amylopectin with α-1-6 glycosidic bonds (circled in red).

called saccharification (Bamforth, 2009). The poor ethanol yield in Warrior could thus be caused by an inhibition of saccharification by these enzymes.

Though starch is composed of a single monomer it has a complex structure. The complexity arises from the inclusion of α-1-6 glycosidic bonds; this bond produces a 'branch' (Figure 4.1). It has been shown that an increased proportion of branching in the starch structure can reduce digestion rates (Ao *et al.*, 2007) and by extension, the ethanol yield. Therefore a β-limit digest was performed to study the proportion of starch before and after the branch point in starch. When β-amylase is used to digest starch it cleaves successive maltose residues to the branch point at which point it stops. Once this was complete an aliquot of the sample was taken and the remaining β-limit dextrin was digested with α-amylase and amyloglucosidase. By comparing the glucose content of the two samples the amount of starch before and after the branch point could be calculated. This method relied on the assumption that enzyme activity was equal in the two samples. If enzyme activity were different (e.g. due to an enzyme inhibitor) then the result would not represent the proportion of starch before and after the branch point. It would represent the ability of the enzymes to degrade starch before and after the branch

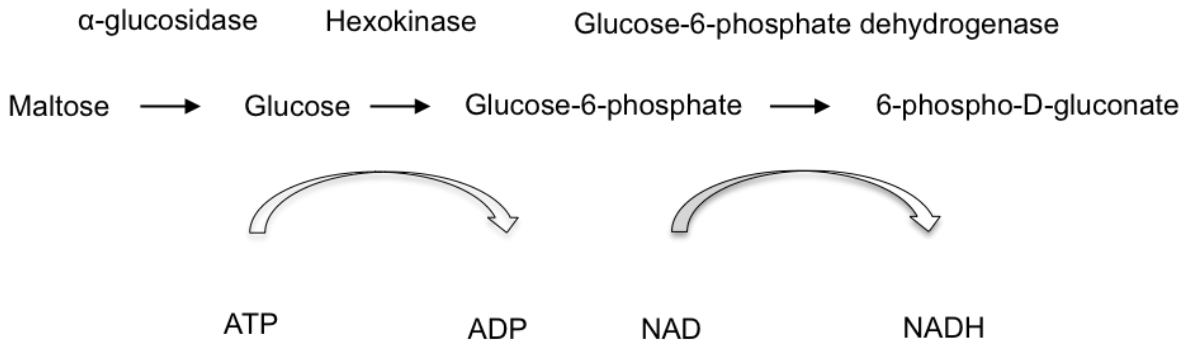

Figure 4.2 ***Enzyme linked spectrophotometric assay of glucose****. Serial conversion from glucose to 6-phospho-D-gluconate, the amount of glucose in the sample is directly proportional to the increase in absorbance at 340nm as NADH is generated*

point. The major issue with using this method was that the enzyme of interest was producing glucose at the same time as the detection pathway was consuming the glucose (Figure 4.2). The consequence of this was that extensive control experiments were needed to ensure the enzyme of interest was the only enzyme (if at all), which is affecting the rate of glucose generation. The results of these are outlined in the following chapter. The analysis of enzymatic breakdown products was completed by mass spectrometry using matrix assisted laser desorption ionisation (MALDI). The advantage of this approach is that differences in the oligosaccharide fragments produced as intermediates during digestion would be detected. MALDI is a soft ionization technique, which means it is less likely to fragment fragile molecules like sugars thus aiding their detection (Karas *et al.*, 1987). The matrix used was a proton donating molecule (α-cyano-4-hydroxycinnamic acid (Beavis *et al.*, 1992)) but with the aqueous sample obtained from enzymatic digestion, uniform application onto target plates could differ between samples. Therefore several replicates were used and each whole spot was analysed. The major limitation of this approach was that detected masses couldn't be used to directly identify a molecule, this was because many molecules could have be present that were of the same or very similar masses. For example maltose and sucrose

have similar molar masses and could not be separately identified using MALDI alone. Also, salts such as potassium and sodium could form adducts with ions generated by MALDI (Leite *et al.*, 2004). These adduct ions could make analysis more complex as the detected mass of a specific molecule could change. Principal component analysis was used to screen for masses, which were different between the two varieties. This was required as the datasets obtained from mass spectrometry is extremely large and complex. The main limitation of using this method of analysis was that any difference in detected masses, however small, would be detected which could result in a false positive. Therefore PCA was used to screen for divergent masses and the identified masses were then statistically analysed using an unpaired t-test on the percentage ion count of the detected spectrum of each spot.

Since the purpose of this experiment was to compare the two varieties it was very important to use homogenous material. Warrior and Viscount are nationally listed commercial wheat varieties and as such are genetically uniform and stable as certified by the HGCA. To remove environmental variation all samples were kindly provided by RAGT (Cambridge) from plots grown in three different years (2010, 2011 and 2012) with the same fertiliser regime.

4.2 Hypotheses

1. The total starch content in Warrior and Viscount grain is the same
2. The starch properties in Warrior and Viscount grain are the same
3. The products of starch breakdown are different in Warrior and Viscount

4.3 Results

4.3.1 Total starch content of wheat grain

The glucose content of the two wheat varieties was determined by hydrolysing starch with 0.565 N hydrochloric acid (Figure 4.3) or with the amylase enzymes; α-amylase, α-glucosidase and isoamylase from a known amount of purified starch (Figure 4.4). The yield of glucose from acid hydrolysis was not significantly different between the two varieties (unpaired t-test, P=0. 0.6970, df=16) and the yield of glucose from enzymatic hydrolysis was also not significantly different between the two varieties (unpaired t-test, P=0.2075, df=16). Though the results were not significantly different there was a large degree of variation in the values, but the range of variation was similar between the two varieties indicating that the variation was variety independent. It should be noted that the overall yield of glucose from enzymatic hydrolysis is slightly less than acid hydrolysis. This is likely due to the amylase enzymes not fully digesting the starch.

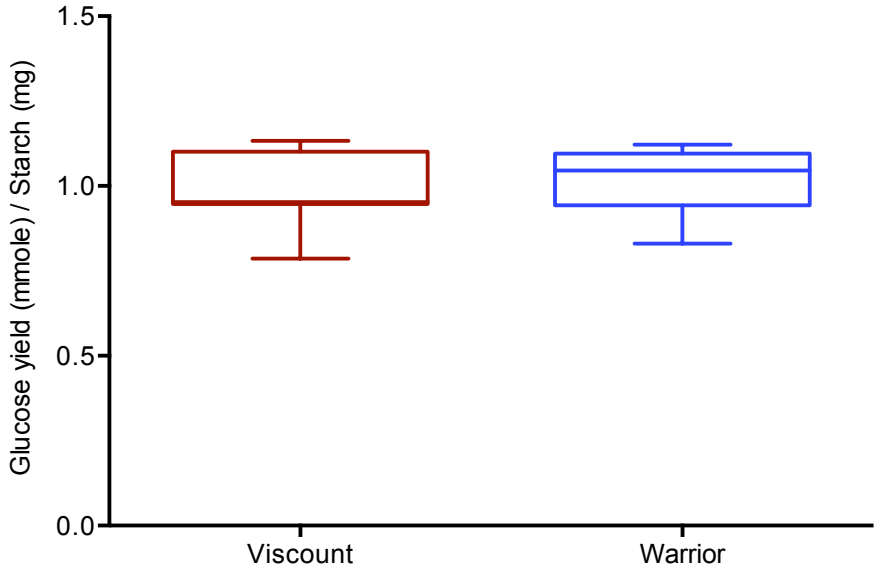

Figure 4.3 ***Starch content of Warrior and Viscount wheat by acid hydrolysis****. Starch was purified (Chapter 2) and hydrolysed with hydrochloric acid. The amount of glucose was then measured using the enzyme-linked spectrophotometric assay (Chapter 2). Each box was plotted using the Tukey method. The difference between the two means is not significant (unpaired t-test, n=9).*

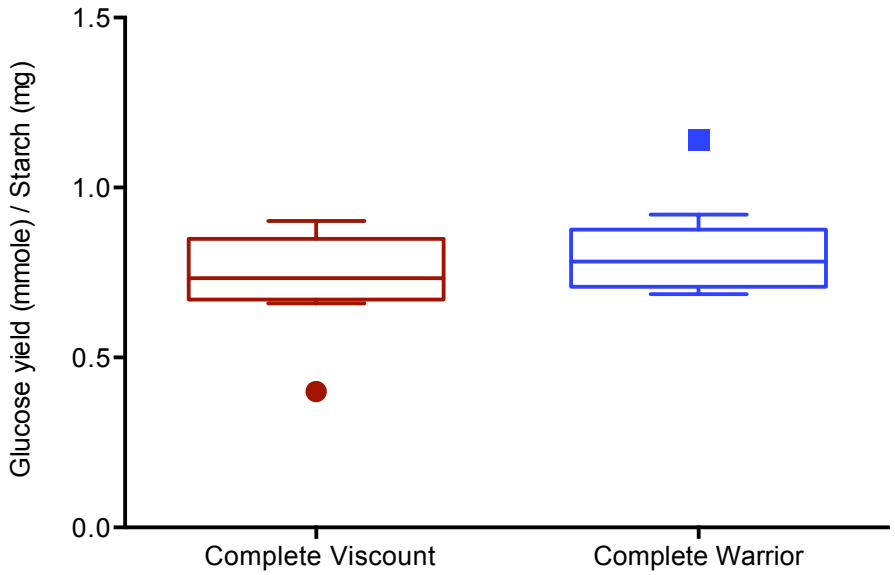

Figure 4.4 ***Starch content of Warrior and Viscount wheat by enzymatic hydrolysis****. Starch was purified (Chapter 2) and hydrolysed with enzymes. The amount of glucose was then measured using the enzyme-linked spectrophotometric assay (Chapter 2). Each box was plotted using the Tukey method. The difference between the two means is not significant (unpaired t-test, n=9).*

4.3.2 Amylase digestion rate of starch

The initial digestion rate of purified starch with two different enzyme combinations was measured. The first enzyme combination was with α-amylase, amyloglucosidase and Isoamylase and the second was with amyloglucosidase alone (Table 4.1). The initial rate of reaction for Viscount and Warrior digested with α-amylase, amyloglucosidase and Isoamylase was not significantly different (unpaired t-test, P=0.5, n=3). The initial rate of reaction for Viscount and Warrior digested with amyloglucosidase alone was significantly different (unpaired t-test, P=0.005, n=3).

Table 4.1 ***Initial rates of two amylase preparations on Warrior and Viscount starch****. Purified Warrior and Viscount starch was digested with α-amylase, amyloglucosidase and Isoamylase or amyloglucosidase alone. The reaction progress was followed by measuring the generation of NADH at 340nm for 30min. The initial rate was measure for 10min. The difference between the amyloglucosidase digest initial rates is significant (unpaired t-test, P=0.005, n=3).*

Sample	Initial rate (μmol/min^{-1})	Standard deviation
Viscount (α-amylase, amyloglucosidase and Isoamylase)	4.35^{ns}	0.71
Warrior (α-amylase, amyloglucosidase and Isoamylase	4.53^{ns}	0.21
Viscount (amyloglucosidase)	15.3**	0.68
Warrior (amyloglucosidase)	23.6**	1.68

4.3.3 β-limit digest of Warrior and Viscount starch

The proportion of recovered glucose before and after the branch point of the two wheat varieties has been determined by using a β-limit digest (Figure 4.5). The amount of glucose recovered after the β-amylase digest (before the branch point) was not significantly different between the two varieties (unpaired t-test, P=0.5881, df=15). However the yield of glucose from the β-amylase digest of Warrior was found to be slightly greater than Viscount. In contrast, the amount of glucose recovered after the branch point (digested with α-amylase, isoamylase and amyloglucosidase) was significantly different (unpaired t-test, P=0.0485, df=16). The starting weight of starch was ~20mg (glucose yield has been normalized against exact measured weight). Therefore the theoretical total glucose yield is 20mg; this was within the range of Viscount when both the amount of glucose measured before and after the branch is totaled. However this was not the case for Warrior, the glucose yield after the branch point was far lower than would be expected.

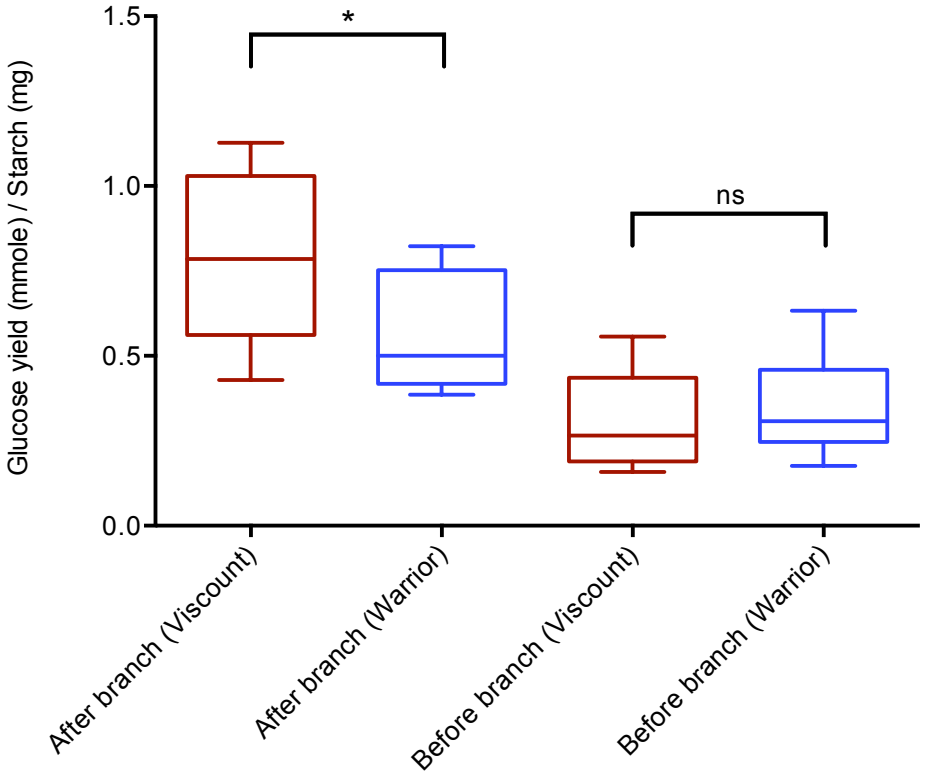

Figure 4.5 ***β-limit digest of Warrior and Viscount starch****. Starch was extracted (Chapter 2) and hydrolysed with β-amylase, an aliquot was then removed (β-limit). The remaining β-limit dextrin was then completely hydrolysed using α-amylase, isoamylase and amyloglucosidase (Isoamylase). The amount of glucose in each aliquot was then measured using the enzyme-linked spectrophotometric assay (Chapter 2). Each box represents the mean of nine digestion procedures and the boxes are plotted using the Tukey method. The difference between the β-limit means is not significant (unpaired t-test). The difference between the Isoamylase means is significant (unpaired t-test, P=0.05, n=9).*

4.3.4 Mix analysis of Warrior and Viscount starch

The β-limit digest was repeated with samples composed of a mixture of Warrior and Viscount starch. Three mixes were prepared of 25% Warrior to Viscount, 50% Warrior to Viscount and 75% Warrior to Viscount. All percentages stated refer to the amount of Warrior starch in the sample; the remaining percentage was Viscount starch (Table 4.2). Figure 4.6 shows a negative correlation between the amount of Warrior starch in the sample and glucose yield from the isoamylase digest. Not only that but Warrior has a potent effect on glucose yield; only a small amount of Warrior starch is required to reduce glucose yield. As can be seen in Figure 4.6 and Table 4.2 the decrease in glucose yield is non-linear.

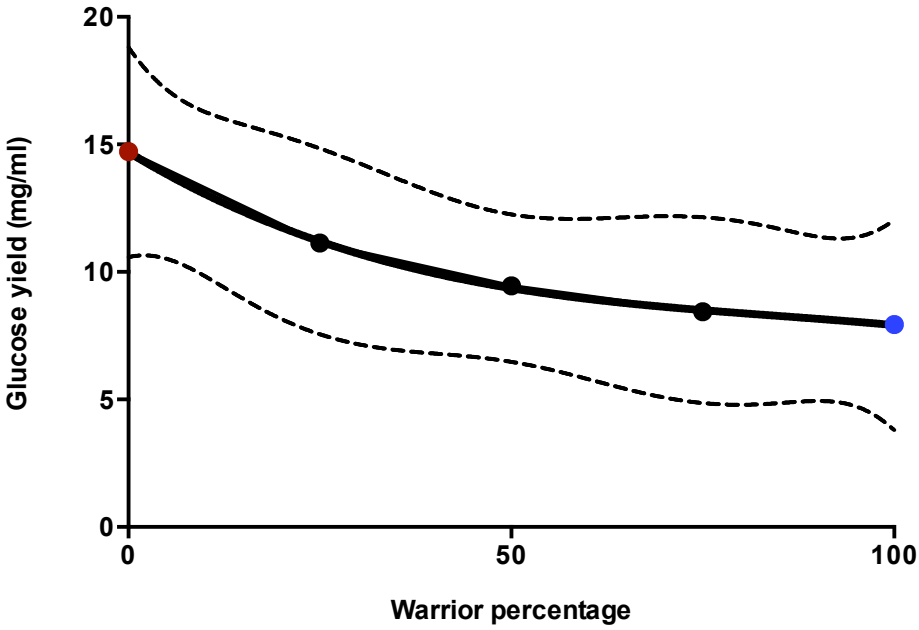

Figure 4.6 ***Mix analysis of Warrior and Viscount starch****. Starch was extracted (Chapter 2) and mixed proportionally (X-axis). The samples were then hydrolysed with β-amylase and the remaining starch was then completely hydrolysed using α-amylase, isoamylase and amyloglucosidase. The amount of glucose in the Isoamylase digest was then measured using the enzyme-linked spectrophotometric assay (Chapter 2). Each point represents the mean of nine separate digestion procedures. Viscount is represented by the red point and Wariror by the blue point The plotted line is a third order polynomical curve with the 95% confidence interval (n=72).*

Table 4.2 ***Compositions of samples for mix digest****. All samples were weighed out exactly, mixed and solubilised.*

Warrior %	Warrior (mg)	Viscount (mg)	Theoretical yield (**Figure 4.4**)	Actual yield
0	0	20	15	14.7
25	5	15	15	11.1
50	10	10	15	9.45
75	15	5	15	8.44
100	20	0	15	7.93

4.3.5 The effect of Warrior starch on amyloglucosidase activity

A concentration gradient of starch was used to calculate the enzyme kinetics of amyloglucosidase when digesting Warrior and Viscount starch. The sample was digested with amyloglucosidase (EC 3.2.1.3, 5.6 Units/mL) and the rate of the reaction was followed using the enzyme linked spectrophotometric assay (Chapter 2). From these data the enzyme constants Vmax and K_m were calculated using a non-linear method. Figure 4.7 was the Lineweaver-Burke plot derived from the data, each point was the average of three batches from three separate years (2010, 2011 and 2012). Each batch has been measured three times; therefore the total number of measurements is nine. The Vmax for Warrior and Viscount respectively was calculated as 0.1115 and 0.07683 respectively. The K_m of Warrior was found to be 15.58 compared to 6.798 for Viscount.

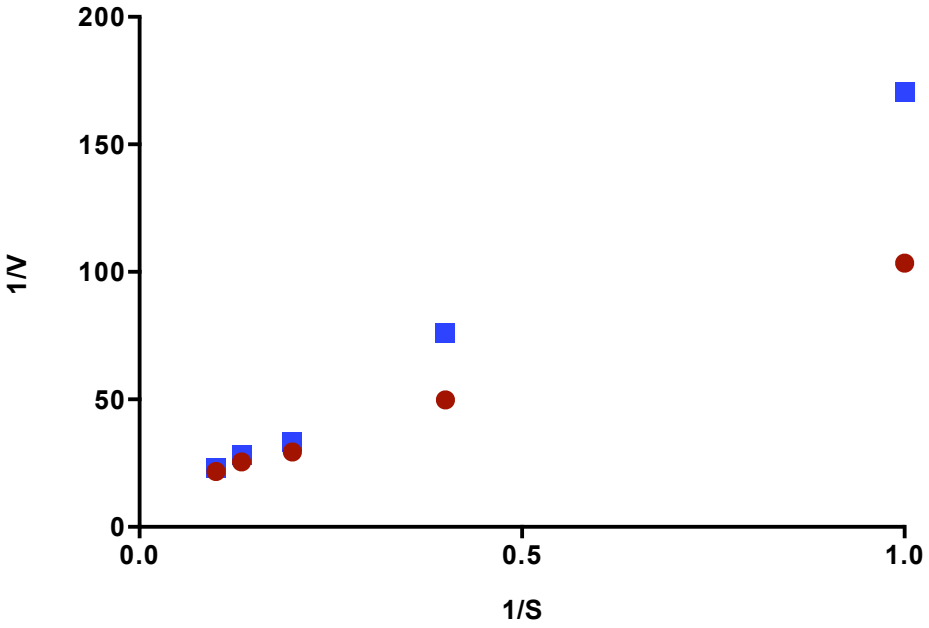

Figure 4.7 ***Enzyme kinetics of amyloglucosidase with Warrior and Viscount starch****. A concentration gradient of starch from either variety was digested with amyloglucosidase and the rate of the reaction was followed using the enzyme linked spectrophotometric assay (Chapter 2). Each point represents the initial rate of reaction of nine assays plotted against the reciprocals of substrate concentration and velocity. Warrior is in blue and Viscount is in red. (n=9).*

4.3.6 Enzymatic inhibition by Warrior starch

To investigate the effect of Warrior starch on the amylase enzymes various enzymatic assays were performed. To observe the effect of Warrior starch on enzyme activity a fixed amount of maltose (90% of amyloglucosidase Vmax) was added to a concentration gradient of starch. The samples were then digested with amyloglucosidase (EC 3.2.1.3, 5.6 Units/mL) and the generation of glucose was measured using an enzymatic assay (Chapter 2). The data gathered was used to produce a Lineweaver-Burke plot (Figure 4.8). The graph showed that the warrior starch was inhibiting the digestion of maltose into glucose, however at high Warrior starch concentrations the inhibitory effect was lost. The Vmax for Warrior and Viscount respectively was calculated as 2.139 and 0.7414 respectively. The K_m of Warrior was found to be 41.57 compared to 1.583 for Viscount.

To observe the nature of inhibition by Warrior a fixed amount of starch was added to a concentration gradient of maltose (the lowest concentration was in excess of 90% of Vmax). If inhibition was competitive then no effect should have been observed and if inhibition is non-competitive then the previous graph (Figure 4.8) should have been reproduced. The samples were digested with amyloglucosidase (EC 3.2.1.3, 5.6 Units/mL) and the generation of glucose was measured using an enzymatic assay (Chapter 2). The data gathered was used to produce a Lineweaver-Burke plot (Figure 4.9). The graph showed that adding excess maltose would remove the inhibitory effect of Warrior. The Vmax for Warrior and Viscount respectively was calculated as 0.0826 and 0.02387 respectively. The K_m of Warrior was found to be 41.83 compared to 8.997 for Viscount.

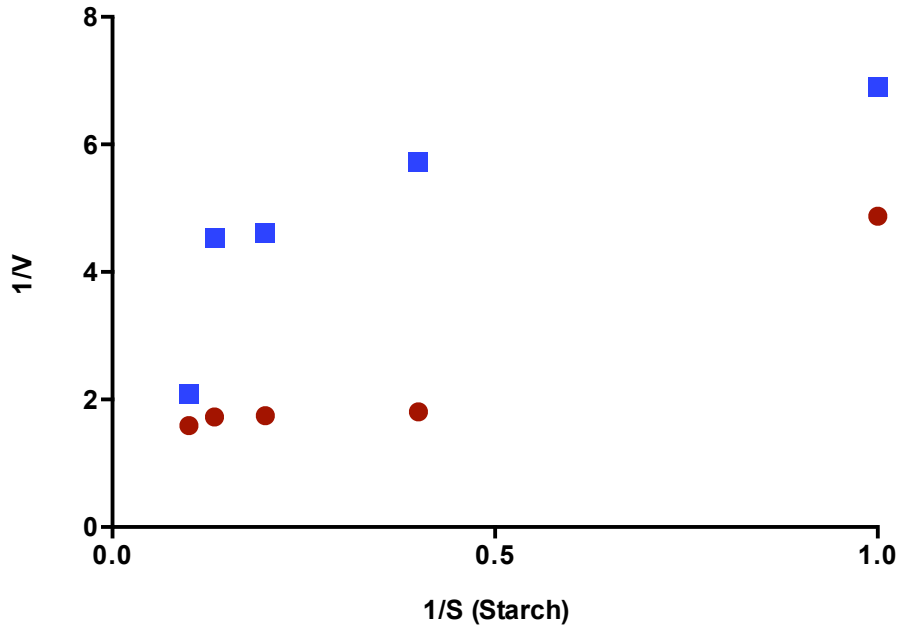

Figure 4.8 ***Lineweaver-Burke plot of starch breakdown by amyloglucosidase****. A fixed amount of maltose was added to a concentration gradient of starch from either variety. The sample was then digested with amyloglucosidase and the rate of the reaction was followed using the enzyme linked spectrophotometric assay (Chapter 2). Each point represents the initial rate of reaction plotted against the reciprocals of substrate concentration and velocity. Warrior is in blue and Viscount is in red. (n=3)*

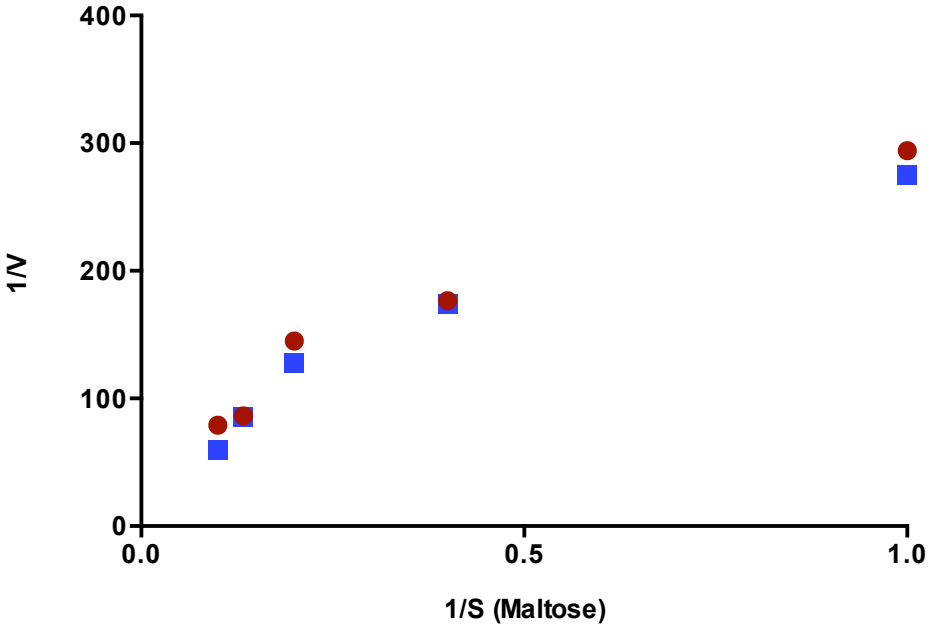

Figure 4.9 ***Lineweaver-Burke plot of maltose breakdown by amyloglucosidase****. A fixed amount of starch from either variety was added to a concentration gradient of maltose. The sample was then digested with amyloglucosidase and the rate of the reaction was followed using the enzyme linked spectrophotometric assay (Chapter 2). Each point represents the initial rate of reaction of three assays plotted against the reciprocals of substrate concentration and velocity. Warrior is in blue and Viscount is in red. (n=3)*

4.3.7 Are the coupling enzymes inhibited?

In order to definitively associate the slow rate of reaction to amyloglucosidase a control assay was carried out. In this assay different glucose concentrations was added to a fixed amount of starch (as in Figure 4.8 except maltose was replaced with glucose). If coupling enzymes were having a limiting effect then the results of Figure 4.8 would be replicated. The sample was digested with the coupling enzymes only hexokinase, (EC 2.7.1.1, 1.1 Units/mL) and glucose-6-phosphate dehydrogenase (EC 1.1.1.49, 1.5 Units/mL)) and the rate of the reaction was followed using the enzyme linked spectrophotometric assay (Chapter 2). In Figure 4.10 no differences in the rates of reaction were observed as seen by the fitted linear regressions.

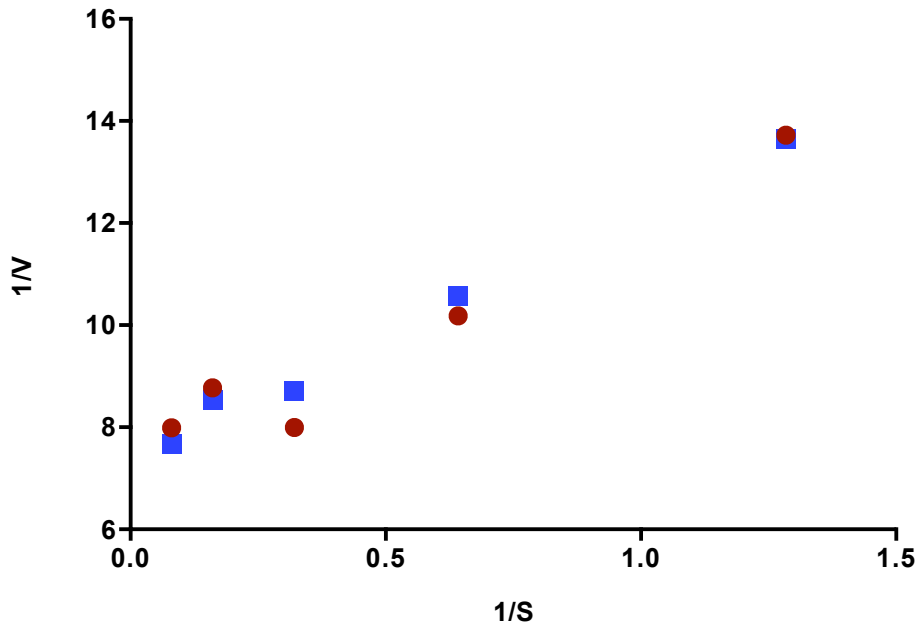

Figure 4.10 ***Enzyme kinetics of coupling enzymes with Warrior and Viscount starch****. A concentration gradient of glucose was added to a fixed amount of starch from either variety. The rate of glucose breakdown was followed using the enzyme linked spectrophotometric assay (Chapter 2). Each point represents the initial rate of reaction of three assays plotted against the reciprocals of substrate concentration and velocity. Warrior is in blue and Viscount is in red. (n=3)*

4.3.8 Is the inhibitor a soluble low MW component of starch?

To determine if a low MW soluble inhibitor was responsible for the reduction in the enzyme kinetics of amyloglucosidase, dialysis was used to separate low MW molecules from solubilised starch. Solubilised starch was dialysed with a molecular weight cut off of 12-14 kDa. Warrior or Viscount dialysate was added to the reaction mixture in the same volume ratio as the solubilised starch. The sample was digested with amyloglucosidase (EC 3.2.1.3, 5.6 Units/mL) and the rate of the reaction was followed using the enzyme linked spectrophotometric assay (Chapter 2). From these data the enzyme constants Vmax and K_m were calculated using a non-linear method. Figure 4.11 was the Lineweaver-Burke plot derived from the data collected when Warrior dialysate has been added to the reaction mixture. Likewise Figure 4.12 is derived from the data collected when Viscount dialysate has been added to the reaction mixture. Each point was the average of three batches from three separate years. Each batch has been measured three times; therefore the total number of measurements was nine.

Figure 4.11 shows the difference in amyloglucosidase kinetics (Figure 4.7) between Warrior and Viscount appears to be lost once Warrior dialysate was added to each variety. However the K_m calculated using the more accurate non-linear method is 6.072 for Warrior and 1.174 for Viscount. The calculated Vmax for Warrior is 0.04566 and 0.02353 for Viscount. Therefore the amyloglucosidase kinetics of Viscount do not appear to be affected by the added Warrior dialysate.

Figure 4.12 shows the difference in amyloglucosidase kinetics (Figure 4.7) between Warrior and Viscount was maintained when Viscount dialysate was added to each

variety. The K_m calculated using the non-linear method was 15.52 for Warrior and 8.185 for Viscount. The calculated Vmax for Warrior was 0.2257 and 0.1507 for Viscount. Therefore the amyloglucosidase kinetics of Warrior starch were not improved by adding Viscount dialysate.

To remove the effect of starch on the assay it was replaced with maltose. This would allow any effect observed to be directly attributed to the presence of the dialysate. Warrior or Viscount dialysate was added to the reaction mixture with a concentration gradient of maltose. The sample was digested with amyloglucosidase (EC 3.2.1.3, 5.6 Units/mL) and the rate of the reaction was followed using the enzyme linked spectrophotometric assay (Chapter 2). From these data the enzyme constants Vmax and K_m were calculated using a non-linear method.

Figure 4.13 shows the difference in amyloglucosidase kinetics (Figure 4.7) between Warrior dialysate and Viscount dialysate was lost in the presence of maltose. The K_m calculated using the non-linear method is 5.625 for Warrior dialysate and 4.305 for Viscount dialysate. The calculated Vmax for Warrior is 0.04240 and 0.03607 for Viscount. In the presence of maltose the warrior dialysate reduces the rate of reaction of amyloglucosidase. However the effect is slight and is not able to fully replicate the inhibition, which has been previously demonstrated (Figure 4.7).

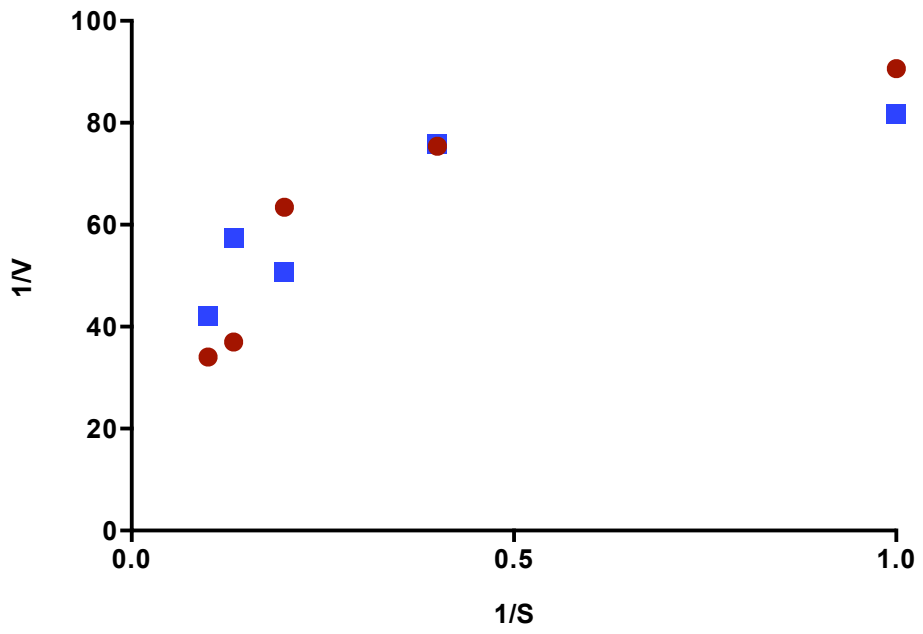

Figure 4.11 ***Enzyme kinetics of amyloglucosidase with Warrior and Viscount starch + Warrior dialysate****. . A concentration gradient of starch from each variety had a fixed amount of Warrior dialysate added. The rate of reaction was followed using the enzyme linked spectrophotometric assay (Chapter 2). Each point represents the initial rate of reaction of three assays plotted against the reciprocals of substrate concentration and velocity. Warrior is in blue and Viscount is in red.*

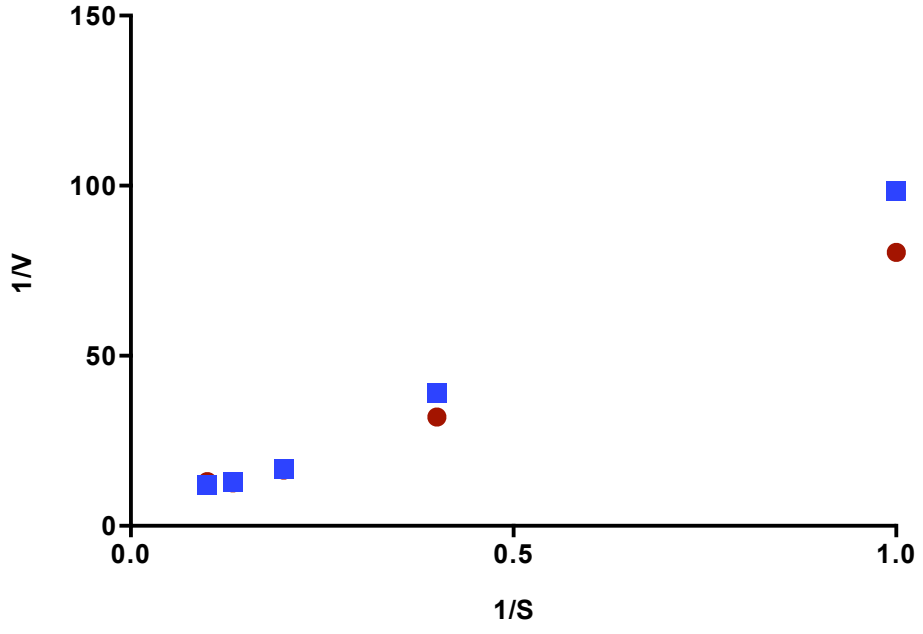

Figure 4.12 ***Enzyme kinetics of amyloglucosidase with Warrior and Viscount starch + Viscount dialysate****. A concentration gradient of starch from each variety had a fixed amount of Viscount dialysate added. The rate of reaction was followed using the enzyme linked spectrophotometric assay (Chapter 2). Each point represents the initial rate of reaction of three assays plotted against the reciprocals of substrate concentration and velocity. Warrior is in blue and Viscount is in red.*

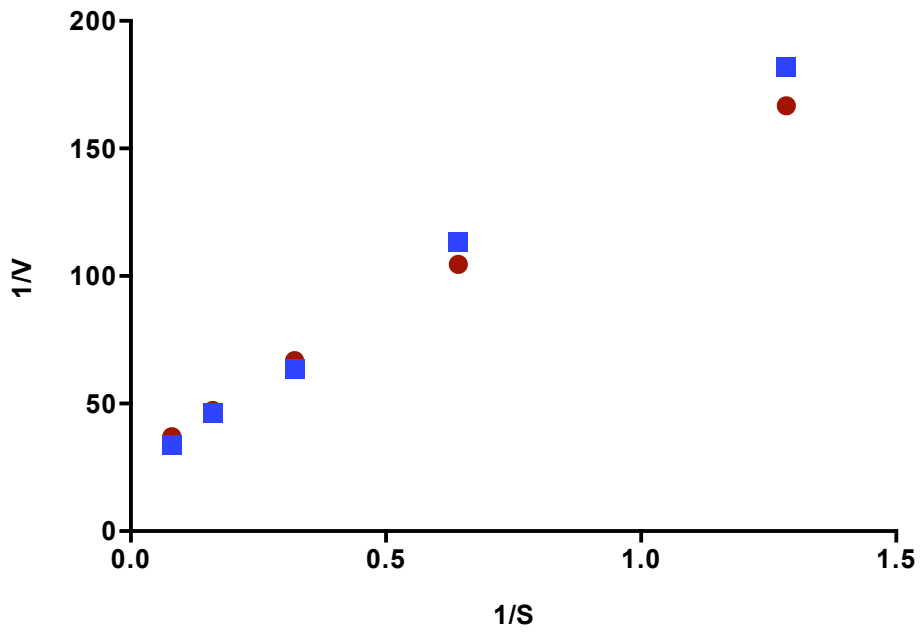

Figure 4.13 ***Enzyme kinetics of amyloglucosidase with Maltose with dialysates****. A concentration gradient of maltose had a fixed amount of warrior or Viscount dialysate added. The rate of reaction was followed using the enzyme linked spectrophotometric assay (Chapter 2). Each point represents the initial rate of reaction of three assays plotted against the reciprocals of substrate concentration and velocity. Warrior dialysate is in blue and Viscount dialysate is in red.*

4.3.9 Analysis of amyloglucosidase starch digests by Mass spectrometry

Warrior and Viscount starch solutions (1-10mg/ml), which had previously been digested with amyloglucosidase (Figure 4.7) were analysed by MALDI (Chapter 2). The mass spectra obtained (Figure 4.14) were visualised using principal component analysis (PCA), this was completed to establish if specific masses detected via MALDI could separate the two varieties. Three separate digests were analysed twice. Figure 4.15 shows the PCA plot of the centroided spectra of the 7.5mg/ml concentration used in the calculation of amyloglucosidase kinetics. The points on the plot grouped according to variety, as they could be separated based on their composition. To identify the cause of the separation observed further analyses were completed. The PCA plots of the centroided spectra of the concentrations; 1mg/ml, 2mg/ml, 5mg/ml, 10mg/ml used in the calculation of amyloglucosidase kinetics showed no separation (Appendix 9.1.1). The points on the plots did not group according to variety, as they couldn't be separated based on their composition.

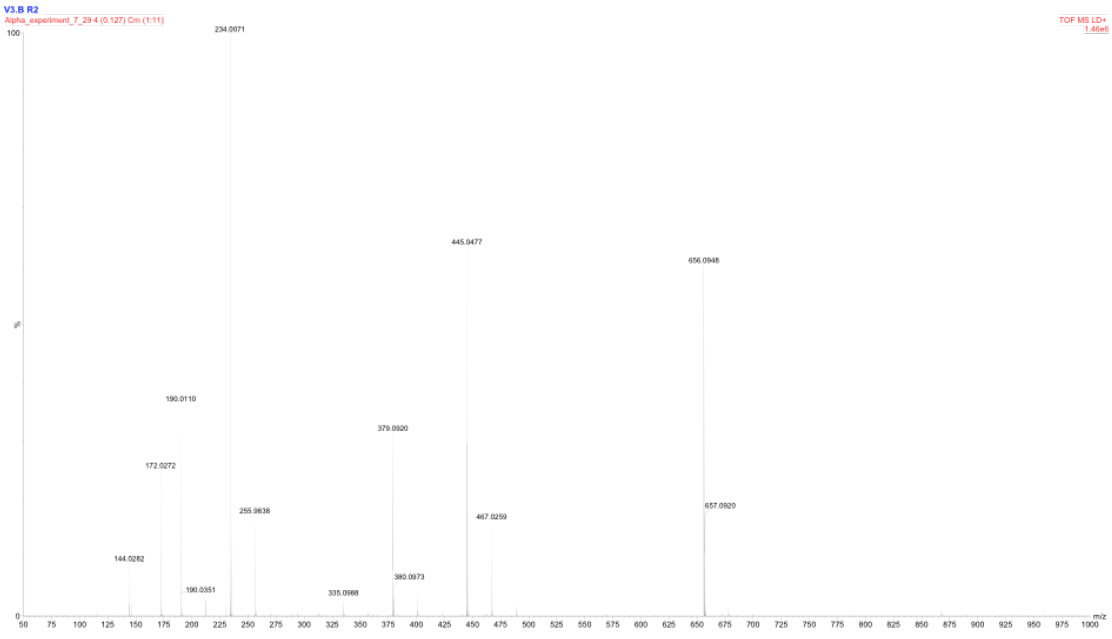

Figure 4.14 Mass spectrum of Viscount starch digested with alpha-amylase.

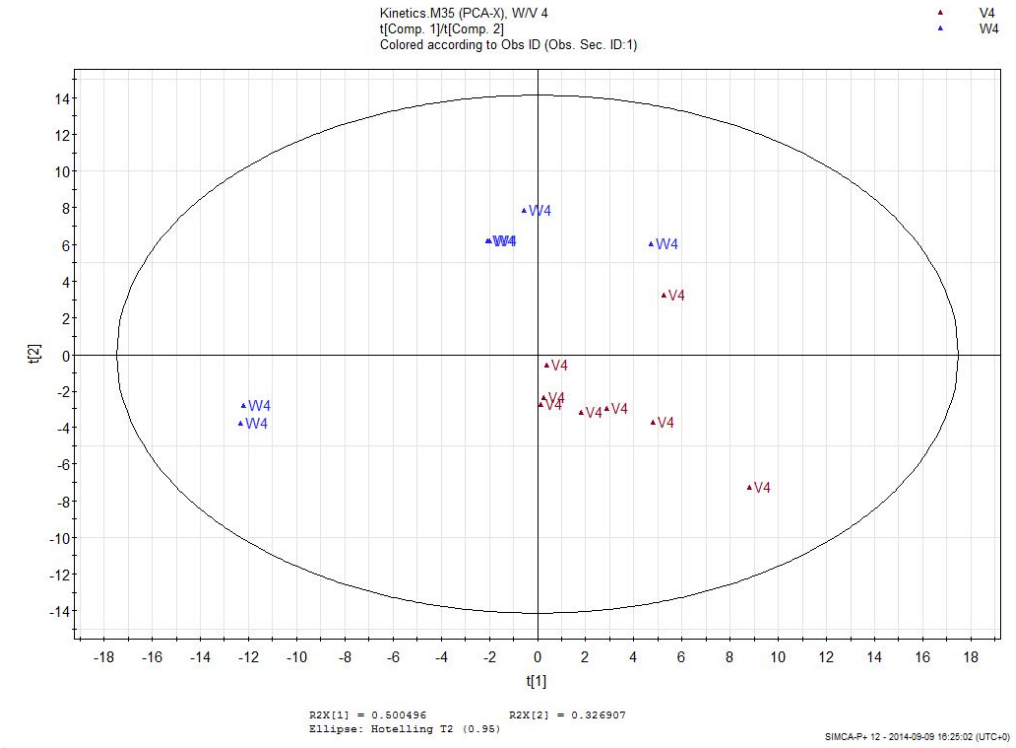

Figure 4.15 ***PCA plot of amyloglucosidase kinetics in 7.5mg/ml Warrior and Viscount starch****. Amyloglucosidase digested starch (7.5mg/ml) was analysed by MALDI. Collected spectra were centroided, and analysed by PCA. Each point represents one of two analytical replicates of one of three separate digests.*

4.3.10 Identification of outliers by partial least squares discriminant analysis (PLS-DA)

To identify masses that differed between Warrior and Viscount starch solutions, which had previously been digested with amyloglucosidase (Figure 4.7) and analysed by MALDI (Chapter 2). The data obtained which was visualised using principal component analysis (PCA) was further analysed using PLS-DA. This allowed the identification of masses, which differed between the two Varieties after the amyloglucosidase digest. The PLS-DA was completed on the PCA plot of the data from the 7.5mg/ml Warrior/Viscount starch content and masses which corresponded to the CHCA matrix were excluded from this analysis to remove sample independent variation from the analysis.

Figure 4.16 shows the PLS-DA plot of 7.5mg/ml Warrior and Viscount starch. This plot showed that the two varieties could be separated based on the intensity of different masses in the samples.

Figure 4.18 is the loadings plot for the PLS-DA plot of 7.5mg/ml Warrior and Viscount starch. The loadings plot showed the masses which cause the separation observed in Figure 4.16. The masses on the extreme right of the plot were separating Viscount from Warrior i.e. these masses were of a greater abundance in Viscount than Warrior and vice versa. The top 10 masses which separated the two varieties were then identified and listed (Figure 4.19 and Figure 4.20).

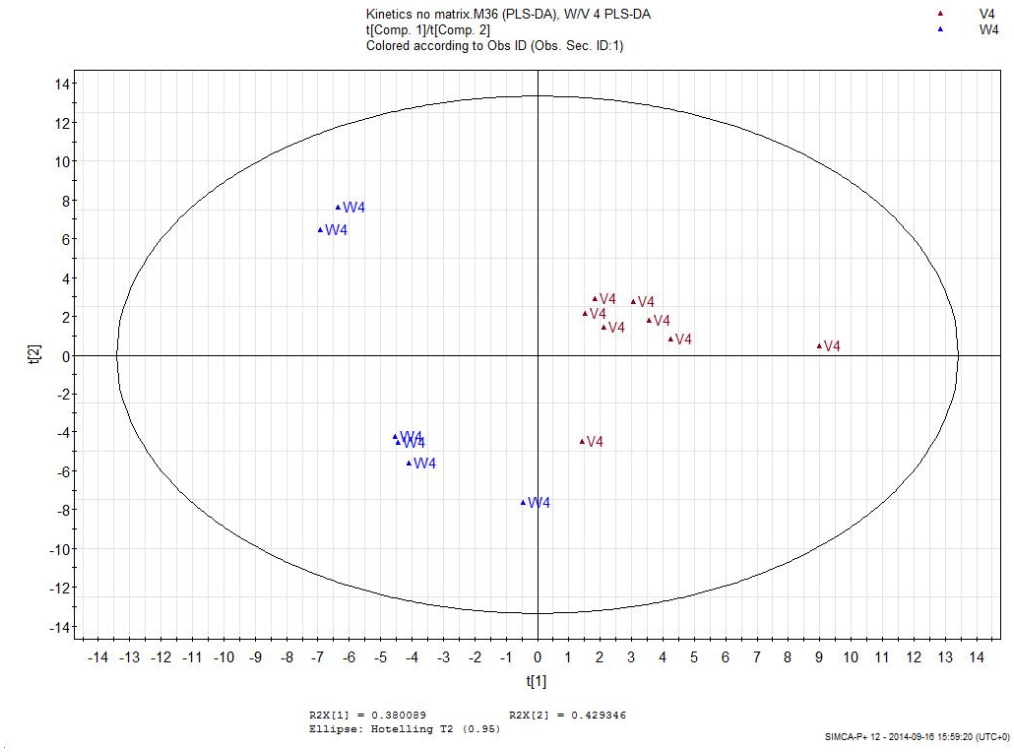

Figure 4.16 ***PLS-DA plot of amyloglucosidase kinetics in 7.5mg/ml Warrior and Viscount starch****. Amyloglucosidase digested starch (7.5mg/ml) was analysed by MALDI. Collected spectra were centroided, and analysed by PLS-DA. Each point represents one of two analytical replicates of one of three separate digests.*

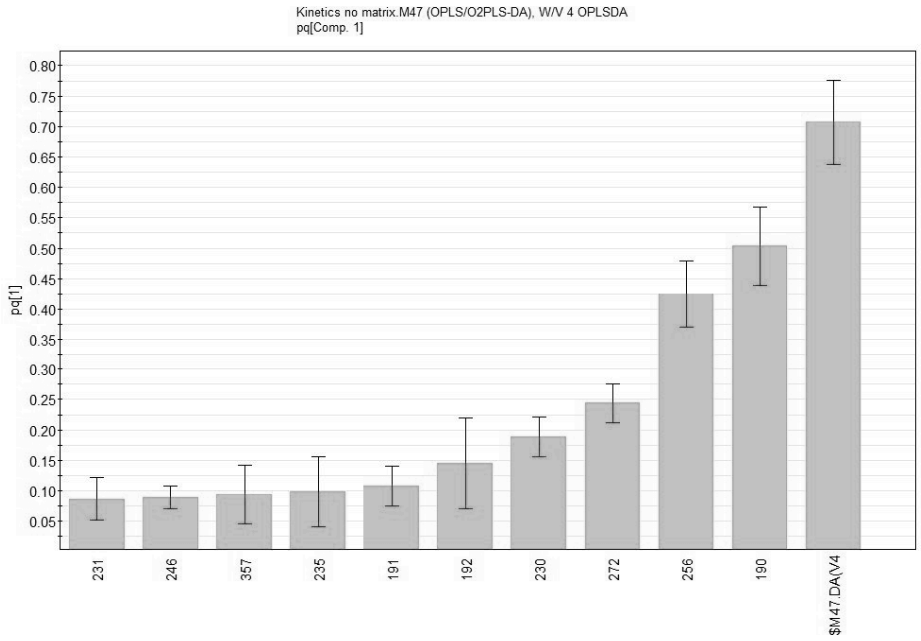

Figure 4.17 ***Loading plot of the OPLS-DA model with standard errors of Warriror amyloglucosidase digest****. Amyloglucosidase digested starch (7.5mg/ml) was analysed by MALDI. Collected spectra were centroided, and analysed by PLS-DA. Each bar represents a mass that separates Warrior from Viscount; only the ten most discriminating masses are shown.*

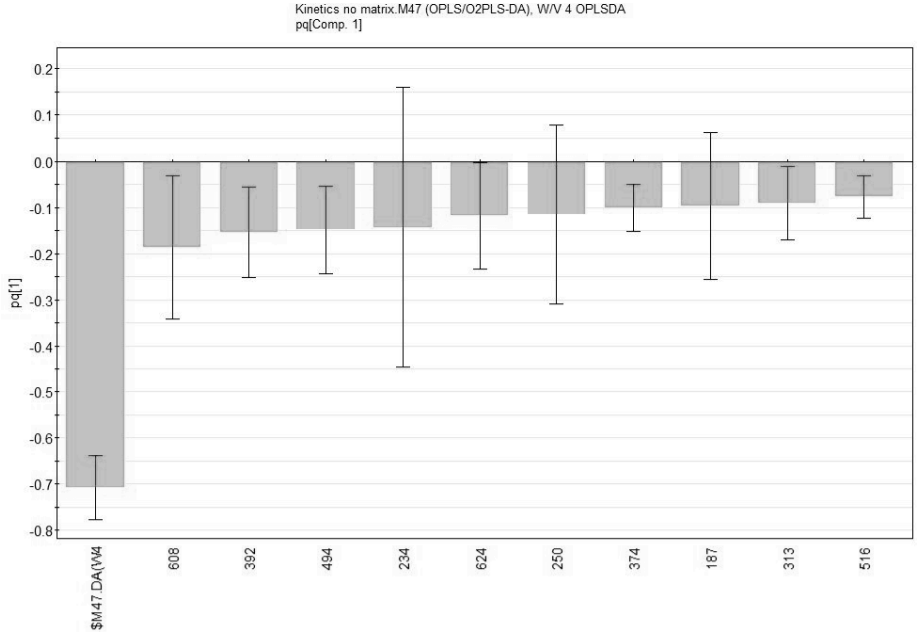

Figure 4.18 ***Loading plot of the OPLS-DA model with standard errors of Warriror amyloglucosidase digest****. Amyloglucosidase digested starch (7.5mg/ml) was analysed by MALDI. Collected spectra were centroided, and analysed by PLS-DA. Each bar represents a mass that separates Warrior from Viscount; only the ten most discriminating masses are shown.*

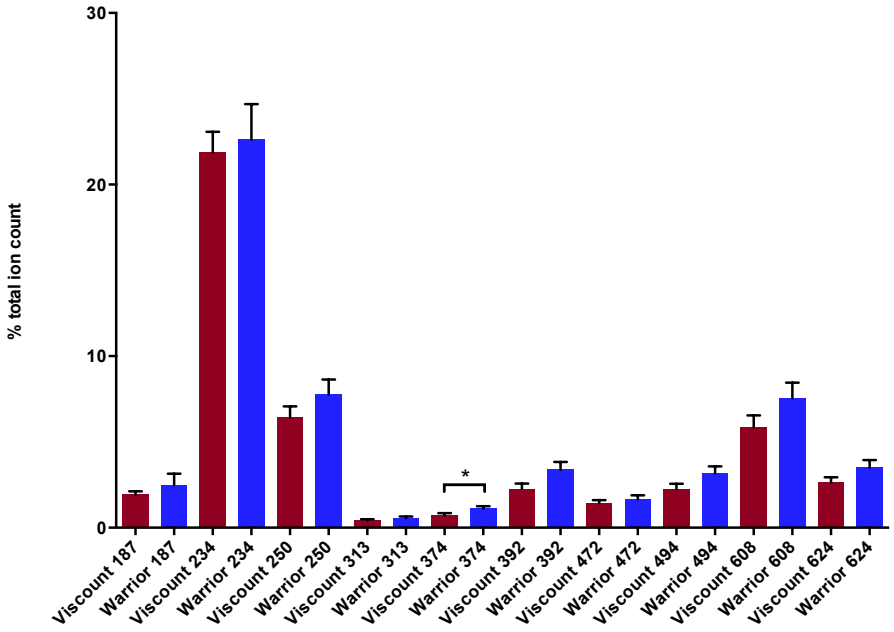

Figure 4.19 ***Comparison of masses separating with Warrior compared to Viscount****. Amyloglucosidase digested starch was analysed by MALDI. Each bar represents the average percentage total ion count of the mass of interest (x-axis), each bar is an average of two separate digests from each starch concentration, n=60.*

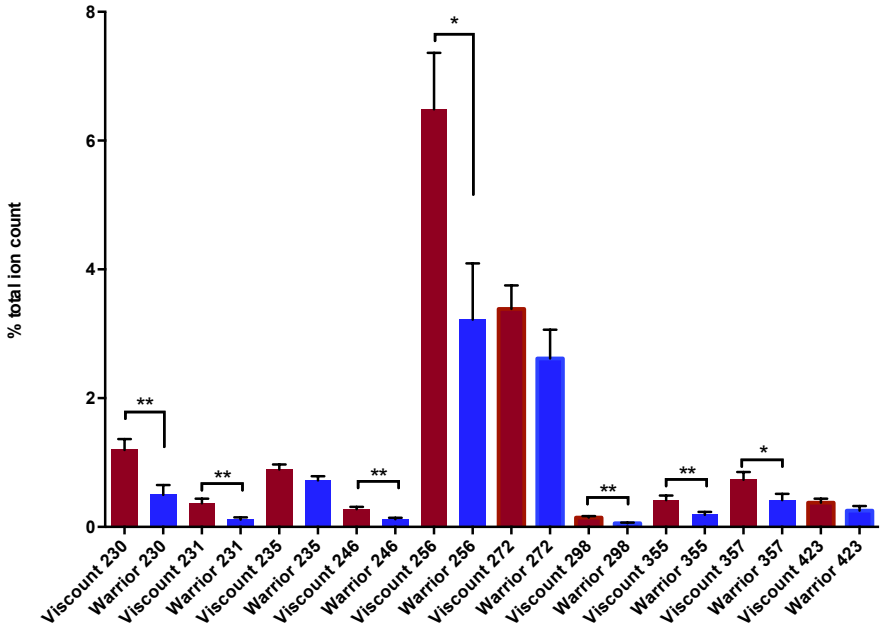

Figure 4.20 ***Comparison of masses separating with Viscount compared to Warrior****. Amyloglucosidase digested starch was analysed by MALDI. Each bar represents the average percentage total ion count of the mass of interest (x-axis), each bar is an average of two separate digests from each starch concentration, n=60.*

4.3.11 Analysis of α-amylase starch digests by Mass spectrometry

Warrior and Viscount starch solutions, digested with α-amylase (Chapter 2) were analysed by MALDI (Chapter 2). Unlike amyloglucosidase the kinetics of α-amylase activity could not be measured, as the maltase activity of α-amylase is not great enough to accurately represent the breakdown rate of starch. Therefore the digest products were analysed using MALDI. The data obtained was visualised using principal component analysis (PCA), this was completed in order to establish if specific masses detected via MALDI could separate the two varieties. Three separate digests were analysed twice.

The PCA plots of the centroided spectra of all concentrations used in the α-amylase digestion showed no separation (Appendix 9.1.2). The points on the plots did not group according to variety, as they couldn't be separated based on their composition. An example PCA plot is shown for the highest starch concentration (Figure 4.21).

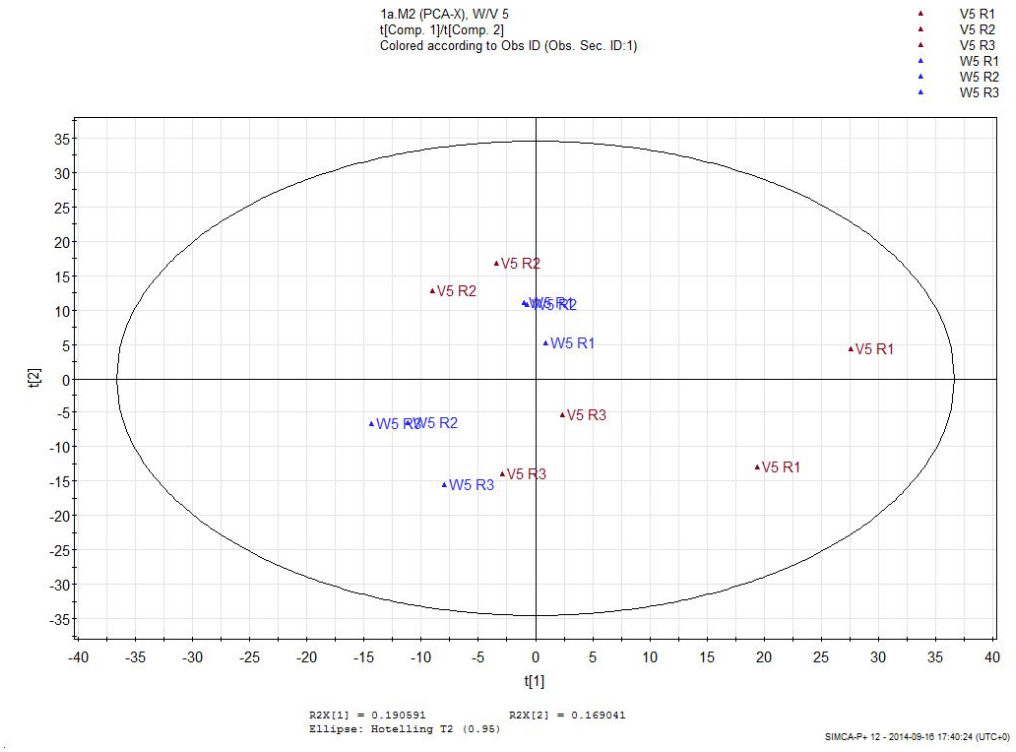

Figure 4.21 ***PCA plot of α-amylase digest in 10mg/ml Warrior and Viscount starch****. α-amylase digested starch (10mg/ml) was analysed by MALDI. Collected spectra were centroided, and analysed by PCA. Each point represents one of two analytical replicates of one separate digest.*

4.4 Discussion

The evidence outlined in this chapter showed for the first time that starch from two wheat varieties performs differently under amyloglucosidase digestion. The first hypothesis stated that total starch content in Warrior and Viscount is the same; this hypothesis must be accepted, as total starch content as measured by acid hydrolysis and enzyme hydrolysis was not different between the two varieties. The second hypothesis stated that the starch properties in Warrior and Viscount are the same. This hypothesis must be rejected as the digestion of the β-limit dextrin and the activity of amyloglucosidase on boiled starch was different in the two varieties. The third hypothesis stated that the products of starch breakdown are the same in the two varieties. This hypothesis can be rejected as differences were found in between the starch breakdown products in Warrior and Viscount.

Amylase enzymes of various biological origins have been studied extensively for their various roles in starch degradation (Sun & Henson, 1991; Planchot *et al.*, 1995; Bijttebier *et al.*, 2010). However the performance of different starches to degradation has been studied far less and comparisons have been limited to between species (Zhang *et al.*, 2013a). In the previous experiments it was shown that Warrior starch is recalcitrant to degradation by amyloglucosidase (Figure 4.6/Figure 4.7). The inhibition was removed when maltose was added to the reaction, which proved the inhibition occurred at the active site (Figure 4.9). These data indicated that the inhibition of amyloglucosidase originated from the starch itself. However from these data it was not clear whether the inhibition was caused by a structural element of starch or a soluble molecule. To separate the two potential sources of inhibition the starch was dialysed and soluble

components were removed. However there was little evidence for a soluble inhibitor since no inhibition of Viscount starch with the added soluble component from Warrior starch could be identified (Figure 4.12). Screening the breakdown products of amyloglucosidase digestion and alpha amylase digestion was also unable to identify any potential inhibitors of starch breakdown (Figure 4.19). On the basis of this, and the weight of evidence from the previous chapter it can be deduced that the organisation of starch at either a molecular or supramolecular level affects the degradation of starch by amyloglucosidase. If this can be proved to be true this would have implications in the conversion of starch to glucose for fermentation; as amyloglucosidase inhibition would reduce the yield of ethanol from Warrior starch.

Starch content is typically measured using amylase enzymes such as the widely used method of McCleary (McCleary *et al.*, 1997). However equal performance of the enzymes could not be guaranteed in either variety therefore an enzyme independent method also had to be used. Figure 4.3 shows the yield of glucose after acid hydrolysis is the same in both of the varieties. This result is complemented by the measurement of starch content by enzymatic hydrolysis, where the yield of glucose after hydrolysis with α-amylase, isoamylase and α-glucosidase was the same. Therefore it can be concluded that equal weights of extracted starch from both varieties contain the same amount of glucose. It is important to note in the context of the subsequent experiments that the functional role of α-glucosidase is very different to amyloglucosidase as α-glucosidase functions mostly to remove maltose competitive inhibition from α-amylase (Sun & Henson, 1991). This is unlike amloglucosidase which will also digest starch at comparable rates to α-amylase but also removes maltose inhibition from α-amylase (Zhang *et al.*, 2013a).

The method used to quantify glucose from all of the enzyme digests was an enzyme linked spectrophotometric method derived from the method of Bergmeyer (Bergmeyer, 1984). Other methods which exploit increasing absorbance include the phenol-sulphuric acid method (Buysse & Merckx, 1993) and the glucose oxidase/peroxidase method (McCleary & Codd, 1991). However the Bergmeyer method was chosen as it is specific for hexose sugars, therefore pectin and hemicellulose, which are both composed of pentose sugars would not affect the starch signal.

The next experiment to be completed was intended to calculate the proportion of starch before and after the branch point. β-amylase was used in the first digest and cleaved maltose units until the branch point in amylose or amylopectin. The maltose produced was measured using the enzyme linked spectrophotometric assay (Figure 4.2) the result of which was outlined in Figure 4.5. The two wheat varieties of interest produced the same amount of maltose from this digestion (unpaired t-test, n.s.), therefore it can be concluded that they have the same proportion of starch before the branch point. However the amount of glucose yielded after digestion of the remaining β-limit dextrin was not the same between the two varieties (unpaired t-test, P=0.05). Since the same amount of starch was used as substrate in the digestion and the starch has previously been shown to produce the same amount of glucose then this difference could not be due to a smaller proportion of glucose after the branch point in Warrior. The conclusion from this experiment therefore was that Warrior starch was resistant to digestion when commercial amylase enzymes are used. This conclusion was seemingly in contrast to

the measurement of starch content by amylase enzymes outlined previously (Figure 4.4) however the enzymes used was different in these experiments.

To test the hypothesis that Warrior starch inhibits enzyme activity an experiment was performed in which starch from both varieties was mixed (Figure 4.6). The result of this experiment showed that Warrior starch disproportionately reduced the yield of glucose. That meant adding only a small amount of Warrior starch was needed to reduce glucose yield; as can be seen on Figure 4.6 the relationship between proportion of warrior in the sample and glucose yield is negative and non-linear. This means adding only a small amount of Warrior starch was needed to reduce glucose yield. The conclusion from this experiment is therefore, Warrior starch inhibits enzyme activity. Interestingly the effect seen in this experiment is consistent with the guidance issued by the HGCA; Warrior reduces the efficiency of the distillation procedure even if ground Warrior is in a mixture with other flours (HGCA, 2011).

Enzymatic assays were used to measure the activity of amyloglucosidase, which is a key enzyme in the conversion of starch to glucose (Smith *et al.*, 2006). Though amyloglucosidase can degrade starch alone it is included in enzymatic digests of starch (Smith *et al.*, 2006), as it will hydrolyse maltose more efficiently than α-amylase. Therefore the addition of amyloglucosidase to starch prevents the competitive inhibition of α-amylase by maltose (Sun & Henson, 1991), though this inhibition is not particularly potent. Amyloglucosidase will also work synergistically with α-amylase to hydrolyse starch granules; when starch granules are digested with amyloglucosidase and α-amylase the granules will exhibit larger and more numerous holes on the granule

surface (SEM) compared to when digested with α-amylase alone (Sun & Henson, 1990).The first amyloglucosidase assay completed used a fixed amount of maltose (90% of maltose Vmax) with a concentration gradient of starch from each variety (Figure 4.8). By using this concentration of maltose it was concluded that the reduction in rate of absorbance increase can be attributed to inhibition of the amyloglucosidase by the warrior starch.

To further investigate the nature of the amyloglucosidase inhibition the previous experiment was reversed, in that there was a concentration gradient of maltose (in excess of 90% Vmax) with a fixed amount of starch of either variety. Figure 4.9 shows the Linewaver-Burke plot for both varieties, the fitted linear regression overlap. This shows that adding excess maltose removes the inhibitory effect; therefore amyloglucosidase must be inhibited at the active site. i.e. inhibition is not allosteric.

The enzyme constants of amyloglucosidase were then calculated using the non-linear method. The Vmax for Warrior and Viscount respectively was calculated as 0.1115 and 0.07683 respectively. This means that the substrate concentration at which Warrior starch saturates the enzyme was higher. The substrate concentration at which the reaction velocity is half-maximal is called K_m. The K_m of Warrior is 15.58 compared to 6.798 for Viscount. This means that more than double the amount of Warrior substrate was required to reach the same rate of reaction as Viscount.

As stated previously the benefit of using an enzyme linked spectrophotometric assay was that it is specific for hexose sugars. However the conclusions from previous experiments suggest that a hexose sugar of some kind could be inhibiting amyloglucosidase it would be possible for the coupling enzymes to be inhibited in some way. To control for this an experiment was completed in which different concentrations of glucose was assayed with a fixed amount of starch (Figure 4.10). There was no difference in the rate of reaction between the two varieties therefore the inhibition can be directly associated with the presence of amyloglucosidase.

Using the non-linear method to calculate amyloglucosidase enzyme constants it could be shown that the enzyme kinetics of amyloglucosidase were unaffected when the respective dialysates were added to each variety (Figure 4.11, Figure 4.12); the Warrior dialysate did not slow the rate of reaction of Viscount and the Viscount dialysate did not increase the rate of reaction of the Warrior starch. Alone (Figure 4.13) the Warrior dialysate was also unable to replicate the inhibition of amyloglucosidase with maltose.

The previous result led to the conclusion that amyloglucosidase was not inhibited by a soluble component of boiled starch. It was therefore possible that an inhibitor is generated during the digest by amyloglucosidase. To identify such an inhibitor MALDI was used to screen the digests for masses that differed between the two varieties during the amyloglucosidase digest. Masses of interest were identified from the mass spectrometric analysis of amyloglucosidase digests using PCA/OPLS-DA. However the masses identified as being more abundant in Warrior than Viscount were not statistically significant, except the mass 374. There was little convincing evidence for the 374 mass

to be an amyloglucosidase inhibitor as it did not correspond to any known amyloglucosidase inhibitors such as gentibiose, malitol and methyl alpha-D-glucoside (Fogarty & Benson, 1983; Ohnishi *et al.*, 1990; Kumar & Satyanarayana, 2009). The 374 mass was present in both samples so it would have been expected to inhibit Viscount digestion also. It was interesting to note however that the masses identified as being of higher abundance in Warrior than Viscount were generally of higher mass. Suggesting the breakdown of starch by amyloglucosidase in the Warrior samples was less advanced.

4.4.1 Conclusion

The evidence presented in this chapter strongly suggests that the organisation of starch at a molecular or supramolecular level in Warrior starch inhibits amyloglucosidase. For example a highly branched starch structure will have more α-1-6 linkages between glucose molecules. Therefore hydrolysis of a more branched starch structure would yield more isomaltose, which is a known and potent inhibitor of amyloglucosidase (Sica *et al.*, 1971; Ohnishi *et al.*, 1990). Secondly, it has been shown that amyloglucosidase action on native starch granules is limited by structural features which can be overcome by adding α-amylase (and vice-versa) (Zhang *et al.*, 2013a). And, furthermore that species to species variation in starch structure affects enzymatic degradation (Warren *et al.*, 2015). It is therefore possible that the organisation of starch a supramolecular level was sufficiently different in these two varieties to cause the phenotype observed in this chapter.

5 Does the Supramolecular structure of starch affect ethanol yield?

5.1 Introduction

The primary objective of this chapter was to determine if the supramolecular structure of starch affects ethanol yield. Therefore the fundamental properties of the starch granules in Warrior and Viscount wheat varieties were studied. Warrior and Viscount crosses were also employed in this chapter to assess the validity of any identified phenotype.

The first aim of this chapter was to measure the size of starch granules in both varieties. This aim was chosen as the weight of evidence from the previous chapter implied that the supramolecular organisation of starch in Warrior inhibited amyloglucosidase activity. Therefore the basic properties of the starch granule in both varieties needed to be measured. Iodine staining allowed the identification and measurement of starch granules; this was to ensure that only starch granules were measured (Figure 5.1). The benefit of using this approach was that it was rapid and simple to perform.

The hypothesis that the crystal properties of the starch granule inhibit saccharification is supported with previous observations stating that starch granules of various botanical origins have different digestion patterns (Planchot *et al.*, 1995). Specifically, potato starch granules have been shown to degrade more slowly compared to maize starches

when degraded with the same enzymes (Warren *et al.*, 2015). As time is a limiting factor in the saccharification step of ethanol production it is reasonable to conclude that a slower rate of granule digestion could cause lower ethanol yield.

The second aim of this chapter was to analyse the properties of the starch crystal and was completed by X-ray powder diffraction (XRD). XRD has been used to classify the crystalline structure of cereal starch granules into three types; A, B and C (Zobel, 1964), and has since been used to analyse the breakdown of starch granules by amylase enzymes. It was shown that the slow digestion of cereal starch was dependent on the A-type (size) supramolecular granules (Zhang *et al.*, 2006b). However due to the complex nature of granule structure, the initial rate of A-type granules breakdown is actually faster than the B-type granules, as suggested by a faster decrease in lamellar peak intensity (Blazek & Gilbert, 2010; Li *et al.*, 2013). Thus it has been widely documented that starch granule structure affects the rate of enzymatic degradation. It is therefore possible that a difference in granule structure alters the efficiency of amylase activity and therefore ethanol yield.

It is very important to understand the limitations of XRD in order for the results to be properly interpreted. XRD produces an image (Figure 5.11), which represents every possible crystalline orientation, unlike the Laue spots seen from single crystal diffraction. This crucial difference means that structure could not be directly inferred but the relative amounts of each crystal lattice could be calculated. Therefore the properties of the crystal structure in the crystalline regions of the starch granule were determined and compared between the varieties.

Since the purpose of this experiment was to compare the two varieties it was very important to use homogenous material. Warrior and Viscount are nationally listed commercial wheat varieties and as such are genetically uniform and stable as certified by the HGCA. To remove environmental variation all samples were kindly provided by RAGT (Cambridge) from plots grown in three different years (2010, 2011, 2012 and 2013) with the same fertiliser regime. The samples from 2013 were harvested from three separate blocks in the field. The three blocks each contained a single row of Warrior and Viscount wheat, from which samples were harvested from the beginning, middle and end of each row.

5.2 Hypotheses

1. Starch granules are smaller in Warrior starch compared to Viscount.
2. The crystal properties of Warrior starch granules prevent efficient enzymatic digestion.

5.3 Results

5.3.1 Measurement of starch granule size in Warrior and Viscount

The Feret diameter distribution of iodine stained starch granules in Warrior and Viscount wheat was measured by light microscopy (Figure 5.1). To reduce sampling error ten pictures were taken at the same magnification as a transect across the center of the slide. Starch granules were measured by their Feret diameter, which calculates the distance between two parallel tangents on opposite sides of a randomly oriented particle (Merkus, 2009). This measure is used when an irregular 3D object is in a 2D plane (Merkus, 2009). It was observed during the experiment that starch granules spread unevenly across the slide with the smaller starch granule distributed towards the edges of the slide while the larger granules remained concentrated in the middle. However by comparing the granule distribution calculated by transect and the granule distribution calculated by imaging the whole slide, the use of a transect method was shown to be accurate.

The starch granule size distribution of wheat was calculated from samples harvested in three consecutive years 2010, 2011 and 2012 (Figure 5.2/Figure 5.3) The two classes of starch granule size were plotted separately in order to visualise the data more easily. The general pattern is that Warrior has smaller and more numerous B-type starch granules (0-15μm) compared to Viscount. This pattern is not replicated with the A-type starch which encompass the 15-50μm size bracket and in several cases the Gaussian distribution line cannot be fitted to the starch granule distribution.

The B-type starch granule size distribution of Warrior and Viscount wheat was assessed from three experimental blocks in the same field, which were grown in the same year (Figure 5.4). Again, Warrior tends to have smaller and more numerous B-type granules than Viscount in block 1 and 2, consistent with the pattern observed in Figure 5.2. However, this observation does not hold true for block 3.

Figure 5.5 shows the A-type starch granule size distribution of Warrior and Viscount wheat from three experimental blocks in the same field grown in 2013. No distinct pattern could be deduced from these graphs and in several cases the Gaussian distribution line cannot be fitted to the starch granule distribution.

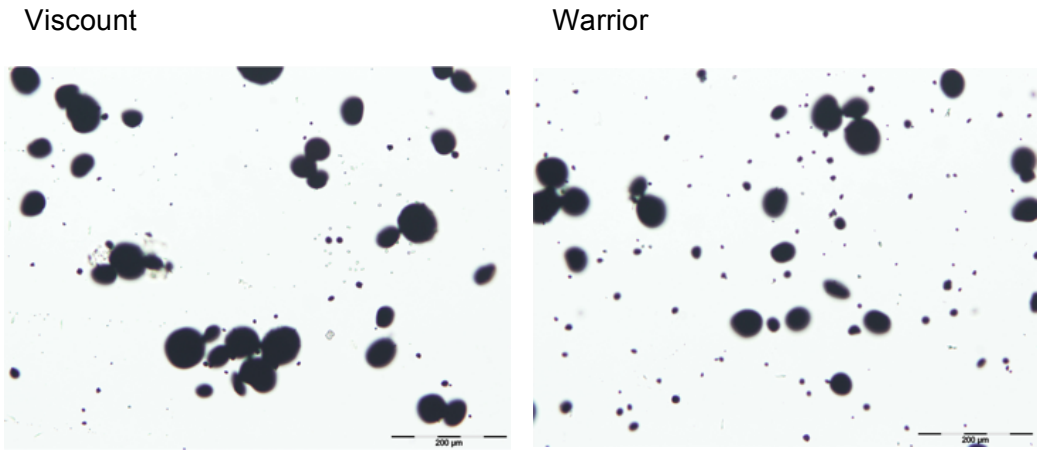

Figure 5.1. ***Warrior and Viscount starch stained with iodine.*** *Sample was prepared from purified starch as in Chapter 2. Granule ferret diameter was measured using imageJ.*

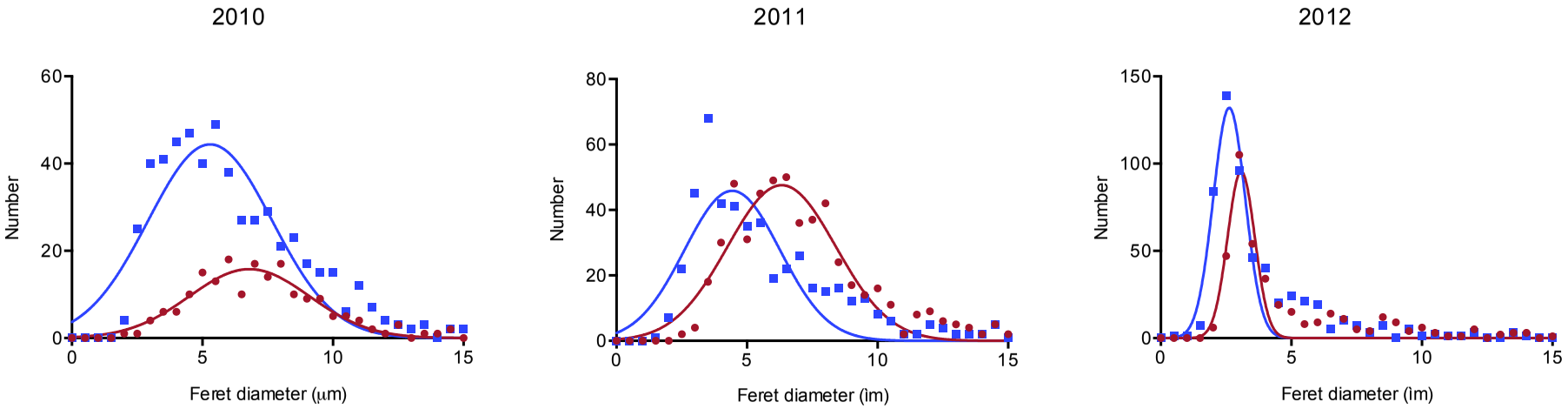

Figure 5.2 ***Feret diameter distribution of starch granules in the B granule size fraction (0-15um).*** *Starch was used from three batches of Warrior and Viscount harvested in separate years. The Gaussian distribution has been fitted to each distribution, from which the area under the curve can be calculated. Viscount is in red and Warrior is in blue (n=10).*

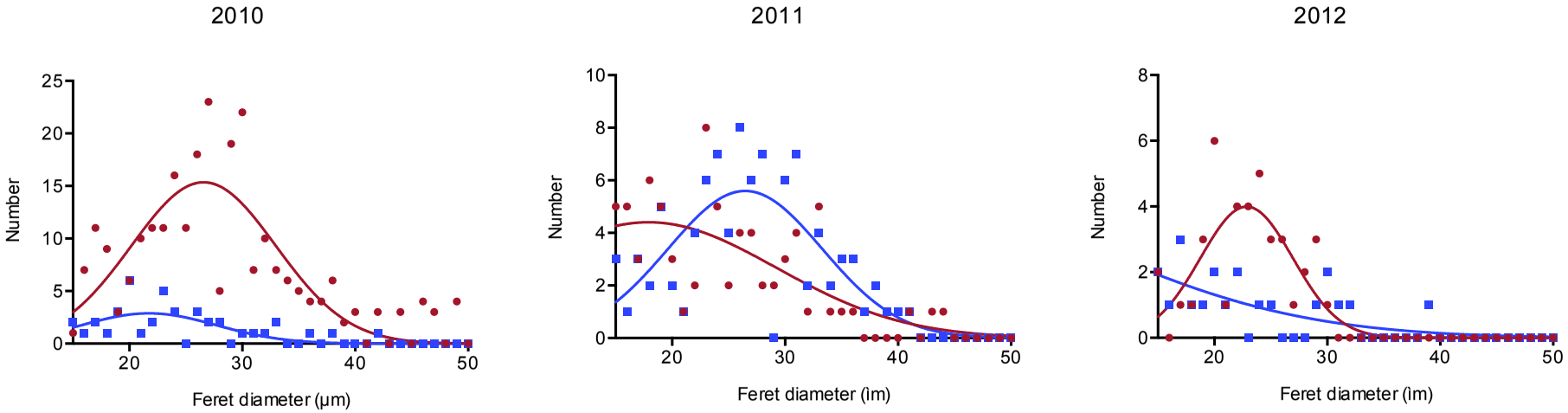

Figure 5.3. ***Feret diameter distribution of starch granules in the A granule fraction (15-50um)****. Starch was used from three batches of Warrior and Viscount harvested in separate years. The Gaussian distribution has been fitted to each distribution, from which the area under the curve can be calculated. Viscount is in red and Warrior is in blue (n=10).*

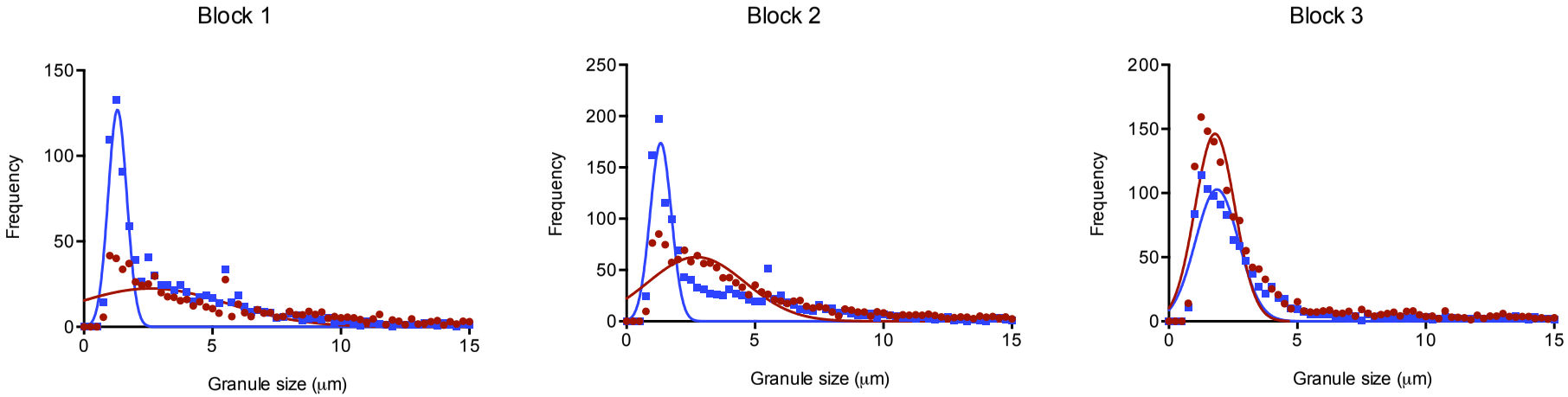

Figure 5.4 ***Feret diameter distribution of starch granules in the B granule size fraction (0-15um)****. Starch from Warrior and Viscount samples harvested in the same year (2013) was used to measure the feret diameter. Samples were harvested from the beginning, middle and end of three separate blocks .The gaussian distribution has been fitted to each distribution, from which the area under the curve can be calculated. Viscount is in red and Warrior is in blue. (n=10)*

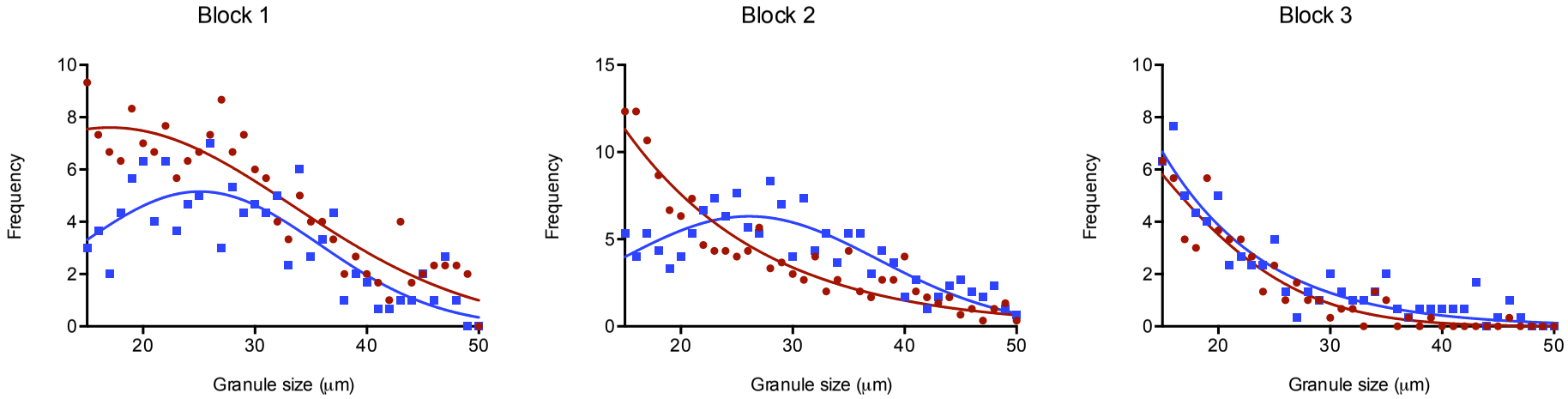

Figure 5.5. ***Feret diameter distribution of starch granules in the A granule size fraction (15-50um)****. Starch from Warrior and Viscount samples harvested in the same year (2013) was used to measure the feret diameter. Samples were harvested from the beginning, middle and end of three separate blocks . The gaussian distribution has been fitted to each distribution, from which the area under the curve can be calculated. Viscount is in red and Warrior is in blue (n=10).*

5.3.2 *Analysis of starch granule size distribution in Warrior and Viscount starch*

In order to further analyse the graphs shown in Figures 5.2-5.5 the area under the Gaussian distribution (AUC) and the Gaussian amplitude and mean was calculated. The AUC was used as a measure of the amount of each granule fraction in each graph. The amplitude and mean of the Gaussian distributions was used to quantify the distributions of B-type granules in the granule fractions.

The Tukey box plot of the area under the curve was measured for the B-type (0-15μm) starch granules from both varieties (Figure 5.6) The two varieties shared similar means and variance, and as such the two datasets were not found to be significantly different (Table 5.1, ANOVA when P=0.5). However, a significant difference was noted between the areas under the Gaussian curve when block was used as a covariable in the analysis (Table 5.1, ANOVA when P=0.5).

Figure 5.7 depicts the Tukey box plot of the area under the curve for the A-type (15-50μm) starch granules from both varieties. Similarly, the means and variance did not significantly vary between the two varieties, rendering the two datasets not statistically different (Table 5.2, ANOVA when P=0.5). It was also found that the area under the Gaussian curve exhibited a significant difference when block was used as a covariable in the analysis (Table 5.2, ANOVA when P=0.5).

The Tukey box plot of the Gaussian amplitude for the B-type (0-15μm) starch granules from both varieties is represented in Figure 5.8. Both varieties again have similar means and variance. The two datasets were found to be significantly different (Table 5.3, ANOVA when P=0.5). It was also found that there was a significant difference between the area under the Gaussian curve when block was used as a covariable in the analysis (Table 5.3, ANOVA when P=0.5), though block was a less significant variable than variety in this parameter.

Figure 5.9 shows the Tukey box plot of the Gaussian mean for the B-type (0-15μm) starch granules from both varieties. Both varieties again have similar means and variance. The two datasets were found to be significantly different (Table 5.4, ANOVA when P=0.5). It was also found that there was a significant difference between the area under the Gaussian curve when block was used as a covariable in the analysis (Table 5.4, ANOVA when P=0.5), though block was an even less significant variable than variety in this parameter.

As the Gaussian distribution could not be accurately plotted on the 15-50μm starch granules sizes, only the area under the curve could be applied to analyse those data.

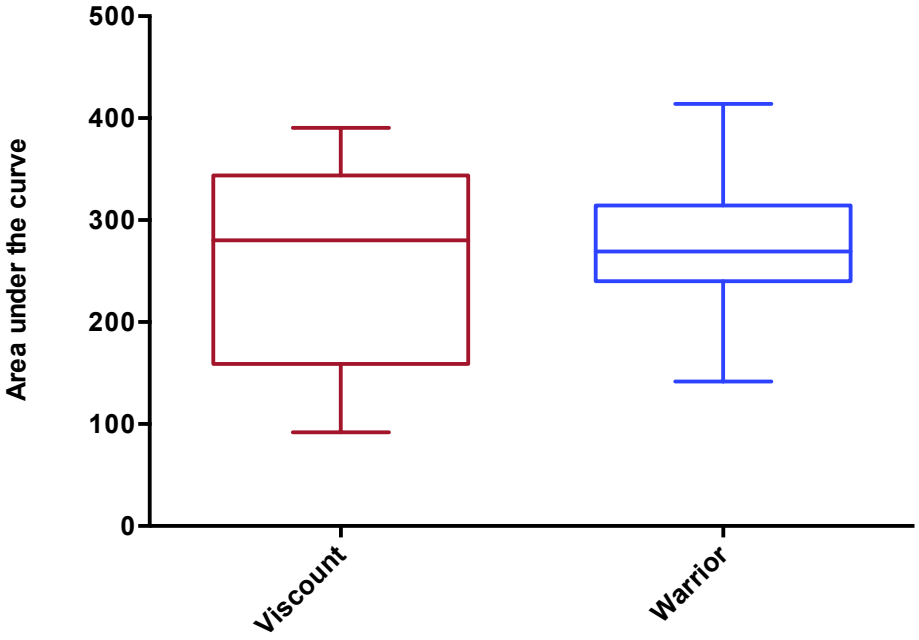

Figure 5.6. ***Tukey box plot of the area under the Gaussian distribution curve for B-type starch granules in Warrior and Viscount wheat****. The area under the Gaussian distribution curves was calculated from all years (2010, 2011, 2012 and 2013) and plotted using the Tukey method. Warrior is in blue and Viscount is in red (n=12).*

Table 5.1. ANOVA table for Area under the curve measurement curve for B-type starch granules in Warrior and Viscount wheat in all four experimental blocks. Dependant variable is log10 of the area under the curve.

Dependent Variable: Area under the curve (log10)

Source		Type III Sum of Squares	df	Mean Square	F	Sig.
Variety	Hypothesis	1756.170	1	1756.170	.174	.705
Block	Hypothesis	78380.785	3	26126.928	2.583	.228
Variety * Block	Hypothesis	30348.928	3	10116.309	3.163	.053

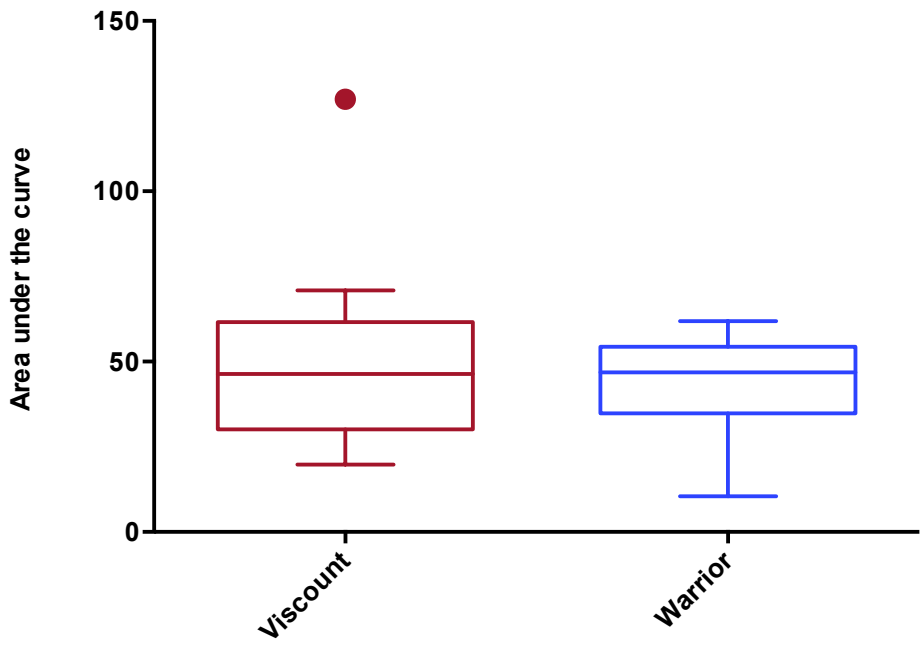

Figure 5.7. ***Tukey box plot of the area under the Gaussian distribution curve for A-type starch granules in Warrior and Viscount wheat****. The area under the Gaussian distribution curves was calculated from all years (2010, 2011, 2012 and 2013) and plotted using the Tukey method. Warrior is in blue and Viscount is in red (n=12).*

Table 5.2. ANOVA table for Area under the curve measurement curve for A-type starch granules in Warrior and Viscount wheat in all four experimental blocks. Dependant variable is the area under the curve.

Dependent Variable: Area under the curve (log10)

Source		Type III Sum of Squares	df	Mean Square	F	Sig.
Variety	Hypothesis	394.065	1	394.065	.672	.472
Block	Hypothesis	1809.845	3	603.282	1.028	.491
Variety * Block	Hypothesis	1759.738	3	586.579	1.184	.347

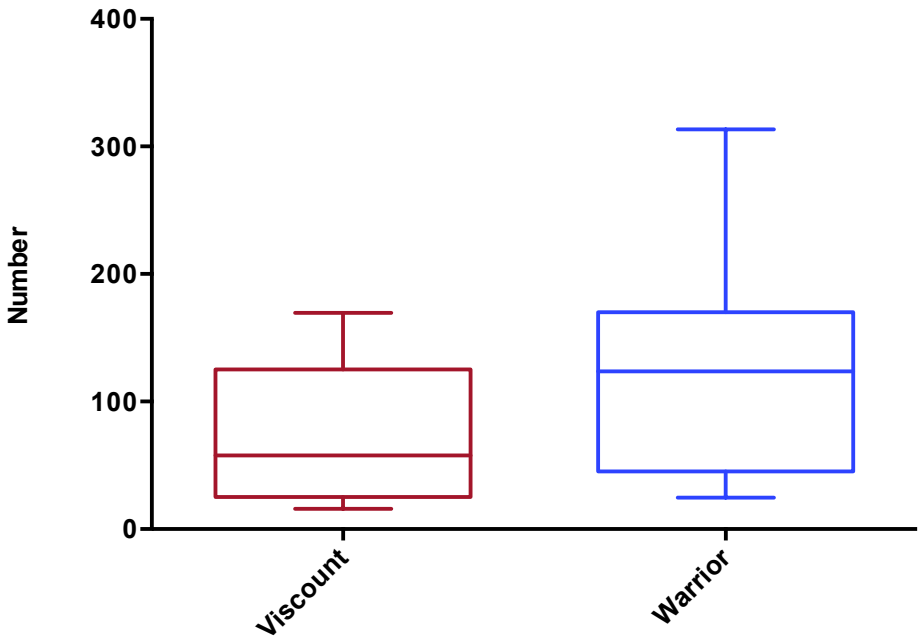

Figure 5.8. ***Tukey box plot of the Gaussian amplitude for B-type starch granules in Warrior and Viscount wheat****. The Gaussian curve amplitude was calculated from all years (2010, 2011, 2012 and 2013) and plotted using the Tukey method. Warrior is in blue and Viscount is in red. (n=12)*

Table 5.3. ANOVA table for Gaussian curve amplitude for B-type starch granules in Warrior and Viscount wheat in all four experimental blocks. Dependant variable is the Gaussian amplitude.

Dependent Variable: Gaussian amplitude

Source	Type III Sum of Squares	df	Mean Square	F	Sig.
Variety	17349.428	1	17349.428	3.830	.068
Block	22793.812	3	7597.937	1.677	.212
Variety * Block	27960.502	3	9320.167	2.057	.146

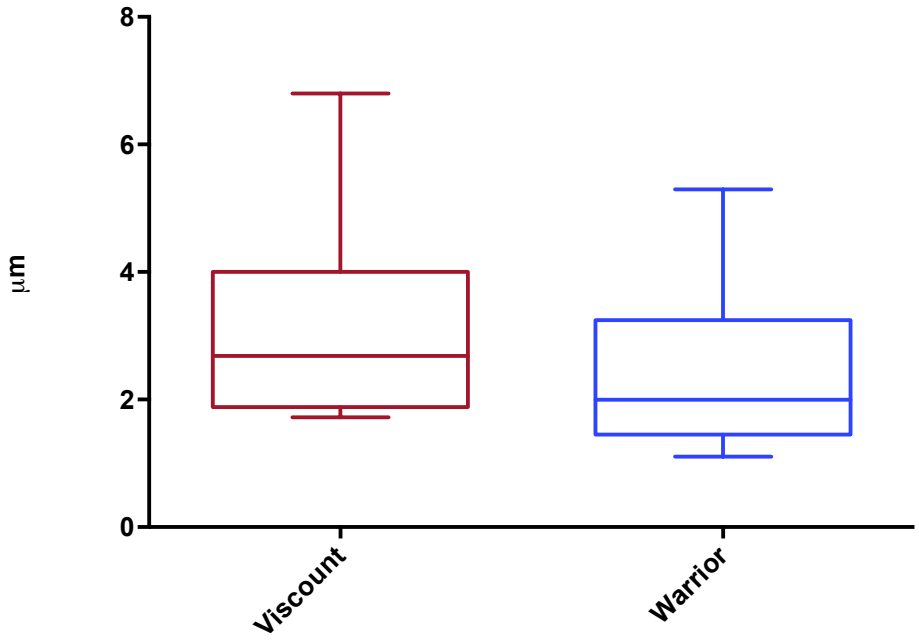

Figure 5.9. ***Tukey box plot of the Gaussian mean for B-type starch granules in Warrior and Viscount wheat****. The Gaussian curve mean was calculated from all years (2010, 2011, 2012 and 2013) and plotted using the Tukey method. Warrior is in blue and Viscount is in red (n=12).*

Table 5.4. ANOVA table for Gaussian curve mean for B-type starch granules in Warrior and Viscount wheat in all four experimental blocks. Dependant variable is the Gaussian mean.

Dependent Variable: Gaussian mean

Source	Type III Sum of Squares	df	Mean Square	F	Sig.
Variety	3.664	1	3.664	3.280	.089
Block	31.018	3	10.339	9.258	.001
Variety * Block	3.055	3	1.018	.912	.457

5.3.3 The relationship between B granule mean size and ethanol yield in Warrior x Viscount crosses

To investigate the relationship between granule size and variety the B-granule Gaussian mean was measured in twelve Warrior and Viscount crosses produced by single seed descent. These crosses were grown with and harvested identically to the Warrior and Viscount samples used previously, with the exception that the crosses were not grown in replicate blocks. The ethanol yield of the crosses analysed has been provided by RAGT and was originally calculated by the Scottish Whiskey research institute (Bringhurst *et al.*, 1996) and correlated to the Gaussian mean. Ethanol yield displayed a significant correlation with mean B-granule size where R^2=0.3472 and P=0.0438 (F test) (Figure 5.10).

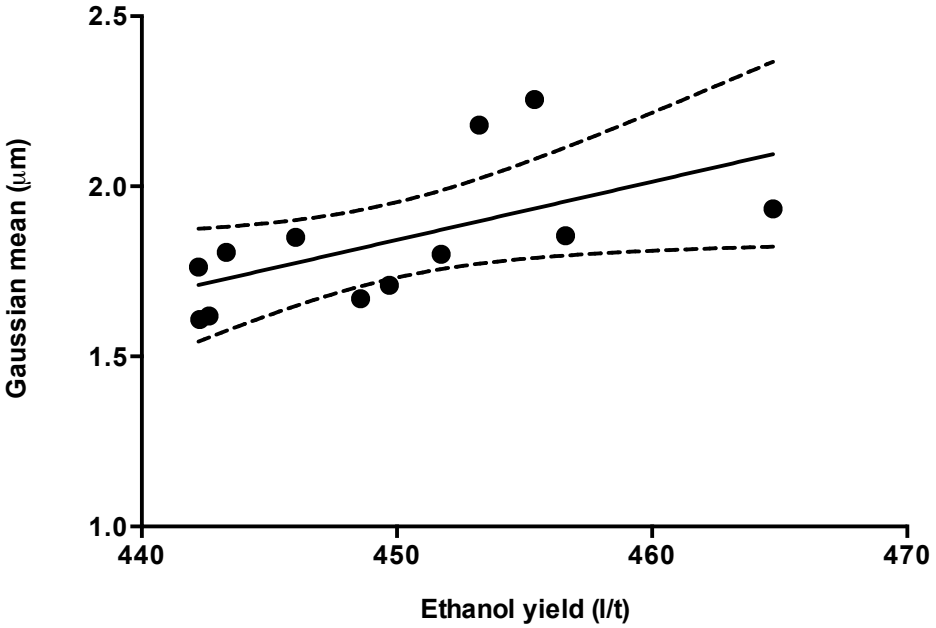

Figure 5.10. ***Correlation between Gaussian mean and ethanol yield in Warrior x Viscount crosses****. As previously, the Gaussian mean of starch granules from Warrior x Viscount crosses was measured and has been plotted against ethanol yield. The line is the linear regression with the 95% confidence interval fitted.* R^2*=0.3473, n=10.*

5.3.4 Analysis of B-granule structure by X-ray crystallography

It was previously demonstrated that B-type starch granules were smaller and occurred in greater quantity in Warrior starch; furthermore this phenotype was associated with a reduced ethanol yield. It is therefore possible that differing granule properties are responsible for the observed correlation. In order to identify any differences in starch granule crystal arrangement x-ray crystallography was used to produce powder diffraction patterns (Figure 5.11). The powder diffraction patterns were then analysed to characterise the crystal properties of the B-starch granule. The parameter analysed represented the diffraction angle of the crystal lattice. The radial profile of the Warrior and Viscount average X-ray diffraction patterns is shown in Figure 5.12. The powder diffraction patterns are typical A-type diffraction patterns that are characteristic of cereal starch (Buléon *et al.*, 1998). Some differences between the two varieties can be seen in the peaks when the diffraction angle is between 19 and 22 degrees (Figure 5.12), the peak in this range is at 20.0 and 21.0 degrees. When the diffraction angle ranges between 17 and 19 degrees (Figure 5.12), the peak is at 17.9 degrees. In all cases the Viscount peak normalised intensity is higher than the Warrior normalised intensity. The plotted standard error of the means for both varieties still overlap slightly, indicating that the difference is small but reproducible.

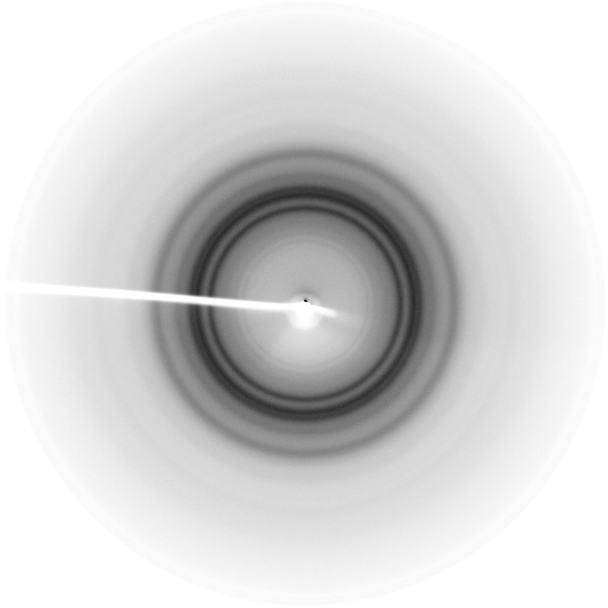

Figure 5.11 ***Powder diffraction pattern of starch granules****. The series of rings represents different crystal lattices with different diffraction angles. The absolute intensity of each ring cannot be compared directly between samples but the relative intensities can be directly compared.*

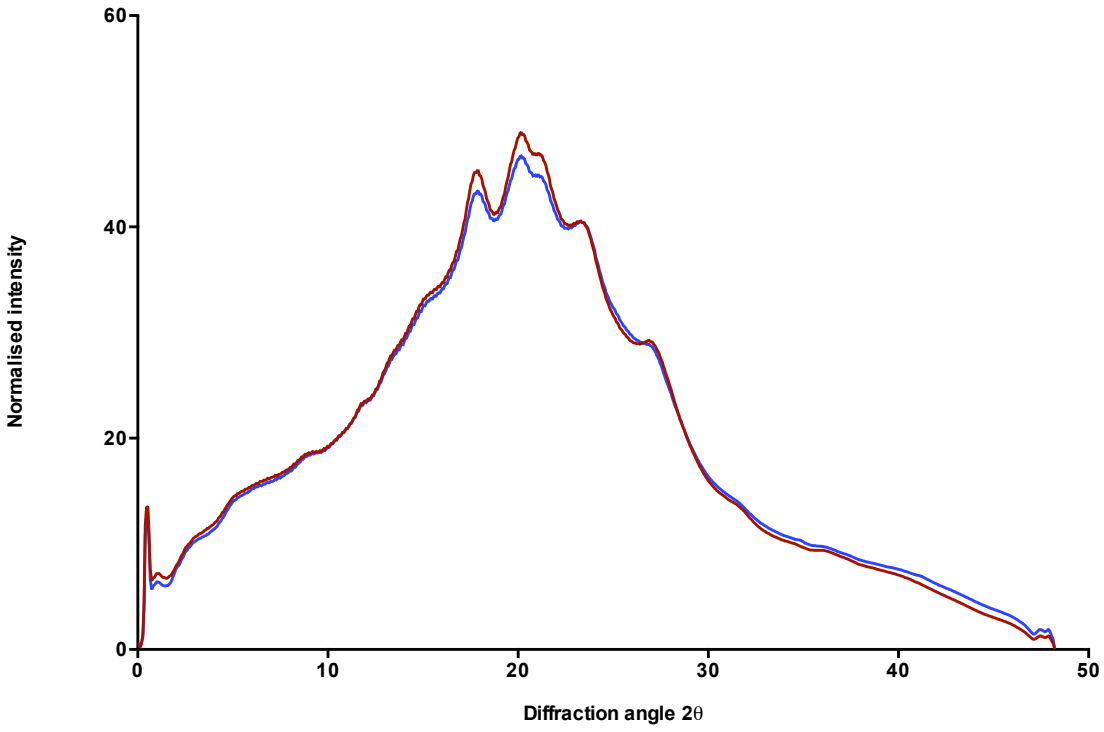

Figure 5.12. ***X-ray powder diffraction pattern of Warrior and Viscount starch B-granules****. Warrior and Viscount B-granules were isolated from purified starch and subjected to X-ray powder diffraction analysis. Collected diffraction patterns were analysed by radial profiling. Images were normalised against the centre of the image. Warrior is in blue and Viscount is in red (n=4).*

5.4 Discussion

The evidence outlined in this chapter shows that the crystal properties of the B-granules are different in both varieties. Furthermore, the B-type granules are more numerous in the Warrior variety. This implies that starch structure in the B-granules is different, a conclusion which offers an explanation for the data gathered in the previous chapter.

The first hypothesis stated that starch granules are the same size in Warrior and Viscount starch. It was shown that B-type starch granules are smaller and more numerous and the amount of starch (as calculated in Figure 5.6) remains the same. Therefore the hypothesis can be rejected. The second hypothesis stated that the crystal properties of the granule are different in Warrior and Viscount. There was evidence to support this hypothesis as differences could be found in the radial intensity of the powder diffraction rings between the two varieties.

It has been shown in this chapter that small B-granule size is correlated with low ethanol yield. This inference is supported by measurement of the starch granule distribution in Warrior and Viscount starch as well as in Warrior and Viscount crosses. The physicochemical properties of A and B type starch granules have been extensively studied by others which allows conclusions to be drawn from the evidence. One hypothesis that could be drawn from the data is that the B-type granules are more resistant to gelatinisation and therefore are less amenable to amylase digestion. However, though B-type starch granules have been shown to have higher gelatinisation temperatures than A-type granules (Zeng *et al.*, 2011; Li *et al.*, 2013) this difference is

Figure 5.13. ***Effect of waterlogging on wheat germination and growth.*** *The panel on the left shows a plot in a section of the field that was not subject to waterlogging. The panel on the right shows a plot in a section of the field that was waterlogged*

not consistent and the opposite phenotype has been observed in some cases (Ao & Jane, 2007). The differences in amylase hydrolysis rates between large and small granules are much more strongly influenced by the absence of pores and channels in the B-granule which prevent efficient degradation (Kim & Huber, 2008; Salman *et al.*, 2009; Blazek & Gilbert, 2010). It is therefore apparent that the observed difference in ethanol yield cannot be explained by a difference in the size of B-type starch granules.

The evidence illustrated in Figure 5.4 and Figure 5.5 showed that starch granule size distribution in wheat harvested from block 3 did not replicate the pattern seen in previous blocks and years. This difference was found to be statistically significant as block was found to be a significant co-variable in the ANOVA analysis. On the basis of this evidence the conclusion that starch granule size is different in the two varieties could not be supported. However block 3 experienced dramatic environmental stress. This was

because block 3 lay at the lowest point in the plot, which was waterlogged for long periods. This manifested as a very low germination rate in the wheat planted in this plot (Figure 5.13). As the environmental conditions in this block varied considerably from the other two blocks it was removed from the statistical analysis.

The difference initially observed was that the B-type starch granules in Warrior were smaller. As the balance of evidence does not support starch granule size affecting ethanol yield it is possible that the molecular structure of starch is responsible for the low ethanol yield phenotype. The highest level of molecular starch organization is the crystal lattice structure of amylopectin. To analyse this property X-ray powder diffraction was used: X-ray diffraction produces an image which represents every possible crystalline orientation (including amylose-lipid complexes). The relative amounts of each crystal lattice could then be calculated, and the properties of the crystal structure were compared between the varieties.

The powder diffraction rings were analysed for the radial profile of intensity at diffraction angles between 3 and 50 degrees. The diffraction pattern for both varieties yielded the classic A-type crystal pattern which is seen in all cereal starches (Buléon *et al.*, 1998) and specifically in B-type starch granules (Zhang *et al.*, 2013b). Small differences in the normalized intensity at certain diffraction angles were observed (Figure 5.12), such that the peak at 17.9, 20.0 and 21.0 degrees is higher in Viscount than Warrior. Since the intensity has been normalised it can be concluded that the contribution of a starch crystal lattice with these diffraction angles is greater in Viscount than Warrior. The crystal lattices in either variety therefore do not contribute uniformly to the starch structure.

5.4.1 Conclusion

It has been previously shown that A-type crystal structure of cereal crops such as wheat is responsible for the slow digestion property of starch (Zhang *et al.*, 2006a) this is in contrast to other crop species with B-type crystallinity such as potato where other structural features such as pore size are more important in determining the rate of digestion (Cai & Shi, 2014). It therefore seems likely that a difference in A-type crystalline structure would affect enzyme activity during saccharification. This is reasonable as A-type crystalline starch has been shown to be important in determining the rate of starch breakdown (Zhang *et al.*, 2006b). Starch synthesis and granule crystallinity is effected and controlled by starch synthase enzymes (Tetlow, 2010). Perturbation of these enzymes during B-granule synthesis (which occurs at a later time than A-granule synthesis (Yin *et al.*, 2012)) would result in a change in the molecular structure of starch, it could also produce the disparity in starch granule size.

6 Is the fine structure of Warrior and Viscount starch different?

6.1 Introduction

The aim of the research in this chapter was to determine if the fine structure of Warrior and Viscount starch was different.

In the previous chapter it was shown by X-ray diffraction that the fundamental structure of the starch is different in the two varieties. It is important to note that the difference was not in the diffraction pattern (e.g. type A/B/C (Zobel, 1964)) but in the relative contribution of the crystal lamella to the powder diffraction pattern. This means that granules possess the same types of crystal lamellae but in different proportions. It has been shown that the branch chain length is an important determinant of X-ray diffraction patterns. A chains with a degree of polymerization of between 6-12 units define the A-type diffraction pattern (Hizukuri *et al.*, 1983; Hizukuri, 1985; Jenkins & Donald, 1995). Therefore it is likely that the chain length in Warrior and Viscount is different. There is also evidence that the digestion rate of starch is affected by amylopectin fine structure. Ao *et al.*, 2007 have shown that reducing the chain length of starch will increase its resistance to enzymatic degradation. This has been complemented by further work, which suggested that the short branches need to be more highly branched to be recalcitrant to enzymatic degradation [168]. Therefore it was essential to investigate if the starch fine structure was different in Warrior and Viscount. As this would explain the disparity in crystal structure seen by x-ray diffraction and the reduced activity of amyloglucosidase (Chapter 4).

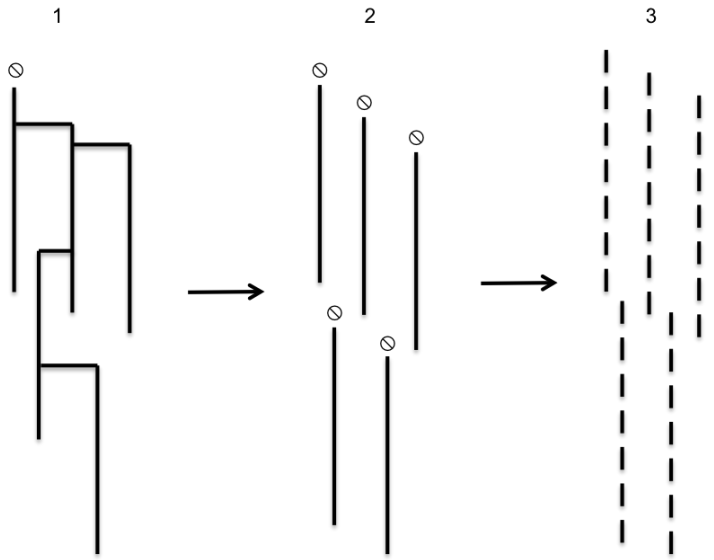

Figure 6.1 ***Starch de-branching method schematic.*** *1 indicates boiled, undigested amylopectin. 2 represents amylopectin treated with isoamylase. This fraction is referred to as "De-branched" in the results section. 3 is the final fraction of de-branched amylopectin which has been treated with β-amylase to depolymerise the oligosaccharides to maltose. This fraction is referred to as "Depolymerised" in the results section. Non-reducing ends are shown with ⊘.*

As shown in Figure 6.1 the approach taken was to de-branch boiled starch with isoamylase (EC 3.2.1.68) and remove a portion, which is subsequently depolymerised with β-amylase (EC 3.2.1.2). The molar concentration of the oligosaccharides produced after de-branching can be used to measure the number of branches. Similarly, the molar concentration of maltose produced after depolymerising is a measure of the amount of maltose in those branches. Therefore both measurements can then be used to approximately calculate the branch chain length.

To quantify the number of oligosaccharides produced after de-branching and maltose produced after depolymerisation, a reducing sugars test was used. The method used was the modified Nelson-Somogyi method (Smogyi, 1952). This method was chosen as it has been shown to the most accurate method (Deng & Tabatabai, 1994) with the

appropriate sensitivity for the expected concentrations of glucose. As a reducing sugars test the ratio of reducing sugars to oligosaccharides (produced after the isoamylase digest) would be 1:1, as each oligosaccharide would only have one reducing end.

The major issue identified in the de-branching experiment was the possibility that β-amylase was inhibited in the depolymerisation step of the experiment. To ensure that this was not an issue an experiment was conducted in which wheat starch was combined in series with control potato starch and digested. The assumption with the control experiment was that if Warrior starch inhibited the β-amylase then a small amount of Warrior starch would disproportionately decrease the reducing sugars yield.

To directly measure the length of the branches produced after the de-branching step electrospray ionisation mass spectrometry (ESI-MS) was used. The benefit of using this technique is that differences in the oligosaccharide produced during digestion would be detected. ESI-MS works by spraying a diluted solution containing the analytes through a needle from a capillary, the needle is charged which allows the generation of singly or multiply charged ions. The droplets evaporate and the analytes of interest are then drawn into the mass spectrometer and detected (Kailemia *et al.*, 2014).

6.2 Hypotheses

1. The fine architecture of starch in Warrior and Viscount is different
2. The average maltooligosaccharide chain length is shorter in Warrior than Viscount

6.3 Results

6.3.1 Glucose determination by Nelson-Somogyi

The Nelson-Somogyi method was used to calculate the amount of reducing sugars in the samples. To do this a glucose calibration curve was generated (Figure 6.2). The selected range was based on the amounts of reducing sugars expected in the experimental samples. The calibration curve is accurate as the standard deviation of each point is very low and the R^2=0.9825. However the X intercept of the calibration curve does not intercept Y at 0.

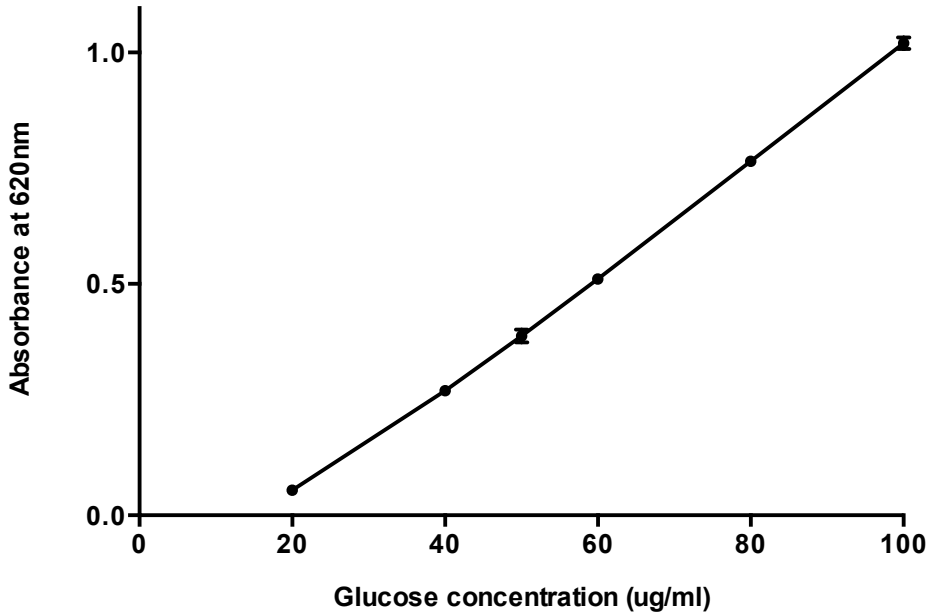

Figure 6.2. ***Glucose calibration curve using the Nelson-Somogyi method.*** *A standard curve of 20-100 µg/ml of glucose was prepared as a solution in dH_2O. Each solution was then used as substrate in the Nelson-Somogyi assay and the absorbance at 620nm was measured 2. Curves were fitted with a third order polynomial and the error is standard error of the mean (n=3).*

6.3.2 Branch measurement of Warrior and Viscount starch

The branch lengths of the two wheat varieties were determined by digesting 10mg of starch with isoamylase (EC 3.2.1.68, 5 units) a subsample was taken and digested with β-amylase (EC 3.2.1.2, 1 unit) to depolymerise the oligosaccharides. Reducing ends were then measured using the Nelson-Somogyi method (Smogyi, 1952).

Figure 6.3 shows the concentration of reducing ends in the de-branched starch sample. The concentration of reducing ends after isoamylase digestion is the same (unpaired t-test, when P=0.5). Therefore the amount of oligosaccharides in the experimental samples after digestion is the same in both varieties.

Figure 6.4 shows the concentration of reducing ends in the depolymerised starch sample. The concentration of reducing ends after Isoamylase digestion and β-amylase digest is significantly different (unpaired t-test, when P=0.05). Therefore the amount of maltose in the experimental samples after digestion is different.

In principle the branch length can be calculated by dividing the concentration of reducing ends in the depolymerised sample by the reducing ends in the de-branched sample. It was therefore calculated that Warrior had an oligosaccharide average length of 12 glucose units and Viscount 16 units.

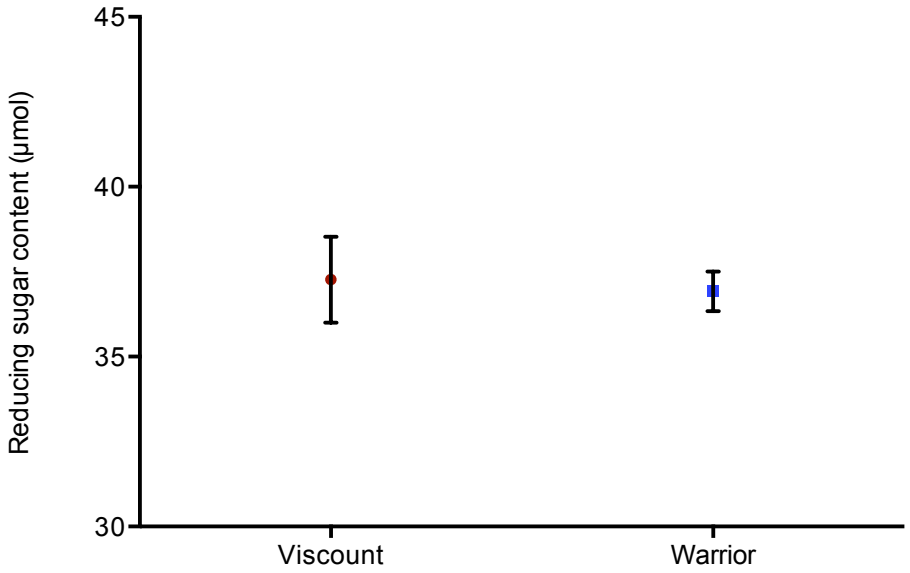

*Figure 6.3**. De-branched Warrior and Viscount starch measured by Nelson-Somoyogyi**. Starch was extracted (Chapter 2) and digested with Isoamylase. The amount of glucose in each aliquot was then measured using the Nelson-Somogyi assay (Chapter 2). Error bars are standard error of the mean. The difference between the means is not significant (unpaired t-test, P=0.5, n=12).*

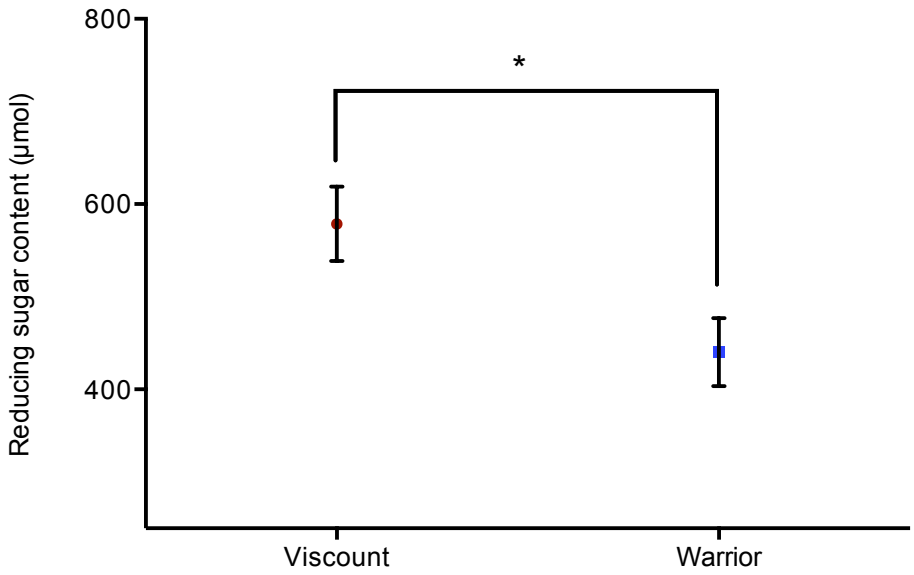

Figure 6.4. ***Depolymerised Warrior and Viscount starch measured by Nelson-Somoyogyi.*** *Starch was extracted (Chapter 2) and digested with Isoamylase and then β-amylase. The amount of glucose in each aliquot was then measured using the Nelson-Somogyi assay (Chapter 2). Error bars are standard error of the mean. The difference between the means is significant (unpaired t-test, P=0.05, n=12).*

6.3.3 Branch measurement control experiment

To control for any potential difference in the activity of the β-amylase or isoamylase enzymes in the branch measurement procedure the depolymerisation digest was repeated with samples composed of a mix of Warrior and Viscount starch with control potato starch (Zulkowsky, 1876). Three mixes were prepared of 25%, 50% and 75% Warrior or Viscount starch with the remaining percentage comprising control potato starch (Table 6.1). Figure 6.5 shows the difference between Warrior and Viscount remains constant regardless of the amount of wheat starch in the sample. If the Warrior starch inhibited the β-amylase then the difference would not be constant.

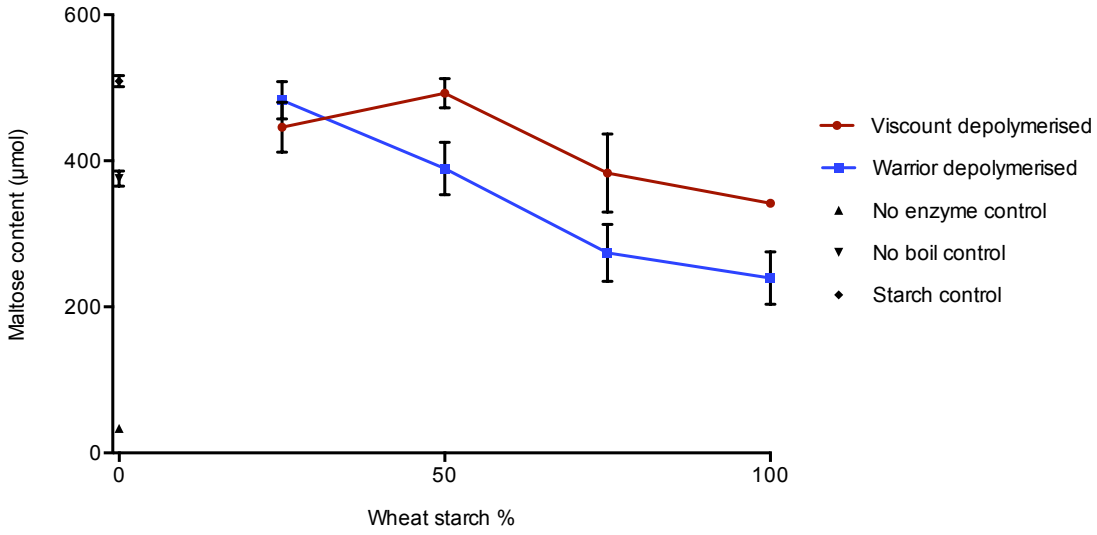

Figure 6.5. ***Branch measurement control experiment****. Starch was extracted (Chapter 2) and mixed proportionally with potato starch. Samples were digested with Isoamylase and then β-amylase (Chapter 2). The amount of glucose in each aliquot was then measured using the Nelson-Somogyi assay (Chapter 2). Error bars are standard error of the mean (n=3).*

Table 6.1 ***Compositions of samples for mix digest****. All samples were weighed out exactly, mixed and solubilised.*

Warrior/Viscount (%)	Warrior/Viscount (mg)	Potato starch (mg)
0	0	10
25	2.5	7.5
50	5	5
75	7.5	2.5
100	10	0

6.3.4 Analysis of de-polymerised starch by mass spectrometry

The starch samples were analysed by ESI-MS to ensure that β-amylase was completely digesting the oligosaccharides produced after the de-branching step. To do this a maltose calibration curve was produced (Figure 6.6) and used to calculate the amount of maltose in the experimental samples as measured by ESI-MS. The calibration curve is accurate and has and R^2 value of 0.9831. Therefore the calibration is less accurate than the glucose calibration using the Nelson-Somogyi method.

The amount of maltose (sodium adduct at 365.2Da) in the depolymerised starch samples was measured by ESI-MS. By using the calibration curve (Figure 6.6) The concentration of maltose in the depolymerised samples was calculated (Table 6.2). This experiment showed that maltose accounts for over 90% of reducing sugar detected in the Nelson-Somogyi assay.

*Table 6.2**. **Concentration of reducing sugars and maltose.** Depolymerised starch samples were measured separately using Nelson-Somogyi and ESI-MS. The proportion of maltose in the reducing sugar population was calculated.*

	Reducing sugars by Nelson-Somogyi (μm)	Maltose by ESI-MS (μm)	Maltose proportion (%)
Viscount	578.7 (± 40.22, n=12)	532.0 (± 174.6, n=3)	92.0%
Warrior	440.1 (± 36.74, n=12)	400.2 (± 91.92, n=3)	91.6%

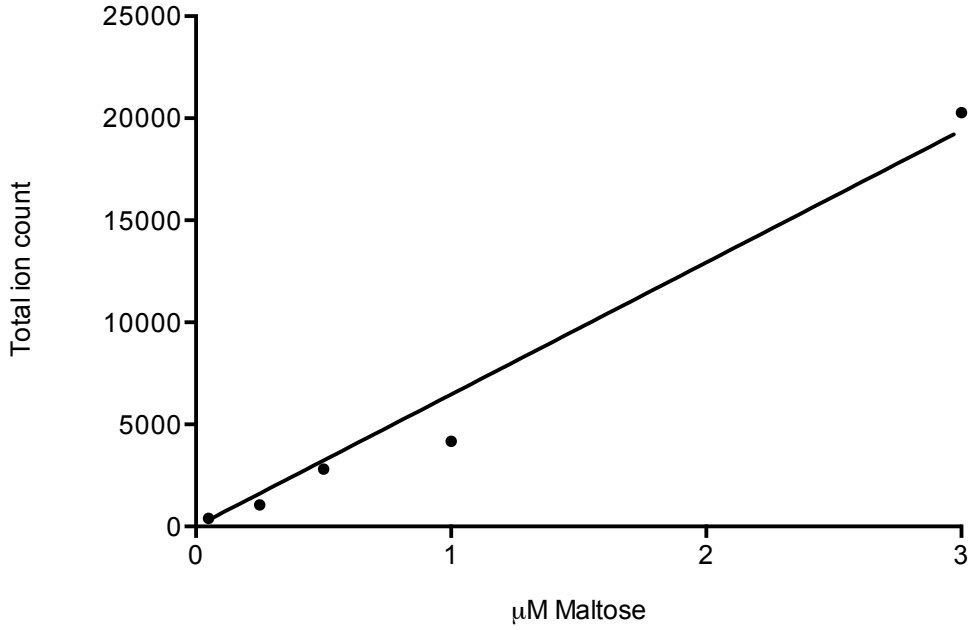

Figure 6.6 ***Maltose calibration curve using ESI-MS.*** *A standard curve of 0.05-3μM of maltose was prepared as a solution. Each solution was then analysed using ESI-MS. The line was fitted using linear regression. Each point represents the total Ion count of the maltose sodium adduct (365.2Da) after a three minute accumulation period.*

6.3.5 Targeted analysis of depolymerised starch by mass spectrometry

ESI-MS was used to characterise the oligosaccharides produced after Warrior and Viscount starch was de-branched. The mass range was selected to encompass the molecular weights of malto-oligosaccharides between five and 15 units long (700-2500Da). Based on the conclusions of the de-branching experiment this selection of oligosaccharides was expected to be greater in abundance in Warrior than Viscount.

Figure 6.7 shows the abundance of eight masses in the de-branched starch sample. Each mass is equivalent to that of a maltooligosaccharide, though it is not possible to unequivocally assign an identity to each of these masses it is reasonable to assume that these masses are maltooligosaccharides as these peaks are not present in the depolymerised starch sample.

Figure 6.7 shows a general trend in that Warrior generally has more abundant low mass maltooligosaccharides whereas there is greater abundance of high mass maltoligosaccharides in Viscount. The mass associated with maltodecaose appears to be the point at which Viscount begins to have more abundant maltooligosaccharide masses. The main issue with this data is that there is a large amount of deviation in the total ion count; this is caused by a large amount of variation between biological replicates. To reduce noise peaks which did not exceed a 1% threshold of the most abundant peak were removed. Therefore it must be noted that n varies between masses.

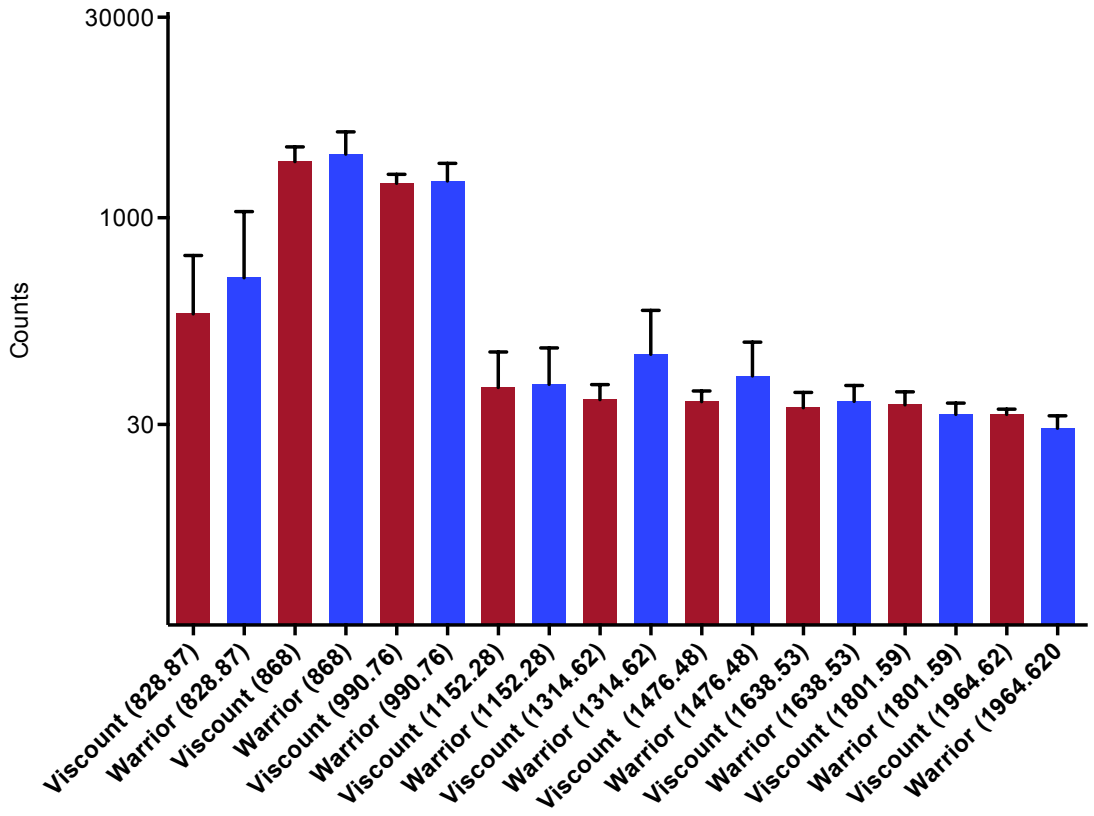

Figure 6.7. ***Oligosaccharide masses in Warrior and Viscount.*** *The total ion count of eight masses corresponding to different oligosaccharides in Warrior and Viscount de-branched starch.*

6.3.6 Non-targeted analysis of depolymerised starch by mass spectrometry

The dataset analysed in Figure 6.7 was also analysed by principal component analysis (PCA), this was completed to establish if masses detected via ESI-MS could separate the two varieties.

The principal component analysis of de-branched starch of Warrior and Viscount identified six outliers that were removed from the analysis. The two varieties grouped together. Several Viscount samples, which are quite different from the rest, specifically samples 1,2 and 7 were removed from the analysis. The Warrior samples seemed to group together more tightly but the difference between the two varieties was not particularly marked.

PLS-DA (Figure 6.8) was used to identify the masses that separate the two varieties; the loadings plot for this analysis is shown in Figure 6.9. This analysis was used to identify the top 10 masses, which separate Warrior and Viscount. The masses identified in both top 10s have been compared between both varieties (Figure 6.10 and Figure 6.11). The significant masses which segregate Warrior from Viscount (Figure 6.10) are not smaller on average compared to Viscount.

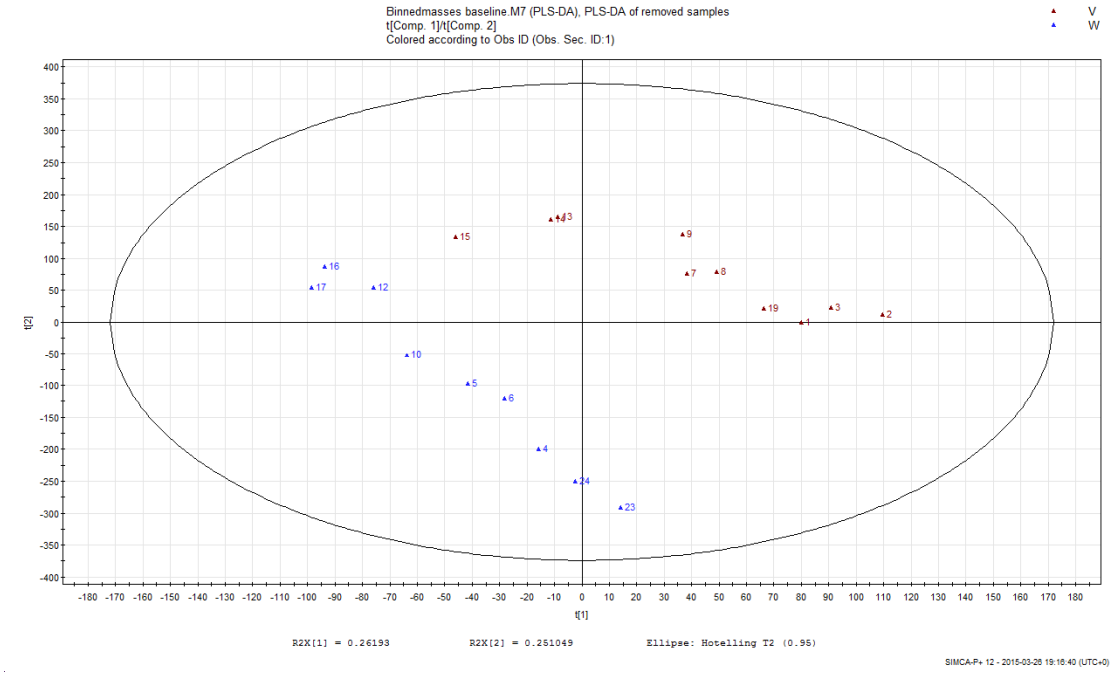

Figure 6.8. ***PLS-DA plot of debranched Warrior and Viscount starch****. De-branched starch was analysed by ESI-MS. Collected spectra were analysed by PLS-DA. Each point represents one analytical replicate. (n=19).*

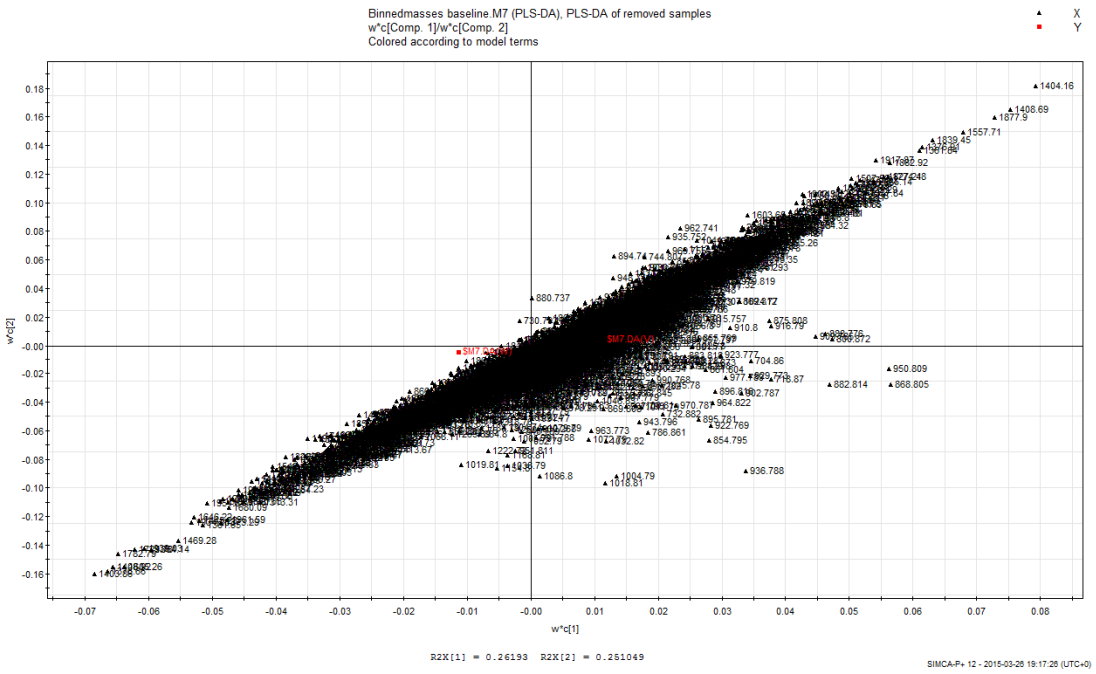

Figure 6.9. ***PLS-DA loadings plot of de-branched Warrior and Viscount starch****. Debranched starch was analysed by ESI-MS. Collected spectra were analysed by PCA and then PLS-DA using variety as the class variable. Each point represents one analytical replicate. (n=19).*

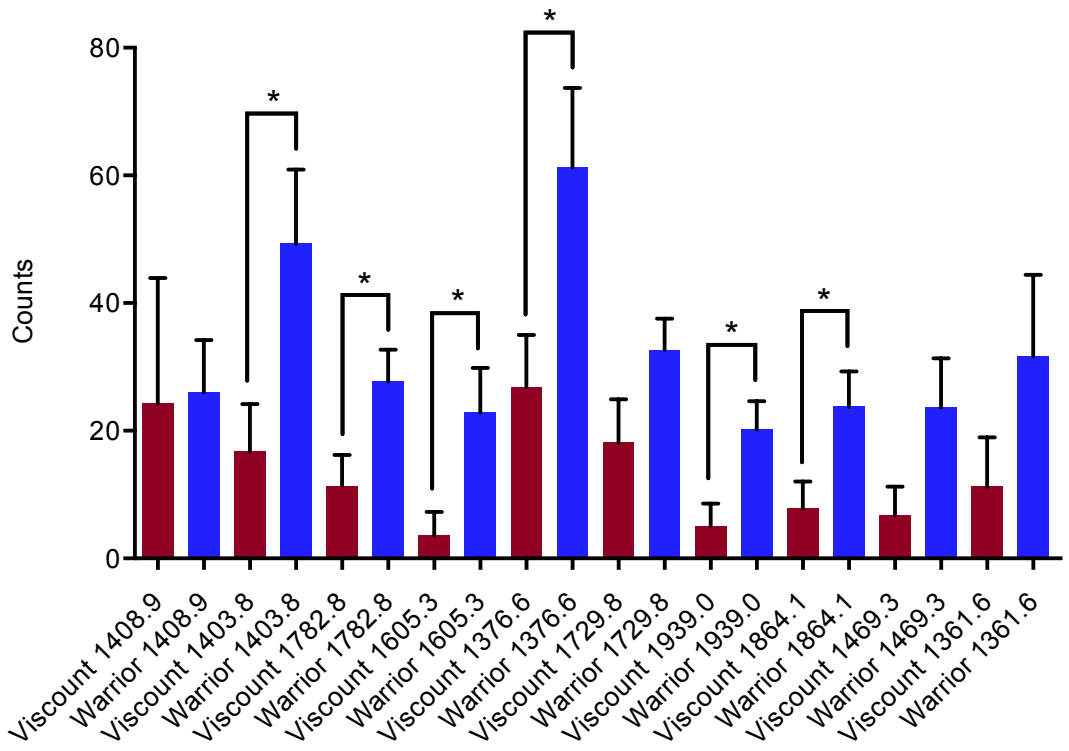

Figure 6.10. ***Comparison of masses separating with Warrior compared to Viscount****. Debranched starch was analysed by ESI-MS. Each bar represents the total ion count of the mass of interest, each bar is an average of three separate digests with three technical replicates, n=12. Masses which are significantly different are marked with an asterisk (P=0.05, Unpaired t-test).*

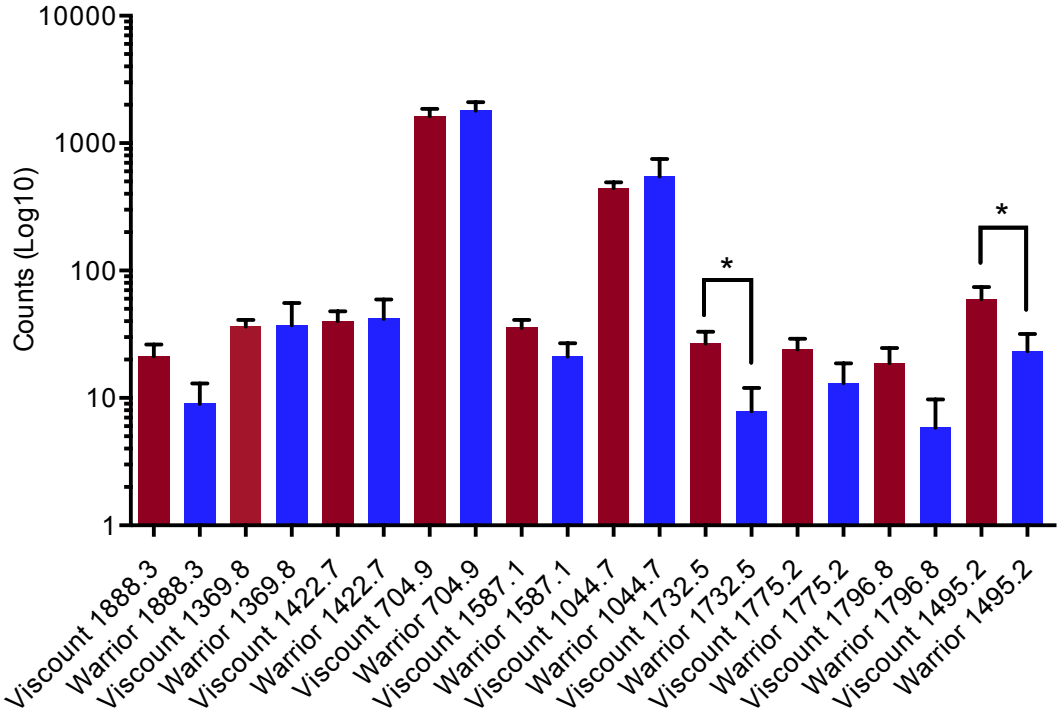

Figure 6.11. ***Comparison of masses separating with Viscount compared to Warrior****. Debranched starch was analysed by ESI-MS. Each bar represents the total ion count of the mass of interest, each bar is an average of three separate digests with three technical replicates, n=12. Masses which are significantly different are marked with an asterisk (P=0.05, Unpaired t-test).*

6.4 Discussion

The evidence presented in this chapter demonstrates that the amylopectin fine structure of Warrior starch is fundamentally different to that of Viscount. This has been demonstrated by measuring the proportions of reducing ends in debranched Warrior and Viscount starch and by analysing the abundance of maltooligosaccharides of various lengths in both varieties. The first hypothesis stated; “The fine architecture of starch in Warrior and Viscount is different”. This hypothesis can be accepted, as the number of reducing ends produced after successive debranching and depolymerisation reactions is different. Furthermore this effect cannot be attributed to inhibition of β-amylase or isoamylase in Warrior starch.

The second hypothesis stated “The average maltooligosaccharide chain length is shorter in Warrior than Viscount”. This hypothesis can be accepted on the balance of the evidence but the actual average chain length could not be calculated. The evidence for this hypothesis is that short maltooligosaccharides are more abundant in Warrior than Viscount and vice versa (Figure 6.7)

The estimated average chain length for Warrior and Viscount calculated using the Nelson-Somogyi assay is consistent with published values of the average chain length of amylopectin chain in wheat starch (Jane *et al.*, 1999) and (Hanashiro *et al.*, 1996). Specifically, the estimated average chain length for Warrior and Viscount was 12 and 16 units respectively, compared to literature values of between 11 and 16 units (Jane *et al.*, 1999).

Shorter amylopectin branch chains are typically associated with lower gelatinization temperatures (Jane *et al.*, 1999), (Singh *et al.*, 2010) and less extensive retrodegradation. The starches with higher gelatinization temperature have previously been associated with improved digestibility with α-amylase (Zhang & Oates, 1999), this effect can be attributed to the inability of the enzyme to penetrate a more retrodegraded structure. Therefore the difference in maltose yield between Warrior and Viscount as a function of the thermal properties of starch does not satisfy the evidence presented in this chapter.

The calibration curve for the Nelson-Somogyi assay was straight but did not intercept Y at 0. This is because the reagent will absorb at 620nm without reducing sugar present. This issue has been documented in the literature regarding this assay (Farnet *et al.*, 2010). Ensuring that the experimental samples were appropriately diluted surmounted the issue.

A more plausible explanation for the difference observed in the previous chapter is that as amylopectin chains become shorter the proportion of α-1-4 linkages to α-1-6 linkages decreases. It has also long been know that the K_m of amyloglucosidase is much higher for isomaltose than it is for maltose (isomaltose being the constituent molecule of the α-1-6 linkage) (Hiromi *et al.*, 1966), (Abe & Naczk, 1985). Therefore the shorter amylopectin branches are, the higher the proportion of α-1-4 linkages to α-1-6 linkages will be, and the more inhibition will occur. This effect has been observed in other types of starches, which have been artificially shortened. When maize and potato starch was

treated with enzymes to reduce the amylopectin chain length the amount of resistant starch increased (Ao *et al.*, 2007), (Zhang *et al.*, 2008b). The authors of these paper suggested that this was due to the proportion of α-1-4 linkages to α-1-6 linkages decreasing.

The first experiment showed that Warrior had the same number of reducing ends after starch de-branching however after those branches were depolymerised by β-amylase less reducing ends were yielded. As each branch has one reducing end and one non-reducing end the amount of reducing sugars measured is representative of the amount of branches. As the same number of branches yielded less reducing sugars (maltose) those branches must be shorter. The reducing sugars were also shown by mass spectrometry to be composed mostly of maltose

In previous chapters it has been observed that amyloglucosidase is inhibited. Therefore inhibition of β-amylase could be an alternative explanation for the reduced reducing sugar yield seen. If this is the case a dose dependent effect should be seen when Warrior starch is mixed with Viscount starch. Warrior starch should disproportionately decrease reducing sugar yield when mixed with control starch. However this effect was not observed (Figure 4.6). In fact the reducing sugar yield increased proportionally. As such substrate inhibition of β-amylase must be rejected as an explanation for the observed difference. On the basis of the evidence collected in these experiments de-branched Warrior starch branches must be shorter. This conclusion allows the first hypothesis stated at the beginning of the chapter to be accepted. However the data did not directly measure the chain length of the maltoligosaccharides. As a consequence of

this mass spectrometry was used to quantify the amount of maltooligosaccharides produced after de-branching.

The de-branched Warrior and Viscount starch was analysed by electrospray mass spectrometry (ESI-MS). The masses, which correspond to eight maltooligosaccharides were extracted from the mass spectra. These eight maltooligosaccharides were chose specifically based on the calculation made after the first de-branching experiment (see text page). Total ion count was used to compare the amount of each maltooligosaccharide as it had been shown that ESI-MS was quantitative (Figure 6.6). The pattern observed in the total ion count of the eight selected masses showed that smaller masses tend to be more abundant in Warrior than Viscount and larger masses were more abundant in Viscount than Warrior, alhough hexaose and heptaose seemed to be exceptions. From this result alone it would be possible to accept the second hypothesis. However analysing the dataset using principal component analysis did not produce the pattern observed previously. However the masses identified as being significantly different in the two varieties were present in very small quantities and as such are likely to contribute little to the phenotype. Therefore the balance of evidence supports the second hypothesis.

6.4.1 Conclusion

It was observed that there was a large degree of deviation in the total ion count between biological replicates. Large variation has been seen previously when maltose in the depolymerised samples was measured by Nelson-Somogyi (Figure 6.3) This large variation is likely to be caused by the technique itself. Analysing oligosaccharides by

conventional ESI-MS is fraught with confounding factors. Firstly oligosaccharides are hydrophilic and as such this reduces the ionization efficiency of the oligosaccharide samples (Zaia, 2004). Secondly the presence of salts (in this case sodium acetate) can cause profound ion suppression (Kailemia *et al.*, 2014). Though the acquisition method was optimised the fundamental properties of the analyte molecules led to the large deviation in total ion count seen in Figure 6.7. In this chapter it has been shown that the amylopectin fine structure is different in Warrior and Viscount starch. Specifically, the branches of amylopectin are shorter in Warrior.

7 General discussion

7.1 Aims

The aims of this thesis were firstly; to identify trait(s) associated with low ethanol yield in Warrior wheat. Secondly, to understand the cause of low ethanol yield in wheat. The work presented in this thesis has achieved the two aims stated in the introduction by characterizing the biochemistry and structure of starch in both varieties. The enzymic digestion of starch to ethanol is inhibited in Warrior by a high proportion of short chains in amylopectin.

Warrior was a chosen as one of the varieties studied, as it was the worst performing variety in its class. Not only did Warrior have an exceptionally low ethanol yield it also reduced ethanol yield when mixed with other varieties. Viscount was selected to compare against Warrior, as it was a high ethanol yielding wheat variety, which shares a parental line with Warrior.

7.2 Endosperm proteins

The relationship between protein content and ethanol yield from wheat is well understood. It has been often observed that when total grain protein increases glucose yield decreases (Gadonna-Widehem *et al.*, 2012) and therefore ethanol yield decreases (Swanston *et al.*, 2014). Specifically the total nitrogen content of a wheat grain can be

used to accurately predict the alcohol yield of wheat (Agu *et al.*, 2009) as grain protein increases as a result of nitrogen application (Xiong *et al.*, 2013). Though this prediction can vary depending on the nitrogen availability during the growing period and the hardness of the wheat grains (Swanston *et al.*, 2012) this effect is likely to be due to the formation of a protein matrix around the starch granules (Stenvert & Kingswood, 1977) preventing enzyme access to the grain. This link has been established as when protein matrices are broken down by enzymes after grain sprouting ethanol yield will increase (Yan *et al.*, 2010). When flour is milled more extensively ethanol yield will increase (Song *et al.*, 2014), (Li *et al.*, 2014). For this reason soft milling wheat varieties are preferred by distilleries, as less energy is required to process the grain for use.

However both Warrior and Viscount wheat varieties are soft milling. Therefore the first hypothesis tested in this thesis was; “Protein content is higher in Warrior than Viscount causing a reduced ethanol yield due to a more extensive protein matrix”. The extraction of total protein from wheat is difficult and many of the published procedures interfere with the estimation of the protein extracted (chapter 3), which has recently been illustrated as being comparable to the industry standard method (Thanhaeuser *et al.*, 2015). The method optimisation allowed the accurate quantification of the protein content of Warrior and Viscount and it was subsequently shown that Warrior had lower protein content than Viscount. Therefore the established paradigm by which protein reduces ethanol yield in wheat based on its abundance does not apply to the Warrior variety.

Explaining the difference in ethanol yield between the two varieties as a result of different protein compositions is not satisfactory either. This is because there is only a

single subunit difference between the two varieties (HMW-glutenin). When this result is compared to the literature there is also little evidence for HMW-glutenins affecting ethanol yield. Burešová (Burešová & Hřivna, 2011) found that glutenin subunits did not significantly change ethanol yield a finding that is supported by Kindred (Kindred *et al.*, 2008) where the authors suggested that selecting for a different class of proteins would improve ethanol yield.

7.3 Starch biochemistry

It was shown that amyloglucosidase; an important industrial enzyme was inhibited by Warrior starch. When an enzyme independent method was used to hydrolyse pure starch both varieties had the same potential to produce glucose. This finding is consistent with the fundamental understanding of the structure of starch (Pérez & Bertoft, 2010). However, as the residence time in the saccharification stage in distilling is limited the rate of the reaction is also important. The rate of reaction for amyloglucosidase when hydrolysing starch is lower in Warrior than Viscount. The rate of amyloglucosidase activity has been measured but the variable tested is often the processing of the substrate rather than the substrate itself such as in Montesinos (Montesinos & Navarro, 2000). Therefore accurate measurements of amyloglucosidase kinetics were made. These measurements showed that Warrior starch was an effective competitive inhibitor of amyloglucosidase. This observation is consistent with the performance of Warrior flour when it is used in distilleries; when Warrior is used as the substrate it will reduce the yield of ethanol even when it is added in small amounts (HGCA, 2011). Numerous studies have identified various inhibitors of amyloglucosidase such as gentibiose, malitol and methyl alpha-D-glucoside (Fogarty & Benson, 1983).

Similarly the competitive inhibitors of amyloglucosidase digestion of maltose are glucose, isomaltose, glycogen (long oligomers) and α-methyl glucosidase (Sica *et al.*, 1971). However mass spectrometry of digests failed to identify such an inhibitor. This finding would seemingly preclude the conclusion that warrior produces/contains a competitive inhibitor of amyloglucosidase activity on starch. However the amount of isomaltose and oligomers cannot be discriminated based on this method as isomaltose has the same mass as maltose and the experiment was not designed to measure the high molecular weight oligomers. There is a precedent for explaining amyloglucosidase inhibition being caused by a disparity in the oligomer population in the digest as it has been shown that when starch is artificially shortened its digestion rate decreases (Ao *et al.*, 2007). As both isomaltose and oligosaccharides are products of the native amylopectin structure the structure of the starch in both varieties was characterised.

7.4 Starch structure

The hypothesis of the two final chapters asked if the structure of Warrior and Viscount could be differentiated. The highest echelon of starch structure analysed was the granule. Higher orders of starch organisation exist but this level is the most complex structure in place when saccharification is carried out during ethanol production (Agu *et al.*, 2006). The results showed that the distribution of the smaller b-type starch granules was different in the Warrior wheat variety compared to Viscount. The two varieties showed the classic bi-modal starch granule distribution (Evers, 1973) and the difference in b-type starch granule size was within variation in starch granule size seen in other varieties (Dengate & Meredith, 1984). Interestingly, the starch granule size distribution of samples collected from an area in the field where the wheat plants were waterlogged for

a prolonged period, had a similar small b-type granule phenotype to wheat which has undergone drought or heat stress (Lu *et al.*, 2014). Once the b-type granules were separated from the a-type granules they were analysed by X-ray diffraction. This allowed the crystal lamellar properties of the b-type granules to be studied in Warrior and Viscount starch granules. The diffraction patterns observed in both varieties exhibited typical patterns for wheat starch granules (Zeng *et al.*, 2011; Zhang *et al.*, 2013b). Despite the overall pattern being consistent with published data the relative intensity of the two varieties was different. Therefore the contribution of the various crystal lamellae in both varieties to the overall starch architecture is different. It is important to remember at this point that the granular structure of the starch is disrupted upon boiling/cooking; treatments used during the enzymatic analysis and in the industrial production of starch (Kim & Huber, 2008). Therefore the molecular structure of amylopectin must be different in the two varieties to produce enzymatic inhibition. And furthermore, must be different in a way which prevents efficient degradation by amyloglucosidase or produces inhibition during digestion.

7.5 Starch fine structure

To compare the fine structure of amylopectin in the two varieties starch from both varieties was de-branched and then depolymerised, the amount of depolymerised starch was different. The average chain length calculated was found to be within the range which is expected in wheat with the majority of chains having a length of between 11 and 16 units (Hanashiro & Takeda, 1998). This was supported by the measurement of chain length by ESI-MS where Warrior was shown to have more abundant short maltooligosaccharide chains and Viscount had more abundant long chains.

The conclusions in this thesis are consistent with other studies on the performance of starch during saccharification. Potato and maize starch which has shorter amylopectin branches is resistant to digestion by amylases (Zhang *et al.*, 2008a) (Zhang *et al.*, 2006b). Although these studies primarily investigated the nutritional value of certain starches the principle is the same. Indeed the rate of saccharification of maize starch can be reduced by increasing the proportion of branches by β-amylosis (Xiong *et al.*, 2014). This result is replicated in the β-limit digest performed in chapter 3 of this thesis (Figure 4.5). With these results it can be concluded that the observations made in this thesis are consistent with those made in other species.

7.6 Final conclusion

The evidence in this thesis supports the conclusion that the amylopectin fine structure of Warrior starch inhibits saccharification and therefore reduces ethanol yield. The inhibition of amyloglucosidase can come from two sources isomaltose and the short chain maltooligosaccharides. Firstly, as shown in chapter 7 Warrior has a more highly branched structure than Viscount. Consequently, there are a higher proportion of α-1-6 linkages to α-1-4 linkages in Warrior. This means that there will be a greater amount of isomaltose produced when the Warrior amylopectin is digested. And as isomaltose is a competitive inhibitor of amyloglucosidase (Pazur & Ando, 1960) there will be greater inhibiton of amyloglucosidase in Warrior starch. Secondly, amyloglucosidase posses both a starch binding and a catalytic domain, both of which are required for enzyme action (Kaneko *et al.*, 1996). Therefore the population of shorter maltoligosaccharides in

Warrior will cause enzyme inhibition by blocking binding of maltooligosaccharides to the active site. This link has not been proved directly but enzymes that exhibit the random multiple attack patterns as amyloglucosidase do not favour amylopectin digestion (Bijttebier *et al.*, 2008) and starches with shorter amylopectin chains are more resistant to hydrolysis(Zhang *et al.*, 2006b).

It should also be noted that amyloglucosidase is added in saccharification to prevent α-amylase inhibition by its product, maltose (Sun & Henson, 1991; Warren *et al.*, 2015). In doing so yields can be increased by 20% (Espinosa-Ramírez *et al.*, 2014). So the actual cause of low ethanol (glucose) yield in Warrior is α-amylase inhibition by maltose. This effect can been seen in this thesis as a difference in glucose yield is not seen when α-glucosidase (3.2.1.33), which does not digest starch, is used to hydrolyse maltose to glucose instead of amyloglucosidase (3.2.1.3).

7.7 Further work

To identify the genetic cause of the phenotype seen in the Warrior variety it will be necessary to screen the crossing population of Warrior and Viscount to identify the locus associated with the lesion. The crossing population has already been collected and processed however a reliable and easily reproducible method for screening the phenotype (shorter amylopectin branches) of interest has not been established. In the opinion of the author the method developed by Morrell (O'Shea *et al.*, 1998) would be the most suitable to screen a large population for this phenotype.

It would also be interesting to measure the activity of certain starch synthases during grain development such as starch branching enzyme III (SBE III) which hydrolyses the α-1,4 link and reattaches the chain with a α-1,6 branch point (Kang *et al.*, 2013). If SBE III was more active or more abundant during the grain-filling phase of development then it is possible that a highly branched amylopectin would be produced. This approach would also need to be complemented by measuring the spatiotemporal distribution of metabolites from which starch is synthesised as their abundance chages over time (Verspreet *et al.*, 2013).

8 References

Abe J-I, Naczk M. **1985**. Kinetic and structural properties of the three forms of glucoamylase of Rhizopus delemar. *Journal of Applied Biochemistry* **7**: 235–247.

Aberle T, Burchard W, Vorwerg W, Radosta S. **1994**. Conformational Contributions of Amylose and Amylopectin to the Structural Properties of Starches from Various Sources. *Starch - Stärke* **46**: 329–335.

Agu RC, Bringhurst TA, Brosnan JM. **2006**. Production of Grain Whisky and Ethanol from Wheat, Maize and Other Cereals. *Journal of the Institute of Brewing* **112**: 314–323.

Agu RC, Swanston JS, Walker JW, Pearson SY, Bringhurst TA, Brosnan JM, Jack FR. **2009**. Predicting Alcohol Yield from UK Soft Winter Wheat for Grain Distilling: Combined Influence of Hardness and Nitrogen Measurements. *Journal of the Institute of Brewing* **115**: 183–190.

Ao Z, Jane J. **2007**. Characterization and modeling of the A- and B-granule starches of wheat, triticale, and barley. *Carbohydrate Polymers* **67**: 46–55.

Ao Z, Simsek S, Zhang G, Venkatachalam M, Reuhs BL, Hamaker BR. **2007**. Starch with a slow digestion property produced by altering its chain length, branch density, and crystalline structure. *Journal of agricultural and food chemistry* **55**: 4540–7.

Awole KD, Kettlewell PS, Hare MC, Agu RC, Brosnan JM, Bringhurst TA. **2011**. Effect of environment and variety on the relationships of wheat grain physical and chemical characteristics with ethanol yield. *Journal of the science of food and agriculture*.

Balat M, Balat H. **2009**. Recent trends in global production and utilization of bio-ethanol fuel. *Applied Energy* **86**: 2273–2282.

Bamforth CW. **2009**. Current perspectives on the role of enzymes in brewing. *Journal of Cereal Science* **50**: 353–357.

Bancel E, Rogniaux H, Debiton C, Chambon C, Branlard G. **2010**. Extraction and proteome analysis of starch granule-associated proteins in mature wheat kernel (Triticum aestivum L.). *Journal of proteome research* **9**: 3299–310.

Barlow KK, Buttrose MS, Simmonds DH, Vesk M. **1972**. The Nature of the Starch-Protein Interface in Wheat Endosperm. *Journal of Cereal Chemistry* **50**: 443–454.

Barsnes H, Vaudel M, Colaert N, Helsens K, Sickmann A, Berven FS, Martens L. **2011**. compomics-utilities: an open-source Java library for computational proteomics. *BMC bioinformatics* **12**: 70.

Beavis RC, Chaudhary T, Chait BT. **1992**. α-Cyano-4-hydroxycinnamic acid as a matrix for matrixassisted laser desorption mass spectromtry. *Organic Mass Spectrometry* **27**: 156–158.

Bechtel DB, Zayas I, Kaleikau L, Pomeranz Y. **1990**. Size-Distribution of Wheat Starch Granules During Endosperm Development. *Cereal Chemistry* **67**: 59–63.

Beddington JR. **2009**. Food, energy, water and the climate: a perfect storm of global events.

BeMiller JN, Whistler RL. **2009**. *Starch: chemistry and technology.* (JN BeMiller and RL Whistler, Eds.). London: Academic Press Limited.

Bennett MD, Smith JB, Barclay I. **1975**. Early Seed Development in the Triticeae. *Philosophical Transactions of the Royal Society B: Biological Sciences* **272**: 199–227.

Bergmeyer. **1984**. Determination of glucose concentration by enzyme linked spectrophotometric assay. Methods of enzymatic analysis.119–126.

Bertoft E, Piyachomkwan K, Chatakanonda P, Sriroth K. **2008**. Internal unit chain composition in amylopectins. *Carbohydrate Polymers* **74**: 527–543.

Bijttebier A, Goesaert H, Delcour JA. **2008**. Amylase action pattern on starch polymers. *Biologia* **63**: 989–999.

Bijttebier A, Goesaert H, Delcour JA. **2010**. Hydrolysis of amylopectin by amylolytic enzymes: structural analysis of the residual amylopectin population. *Carbohydrate research* **345**: 235–42.

Blazek J, Gilbert EP. **2010**. Effect of enzymatic hydrolysis on native starch granule structure. *Biomacromolecules* **11**: 3275–89.

Bradford MM. **1976**. A rapid and sensitive method for the quantitation of microgram quantities of protein utilizing the principle of protein-dye binding. *Analytical biochemistry* **72**: 248–54.

Branlard G, Bancel E. **2007**. Protein extraction from cereal seeds. *Methods in molecular biology (Clifton, N.J.)* **355**: 15–25.

Bringhurst TA, Brosnan JM, McInnes B, Steele GM. **1996**. Methods for determining the fermentability and predicted spirit yield of distilling malts. *Journal of the Institute of Brewing* **102**: 433–437.

Brocklehurst PA. **1977**. Factors controlling grain weight in wheat. *Nature* **266**: 348–349.

Brune A. **2014**. Symbiotic digestion of lignocellulose in termite guts. *Nature reviews. Microbiology* **12**: 168–80.

Buléon a, Colonna P, Planchot V, Ball S. **1998**. Starch granules: structure and biosynthesis. *International journal of biological macromolecules* **23**: 85–112.

Burešová I, Hřivna L. **2011**. Effect of wheat gluten proteins on bioethanol yield from grain. *Applied Energy* **88**: 1205–1210.

Buysse J, Merckx R. **1993**. An Improved Colorimetric Method to Quantify Sugar Content of Plant Tissue. *Journal of Experimental Botany* **44**: 1627–1629.

Cai L, Shi Y-C. **2014**. Preparation, structure, and digestibility of crystalline A- and B-type aggregates from debranched waxy starches. *Carbohydrate polymers* **105**: 341–50.

Cao YN, Hu WG, Wang CS. **2012**. Expression profiles of genes involved in starch synthesis in non-waxy and waxy wheat. *Russian Journal of Plant Physiology* **59**: 632–639.

Clarke B, Liang R, Morell MK, Bird AR, Jenkins CLD, Li Z. **2008**. Gene expression in a starch synthase IIa mutant of barley: changes in the level of gene transcription and grain composition. *Functional & integrative genomics* **8**: 211–21.

Compton SJ, Jones CG. **1985**. Mechanism of dye response and interference in the Bradford protein assay. *Analytical Biochemistry* **151**: 369–374.

Cook WH, Rose RC. **1934**. Solubility of Gluten. *Nature* **134**: 380–381.

Curtis BC, Rajaram S, Macpherson HG. **2002**. Bread Wheat. In: Curtis BC, Rajaram S, Gómez Macpherson H, eds. FAO. FAO, 567.

Cutler R, Von Lingen A. **2003**. The European Parliament and European Union Security and Defence Policy. *European Security* **12**: 1–20.

Deng SP, Tabatabai MA. **1994**. Colorimetric determination of reducing sugars in soils. *Soil Biology and Biochemistry* **26**: 473–477.

Dengate H, Meredith P. **1984**. Variation in size distribution of starch granules from wheat grain. *Journal of Cereal Science* **2**: 83–90.

Diezel W, Kopperschläger G, Hofmann E. **1972**. An improved procedure for protein staining in polyacrylamide gels with a new type of Coomassie Brilliant Blue. *Analytical Biochemistry* **48**: 617–620.

Dupont FM, Altenbach SB. **2003**. Molecular and biochemical impacts of environmental factors on wheat grain development and protein synthesis. *Journal of Cereal Science* **38**: 133–146.

Dupont FM, Vensel WH, Tanaka CK, Hurkman WJ, Altenbach SB. **2011**. Deciphering the complexities of the wheat flour proteome using quantitative two-dimensional electrophoresis, three proteases and tandem mass spectrometry. *Proteome Science* **9**: 10.

Ensus. **2014**. Ensus Ltd.

Espinosa-Ramírez J, Pérez-Carrillo E, Serna-Saldívar SO. **2014**. Maltose and glucose utilization during fermentation of barley and sorghum lager beers as affected by β-amylase or amyloglucosidase addition. *Journal of Cereal Science* **60**: 602–609.

Evans DE, Li C, Eglinton JK. **2010**. The Properties and Genetics of Barley Malt Starch Degrading Enzymes. In: Zhang G, Li C, eds. Advanced Topics in Science and Technology in China. Genetics and Improvement of Barley Malt Quality. Berlin, Heidelberg: Springer Berlin Heidelberg, 143–189.

Evers AD. **1973**. The Size Distribution Among Starch Granules in Wheat Endosperm. *Starch - Stärke* **25**: 303–304.

ExPASy. ENZYME entry 3.2.1.1.

ExPASy. ENZYME entry 3.2.1.3.

FAOSTAT. **2009**. Food and Agricultural commodities production.

FAOSTAT. **2012**. Wheat Production.

Farnet AM, Qasemian L, Guiral D, Ferré E. **2010**. A modified method based on arsenomolybdate complex to quantify cellulase activities: Application to litters. *Pedobiologia* **53**: 159–160.

Feiz L, Wanjugi HW, Melnyk CW, Altosaar I, Martin JM, Giroux MJ. **2009**. Puroindolines co-localize to the starch granule surface and increase seed bound polar lipid content. *Journal of Cereal Science* **50**: 91–98.

Feldman M. **1976**. *Wheats* (N. Simmonds, Ed.). London: Longman.

Fogarty WM, Benson CP. **1983**. Purification and properties of a thermophilic amyloglucosidase from Aspergillus niger. *European Journal of Applied Microbiology and Biotechnology* **18**: 271–278.

Fujita N, Yoshida M, Kondo T, Saito K, Utsumi Y, Tokunaga T, Nishi A, Satoh H, Park J-H, Jane J-L, *et al.* 2007. Characterization of SSIIIa-Deficient Mutants of Rice: The Function of SSIIIa and Pleiotropic Effects by SSIIIa Deficiency in the Rice Endosperm. *Plant Physiology* **144**: 2009–2023.

Gadonna-Widehem P, Debiton C, Marier D, Rhazi L, Branlard G. **2012**. A Laboratory Protocol for Determining Glucose and Maximum Ethanol Production from Wheat Grain: Application to a Complete Genetic Set of Near-Isogenic Waxy Lines. *Journal of Agricultural and Food Chemistry* **60**: 985–990.

Gaillard T, Bowler P. **1987**. Morphology and composition of starch. In: Galliard T, ed. Starch: Properties and Potential. John Wiley & Sons, 62–63.

Giroux MJ, Morris CF. **1998**. Wheat grain hardness results from highly conserved mutations in the friabilin components puroindoline a and b. *Proceedings of the National Academy of Sciences of the United States of America* **95**: 6262–6.

Godet MC, Tran V, Delage MM, Buléon A. **1993**. Molecular modelling of the specific interactions involved in the amylose complexation by fatty acids. *International Journal of Biological Macromolecules* **15**: 11–16.

Godfray HCJ, Beddington JR, Crute IR, Haddad L, Lawrence D, Muir JF, Pretty J, Robinson S, Thomas SM, Toulmin C. **2010**. Food security: the challenge of feeding 9 billion people. *Science (New York, N.Y.)* **327**: 812–8.

Godfrey D, Hawkesford MJ, Powers SJ, Millar S, Shewry PR. **2010**. Effects of crop nutrition on wheat grain composition and end use quality. *Journal of agricultural and food chemistry* **58**: 3012–21.

Godfrey T, West S. **1996**. *Industrial enzymology*. Stockton Press.

Goldemberg J. **2007**. Ethanol for a Sustainable Energy Future. *Science* **315**: 808–810.

Good NE, Winget GD, Winter W, Connolly TN, Izawa S, Singh RMM. **1966**. Hydrogen Ion Buffers for Biological Research. *Biochemistry* **5**: 467–477.

Graham-Rowe D. **2011**. Agriculture: Beyond food versus fuel. *Nature* **474**: S6–8.

Graybosch RA, Morris R. **1990**. An improved SDS-PAGE method for the analysis of wheat endosperm storage proteins. *Journal of Cereal Science* **11**: 201–212.

Greenberg E, Preiss J. **1964**. The occurrence of Adenosine Diphosphate glucose: Glycogen transglucosylase in bacteria. *The Journal of biological chemistry* **239**: 4314–5.

Guo G, Lv D, Yan X, Subburaj S, Ge P, Li X, Hu Y, Yan Y. **2012**. Proteome characterization of developing grains in bread wheat cultivars (Triticum aestivum L.). *BMC Plant Biology* **12**: 147.

Hanashiro I, Abe J, Hizukuri S. **1996**. A periodic distribution of the chain length of amylopectin as revealed by high-performance anion-exchange chromatography. *Carbohydrate Research* **283**: 151–159.

Hanashiro I, Tagawa M, Shibahara S, Iwata K, Takeda Y. **2002**. Examination of molar-based distribution of A, B and C chains of amylopectin by fluorescent labeling with 2-aminopyridine. *Carbohydrate Research* **337**: 1211–1215.

Hanashiro I, Takeda Y. **1998**. Examination of number-average degree of polymerization and molar-based distribution of amylose by fluorescent labeling with 2-aminopyridine. *Carbohydrate Research* **306**: 421–426.

Hannah LC, James M. **2008**. The complexities of starch biosynthesis in cereal endosperms. *Current opinion in biotechnology* **19**: 160–5.

Heick J, Fischer M, Popping B. **2012**. Influence of sample extraction solutions on the detection of wheat proteins by mass spectrometry. *Journal of AOAC International* **95**: 388–93.

HGCA. **2011**. HGCA Recommended List ® winter wheat 2011/12.

Hill L, Smith A. **1991**. Evidence that glucose 6-phosphate is imported as the substrate for starch synthesis by the plastids of developing pea embryos. *Planta* **185**.

Hiromi K, Hamauzu ZI, Takahashi K, Ono S. **1966**. Kinetic studies on gluc-amylase. II. Competition between two types of substrate having alpha-1,4 and alpha-1,6 glucosidic linkage. *Journal of biochemistry* **59**: 411–418.

Hizukuri S. **1985**. Relationship between the distribution of the chain length of amylopectin and the crystalline structure of starch granules. *Carbohydrate Research* **141**: 295–306.

Hizukuri S, Kaneko T, Takeda Y. **1983**. Measurement of the chain length of amylopectin and its relevance to the origin of crystalline polymorphism of starch granules. *Biochimica et Biophysica Acta (BBA) - General Subjects* **760**: 188–191.

Hogg AC, Sripo T, Beecher B, Martin JM, Giroux MJ. **2004**. Wheat puroindolines interact to form friabilin and control wheat grain hardness. *TAG. Theoretical and applied genetics. Theoretische und angewandte Genetik* **108**: 1089–97.

IEA. **2007**. Potential Contribution of Bioenergy to the World's Future Energy Demand. : 12.

Imberty A, Buléon A, Tran V, Péerez S. **1991**. Recent Advances in Knowledge of Starch Structure. *Starch - Stärke* **43**: 375–384.

Imberty A, Chanzy H, Pérez S, Bulèon A, Tran V. **1988**. The double-helical nature of the crystalline part of A-starch. *Journal of Molecular Biology* **201**: 365–378.

Jane J, Chen YY, Lee LF, McPherson AE, Wong KS, Radosavljevic M, Kasemsuwan T. **1999**. Effects of amylopectin branch chain length and amylose content on the gelatinization and pasting properties of starch. *Cereal Chemistry* **76**: 629–637.

Jenkins PJ, Donald AM. **1995**. The influence of amylose on starch granule structure. *International Journal of Biological Macromolecules* **17**: 315–321.

Jeon J-S, Ryoo N, Hahn T-R, Walia H, Nakamura Y. **2010**. Starch biosynthesis in cereal endosperm. *Plant physiology and biochemistry : PPB / Société française de physiologie végétale* **48**: 383–92.

Jones RW, Taylor NW, Senti FR. **1959**. Electrophoresis and fractionation of wheat gluten. *Archives of Biochemistry and Biophysics* **84**: 363–376.

Kailemia MJ, Ruhaak LR, Lebrilla CB, Amster IJ. **2014**. Oligosaccharide analysis by mass spectrometry: A review of recent developments. *Analytical Chemistry* **86**: 196–212.

Kaneko A, Sudo S, Takayasu-Sakamoto Y, Tamura G, Ishikawa T, Oba T. **1996**. Molecular cloning and determination of the nucleotide sequence of a gene encoding an acid-stable α-amylase from Aspergillus kawachii. *Journal of Fermentation and Bioengineering* **81**: 292–298.

Kang G, Li S, Zhang M, Peng H, Wang C, Zhu Y, Guo T. **2013**. Molecular Cloning and Expression Analysis of the Starch-branching Enzyme III Gene from Common Wheat (Triticum aestivum). *Biochemical Genetics* **51**: 377–386.

Karas M, Bachmann D, Bahr U, Hillenkamp F. **1987**. Matrix-assisted ultraviolet laser desorption of non-volatile compounds. *International Journal of Mass Spectrometry and Ion Processes* **78**: 53–68.

Kim K-H, Feiz L, Martin JM, Giroux MJ. **2012**. Puroindolines are associated with decreased polar lipid breakdown during wheat seed development. *Journal of Cereal Science* **56**: 142–146.

Kim H-S, Huber KC. **2008**. Channels within soft wheat starch A- and B-type granules. *Journal of Cereal Science* **48**: 159–172.

Kindred DR, Verhoeven TMO, Weightman RM, Swanston JS, Agu RC, Brosnan JM, Sylvester-Bradley R. **2008**. Effects of variety and fertiliser nitrogen on alcohol yield, grain yield, starch and protein content, and protein composition of winter wheat. *Journal of Cereal Science* **48**: 46–57.

Kosar-Hashemi B, Li Z, Larroque O, Regina A, Yamamori M, Morell MK, Rahman S. **2007**. Multiple effects of the starch synthase II mutation in developing wheat endosperm. *Functional Plant Biology* **34**: 431.

Kovats S, Valentini R. **2014**. *IPCC WGII AR5 Chapter 23*.

Kumar P, Satyanarayana T. **2009**. Microbial glucoamylases: characteristics and applications. *Critical Reviews in Biotechnology* **29**: 225–255.

Kunlan L, Lixin X, Jun L, Jun P, Guoying C, Zuwei X. **2001**. Salt-assisted acid hydrolysis of starch to D-glucose under microwave irradiation. *Carbohydrate Research* **331**: 9–12.

Laemelli UK. **1970**. Cleavage of Structural Proteins during the Assembly of the Head of Bacteriophage T4. *Nature* **227**: 680–685.

Leite JF, Hajivandi MR, Diller T, Pope RM. **2004**. Removal of sodium and potassium adducts using a matrix additive during matrix-associated laser desorption/ionization time-of-flight mass spectrometric analysis of peptides. *Rapid Communications in Mass Spectrometry* **18**: 2953–2959.

Leloir L, Fekete M de, Cardini C. **1961**. Starch and oligosaccharide synthesis from uridine diphosphate glucose. *Journal of Biological Chemistry* **236**.

Leterrier M, Holappa LD, Broglie KE, Beckles DM. **2008**. Cloning, characterisation and comparative analysis of a starch synthase IV gene in wheat: functional and evolutionary implications. *BMC Plant Biology* **8**: 98.

Li E, Dhital S, Hasjim J. **2014**. Effects of grain milling on starch structures and flour/starch properties. *Starch - Stärke* **66**: 15–27.

Li Z, Mouille G, Kosar-Hashemi B, Rahman S, Clarke B, Gale KR, Appels R, Morell MK. **2000**. The structure and expression of the wheat starch synthase III gene. Motifs in the expressed gene define the lineage of the starch synthase III gene family. *Plant Physiology* **123**: 613–24.

Li W, Shan Y, Xiao X, Luo Q, Zheng J, Ouyang S, Zhang G. **2013**. Physicochemical properties of A- and B-starch granules isolated from hard red and soft red winter wheat. *Journal of agricultural and food chemistry* **61**: 6477–84.

Lim S-T, Kasemsuwan T, Jane J-L. **1994**. Characterization of Phosphorus in Starch by 31P-Nuclear Magnetic Resonance Spectroscopy. *Cereal Chemistry* **71**: 488–493.

Liu L, Wang A, Appels R, Ma J, Xia X, Lan P, He Z, Bekes F, Yan Y, Ma W. **2009**. A MALDI-TOF based analysis of high molecular weight glutenin subunits for wheat breeding. *Journal of Cereal Science* **50**: 295–301.

Liu W, Zhang Y, Gao X, Wang K, Wang S, Zhang Y, He Z, Ma W, Yan Y. **2012**. Comparative proteome analysis of glutenin synthesis and accumulation in developing grains between superior and poor quality bread wheat cultivars. *Journal of the science of food and agriculture* **92**: 106–15.

Loomis WD, Battaile J. **1966**. Plant phenolic compounds and the isolation of plant enzymes. *Phytochemistry* **5**: 423–438.

Lu H, Wang C, Guo T, Xie Y, Feng W, Li S. **2014**. Starch composition and its granules distribution in wheat grains in relation to post-anthesis high temperature and drought stress treatments. *Starch - Stärke* **66**: 419–428.

Macedo IC, Seabra JEA, Silva JEAR. **2008**. Green house gases emissions in the production and use of ethanol from sugarcane in Brazil: The 2005/2006 averages and a prediction for 2020. *Biomass and Bioenergy* **32**: 582–595.

Mamone G, De Caro S, Di Luccia A, Addeo F, Ferranti P. **2009**. Proteomic-based analytical approach for the characterization of glutenin subunits in durum wheat. *Journal of mass spectrometry : JMS* **44**: 1709–23.

Martin C, Smith AM. **1995**. Starch biosynthesis. *The Plant Cell* **7**: 971–85.

Martinez D, Berka RM, Henrissat B, Saloheimo M, Arvas M, Baker SE, Chapman J, Chertkov O, Coutinho PM, Cullen D, *et al.* 2008. Genome sequencing and analysis of the biomass-degrading fungus Trichoderma reesei (syn. Hypocrea jecorina). *Nature biotechnology* **26**: 553–560.

McCleary B V., Codd R. **1991**. Measurement of (1 → 3),(1 → 4)-β-D-glucan in barley and oats: A streamlined enzymic procedure. *Journal of the Science of Food and Agriculture* **55**: 303–312.

McCleary B V., Gibson TS, Mugford DC. **1997**. Measurement of total starch in cereal products by amyloglucosidase-α-amylase method: Collaborative study. *Journal of AOAC International* **80**: 571–579.

McComb RB, Bond LW, Burnett RW, Keech RC, Bowers GN. **1976**. Determination of the molar absorptivity of NADH. *Clinical chemistry* **22**: 141–50.

Merkus HG. **2009**. *Particle Size Measurements: Fundamentals, Practice, Quality*. Springer Science & Business Media.

Mikus FF, Hixon RM, Rundle RE. **1946**. The Complexes of Fatty Acids with Amylose. *Journal of the American Chemical Society* **68**: 1115–1123.

Mola-Yudego B, Aronsson P. **2008**. Yield models for commercial willow biomass plantations in Sweden. *Biomass and Bioenergy* **32**: 829–837.

Montesinos T, Navarro J-M. **2000**. Production of alcohol from raw wheat flour by Amyloglucosidase and Saccharomyces cerevisiae. *Enzyme and Microbial Technology* **27**: 362–370.

Morell M. **1997**. Differential expression and properties of starch branching enzyme isoforms in developing wheat endosperm. *Plant Physiology* **113**: 201–208.

Morell MK, Kosar-Hashemi B, Cmiel M, Samuel MS, Chandler P, Rahman S, Buleon A, Batey IL, Li Z. **2003**. Barley sex6 mutants lack starch synthase IIa activity and contain a starch with novel properties. *Plant J* **34**: 173–185.

Morrison WR, Law RV, Snape CE. **1993**. Evidence for Inclusion Complexes of Lipids with V-amylose in Maize, Rice and Oat Starches. *Journal of Cereal Science* **18**: 107–109.

Murphy JD, Power NM. **2008**. How can we improve the energy balance of ethanol production from wheat? *Fuel* **87**: 1799–1806.

NABIM. **2012**. Nabim Wheat Guide 2012.

Nakamura Y. **1996**. Some properties of starch debranching enzymes and their possible role in amylopectin biosynthesis. *Plant Science* **121**: 1–18.

Nelson OE, Rines HW. **1962**. The enzymatic deficiency in the waxy mutant of maize. *Biochemical and Biophysical Research Communications* **9**: 297–300.

O'Shea MG, Morell MK. **1996**. High resolution slab gel electrophoresis of 8-amino-1,3, 6-pyrenetrisulfonic acid (APTS) tagged oligosaccharides using a DNA sequencer. *Electrophoresis* **17**: 681–6.

O'Shea MG, Samuel MS, Konik CM, Morell MK. **1998**. Fluorophore-assisted carbohydrate electrophoresis (FACE) of oligosaccharides: efficiency of labelling and high-resolution separation. *Carbohydrate Research* **307**: 1–12.

Ohnishi M, Matsumoto T, Yamanaka T, Hiromi K. **1990**. Binding of isomaltose and maltose to the glucoamylase from Aspergillus niger, as studied by fluorescence spectrophotometry and steady-state kinetics. *Carbohydrate Research* **204**: 187–196.

Olesen JE, Trnka M, Kersebaum KC, Skjelvåg AO, Seguin B, Peltonen-Sainio P, Rossi F, Kozyra J, Micale F. **2011**. Impacts and adaptation of European crop production systems to climate change. *European Journal of Agronomy* **34**: 96–112.

Osborne TB. **1909**. *The vegetable proteins*. New York [etc.] Longmans, Green.

Patey AL. **1980**. Toxicity of gliadin in coeliac patients. *Lancet* **2**: 427–8.

Payne PI, Holt LM, Lawrence GJ, Law CN. **1982**. The genetics of gliadin and glutenin, the major storage proteins of the wheat endosperm. *Qualitas Plantarum Plant Foods for Human Nutrition* **31**: 229–241.

Pazur JH, Ando T. **1960**. The Hydrolysis of Glucosyl Oligosaccharides with α-d-(1→ 4) and α-d-(1→ 6) Bonds by Fungal Amyloglucosidase. *Journal of Biological Chemistry* **235**: 297–302.

Peat S, Whelan WJ, Thomas GJ. **1956**. 587. The enzymic synthesis and degradation of starch. Part XXII. Evidence of multiple branching in waxy-maize starch. A correction. *Journal of the Chemical Society (Resumed)*: 3025–3030.

Peggy Tao H, Elva Adalsteins A, Kasarda DD. **1992**. Intermolecular disulfide bonds link specific high-molecular-weight glutenin subunits in wheat endosperm. *Biochimica et Biophysica Acta (BBA) - Protein Structure and Molecular Enzymology* **1159**: 13–21.

Peng M, Gao M, Abdel-Aal E-SM, Hucl P, Chibbar RN. **1999**. Separation and Characterization of A- and B-Type Starch Granules in Wheat Endosperm. *Cereal Chemistry* **76**: 375–379.

Peng M, Hucl P, Chibbar RN. **2001**. Isolation, characterization and expression analysis of starch synthase I from wheat (*Triticum aestivum* L.). *Plant Science* **161**: 1055–1062.

Peplow M. **2014**. Cellulosic ethanol fights for life. *Nature* **507**: 152–3.

Pérez S, Bertoft E. **2010**. The molecular structures of starch components and their contribution to the architecture of starch granules: A comprehensive review. *Starch - Stärke* **62**: 389–420.

Piperno DR, Weiss E, Holst I, Nadel D. **2004**. Processing of wild cereal grains in the Upper Palaeolithic revealed by starch grain analysis. *Nature* **430**: 670–3.

Planchot V, Colonna P, Gallant DJ, Bouchet B. **1995**. Extensive degradation of native starch granules by alpha-amylase from *aspergillus fumigatus*. *Journal of Cereal Science* **21**: 163–171.

Qian M, Spinelli S, Payan F, Driguez H. **1997**. Structure of a pancreatic alpha-amylase bound to a substrate analogue at 2.03 Å resolution. *Protein Science*: 2285–2296.

Ribeiro M, Nunes-Miranda JD, Branlard G, Carrillo JM, Rodriguez-Quijano M, Igrejas G. **2013**. One hundred years of grain omics: identifying the glutens that feed the world. *Journal of proteome research* **12**: 4702–16.

Rogers WJ, Payne PI, Seekings JA, Sayers EJ. **1991**. Effect on breadmaking quality of x-type and y-type high molecular weight subunits of glutenin. *Journal of Cereal Science* **14**: 209–221.

Roldán I, Wattebled F, Mercedes Lucas M, Delvallé D, Planchot V, Jiménez S, Pérez R, Ball S, D'Hulst C, Mérida Á. **2007**. The phenotype of soluble starch synthase IV defective mutants of Arabidopsis thaliana suggests a novel function of elongation enzymes in the control of starch granule formation. *The Plant Journal* **49**: 492–504.

Rötter RP, Palosuo T, Pirttioja NK, Dubrovsky M, Salo T, Fronzek S, Aikasalo R, Trnka M, Ristolainen A, Carter TR. **2011**. What would happen to barley production in Finland if global warming exceeded 4°C? A model-based assessment. *European Journal of Agronomy* **35**: 205–214.

Salgó A, Gergely S. **2012**. Analysis of wheat grain development using NIR spectroscopy. *Journal of Cereal Science* **56**: 31–38.

Salman H, Blazek J, Lopez-Rubio A, Gilbert EP, Hanley T, Copeland L. **2009**. Structure–function relationships in A and B granules from wheat starches of similar amylose content. *Carbohydrate Polymers* **75**: 420–427.

Schneider CA, Rasband WS, Eliceiri KW. **2012**. NIH Image to ImageJ: 25 years of image analysis. *Nature Methods* **9**: 671–675.

Scotch Whiskey Association. **2012**. *Statistical Report*.

Searchinger T, Heimlich R, Houghton RA, Dong F, Elobeid A, Fabiosa J, Tokgoz S, Hayes D, Yu T-H. **2008**. Use of U.S. Croplands for Biofuels Increases Greenhouse Gases Through Emissions from Land-Use Change. *Science* **319**: 1238–1240.

Shapter FM, Henry RJ, Lee LS. **2008**. Endosperm and starch granule morphology in wild cereal relatives. *Plant Genetic Resources* **6**: 85–97.

Shevchenko A, Tomas H, Havlis J, Olsen J V, Mann M. **2007**. In-gel digestion for mass spectrometric characterization of proteins and proteomes. *Nature Protocols* **1**: 2856–2860.

Shewry PR. **2009**. Wheat. *Journal of Experimental Botany* **60**: 1537–1553.

Shewry PR, Halford NG, Belton PS, Tatham AS. **2002**. The structure and properties of gluten: an elastic protein from wheat grain. *Philosophical Transactions of the Royal Society B: Biological Sciences* **357**: 133–142.

Shewry PR, Halford NG, Lafiandra D. **2003**. Genetics of Wheat Gluten Proteins. *Advances in Genetics* **49**: 111–184.

Shewry PR, Mitchell RAC, Tosi P, Wan Y, Underwood C, Lovegrove A, Freeman J, Toole GA, Mills ENC, Ward JL. **2012**. An integrated study of grain development of wheat (cv. Hereward). *Journal of Cereal Science* **56**: 21–30.

Shewry PR, Tatham AS, Fido RJ. **1995**. Separation of Plant Proteins by Electrophoresis. Plant Gene Transfer and Expression Protocols. New Jersey: Humana Press, 399–422.

Shewry PR, Underwood C, Wan Y, Lovegrove A, Bhandari D, Toole G, Mills ENC, Denyer K, Mitchell RAC. **2009**. Storage product synthesis and accumulation in developing grains of wheat. *Journal of Cereal Science* **50**: 106–112.

Sica V, Siani A, Bruni CB, Auricchio F. **1971**. Maltase, isomaltase and glucoamylase activities of the acid α-d-glucoside glucohydrolase isolated from cattle liver. *Biochimica et Biophysica Acta (BBA) - Enzymology* **242**: 422–427.

Singh S, Singh N, Isono N, Noda T. **2010**. Relationship of Granule Size Distribution and Amylopectin Structure with Pasting, Thermal, and Retrogradation Properties in Wheat Starch. *Journal of Agricultural and Food Chemistry* **58**: 1180–1188.

Smith TC, Kindred DR, Brosnan JM, Weightman RM, Shepherd M, Sylvester-Bradley R. **2006**. *Wheat as a feedstock for alcohol production*. Cambridge.

Smogyi M. **1952**. Notes on sugar determination. *The Journal of Biological Chemistry* **195**: 19–23.

Song S-H, Lee M-G, Lee H-J, Yoon W-B. **2014**. Analysis of grinding kinetics to control the effect of rice flour particle size on the yield of alcohol and glucose during fermentation. *International Journal of Food Science & Technology*: n/a–n/a.

Statistics | RFA: Renewable Fuels Association.

Stenvert NL, Kingswood K. **1977**. The influence of the physical structure of the protein matrix on wheat hardness. *Journal of the Science of Food and Agriculture* **28**: 11–19.

Sun Z, Henson CA. **1990**. Degradation of Native Starch Granules by Barley Glucosidases. *Plant Physiology* **94**: 320–327.

Sun Z, Henson CA. **1991**. A quantitative assessment of the importance of barley seed α-amylase, β-amylase, debranching enzyme, and α-glucosidase in starch degradation. *Archives of Biochemistry and Biophysics* **284**: 298–305.

Swanston JS, Smith PL, Agu RC, Brosnan JM, Bringhurst TA, Jack FR. **2012**. Variation, across environments within the UK, in grain protein and grain hardness, in wheat varieties of differing distilling quality. *Field Crops Research* **127**: 146–152.

Swanston JS, Smith PL, Gillespie TL, Brosnan JM, Bringhurst TA, Agu RC. **2007**. Associations between grain characteristics and alcohol yield among soft wheat varieties. *Journal of the Science of Food and Agriculture* **87**: 676–683.

Swanston JS, Smith PL, Thomas WT, Sylvester-Bradley R, Kindred D, Brosnan JM, Bringhurst TA, Agu RC. **2014**. Stability, across environments, of grain and alcohol yield, in soft wheat varieties grown for grain distilling or bioethanol production. *Journal of the Science of Food and Agriculture* **94**: 3234–3240.

Taiz, Lincoln. Zeiger E. **2010**. *Plant Physiology*. Sunderland, Massachusetts: Sinauer Associates.

Takeda Y, Guan H-P, Preiss J. **1993**. Branching of amylose by the branching isoenzymes of maize endosperm. *Carbohydrate Research* **240**: 253–263.

Tetlow IJ. **2010**. Starch biosynthesis in developing seeds. *Seed Science Research* **21**: 5–32.

Tetlow IJ, Bowsher CG, Scrase-Field EFAL, Davis EJ, Emes MJ. **2003**. The Synthesis and Transport of ADP-glucose in Cereal Endosperms. *Journal of Applied Glycoscience* **50**: 231–236.

Thanhaeuser SM, Wieser H, Koehler P. **2015**. Spectrophotometric and fluorimetric quantitation of quality-related protein fractions of wheat flour. *Journal of Cereal Science* **62**: 58–65.

Tosi P. **2012**. Trafficking and deposition of prolamins in wheat. *Journal of Cereal Science* **56**: 81–90.

Tosi P, Gritsch CS, He J, Shewry PR. **2011**. Distribution of gluten proteins in bread wheat (*Triticum aestivum*) grain. *Annals of Botany* **108**: 23–35.

Tyson RH, ap Rees T. **1988**. Starch synthesis by isolated amyloplasts from wheat endosperm. *Planta* **175**: 33–38.

United States Congress. **2008**. *Energy Independence and Security Act of 2007*.

Uthayakumaran S, Newberry M, Keentok M, Stoddard FL, Bekes F. **2000**. Basic Rheology of Bread Dough with Modified Protein Content and Glutenin-to-Gliadin Ratios. *Cereal Chemistry* **77**: 744–749.

Vaudel M, Barsnes H, Berven FS, Sickmann A, Martens L. **2011**. SearchGUI: An open-source graphical user interface for simultaneous OMSSA and X!Tandem searches. *Proteomics* **11**: 996–9.

Verspreet J, Hemdane S, Dornez E, Cuyvers S, Pollet A, Delcour JA, Courtin CM. **2013**. Analysis of Storage and Structural Carbohydrates in Developing Wheat (Triticum aestivum L.) Grains Using Quantitative Analysis and Microscopy. *Journal of Agricultural and Food Chemistry* **61**: 9251–9259.

Viikari L, Alapuranen M, Puranen T, Vehmaanperä J, Siika-aho M. **2007**. Thermostable Enzymes in Lignocellulose Hydrolysis. In: Olsson L, ed. Advances in Biochemical Engineering/Biotechnology. Biofuels. Berlin, Heidelberg: Springer Berlin Heidelberg, 121–145.

Vrinten PL. **2000**. Wheat Granule-Bound Starch Synthase I and II Are Encoded by Separate Genes That Are Expressed in Different Tissues. *Plant Physiology* **122**: 255–264.

Warren FJ, Zhang B, Waltzer G, Gidley MJ, Dhital S. **2015**. The interplay of α-amylase and amyloglucosidase activities on the digestion of starch in in vitro enzymic systems. *Carbohydrate Polymers* **117**: 192–200.

Weightman RM, Kindred DR, Clarke S. **2011**. *Cereals for bioethanol : quantifying the alcohol yield of UK hard wheats and the grain yields and N requirements of triticale in the second cereal position*. Cambridge.

Wenger CD, Phanstiel DH, Lee MV, Bailey DJ, Coon JJ. **2011**. COMPASS: a suite of pre- and post-search proteomics software tools for OMSSA. *Proteomics* **11**: 1064–74.

Xiong S, Jiang B, Jiang H, Cui SW, Zhang T. **2014**. Improved the slow digestion property of maize starch using partially β-amylolysis. *Food Chemistry* **152**: 128–132.

Xiong F, Yu X-R, Zhou L, Zhang J, Li B, Liu J, Wang F, Xiong A-S. **2013**. The influence of nitrogen on the development and accumulation of protein bodies in the developing endosperm of wheat caryopses. *Molecular Biology Reports* **41**: 689–695.

Xu T, Zhang X, Dong Y. **2006**. Expression Analysis of HMW-GS 1Bx14 and 1By15 in Wheat Varieties and Transgenic Research of 1By15 Gene. *Agricultural Sciences in China* **5**: 725–735.

Yan S, Wu X, Dahlberg J, Bean SR, MacRitchie F, Wilson JD, Wang D. **2010**. Properties of field-sprouted sorghum and its performance in ethanol production. *Journal of Cereal Science* **51**: 374–380.

Yin Y, Qi J, Li W, Cao L, Wang Z. **2012**. Formation and Developmental Characteristics of A- and B-Type Starch Granules in Wheat Endosperm. *Journal of Integrative Agriculture* **11**: 73–81.

Zaia J. **2004**. Mass spectrometry of oligosaccharides. *Mass Spectrometry Reviews* **23**: 161–227.

Zeng J, Li G, Gao H, Ru Z. **2011**. Comparison of A and B starch granules from three wheat varieties. *Molecules (Basel, Switzerland)* **16**: 10570–91.

Zhang G, Ao Z, Hamaker BR. **2006a**. Slow digestion property of native cereal starches. *Biomacromolecules* **7**: 3252–8.

Zhang G, Ao Z, Hamaker BR. **2008a**. Nutritional property of endosperm starches from maize mutants: A parabolic relationship between slowly digestible starch and amylopectin fine structure. *Journal of Agricultural and Food Chemistry* **56**: 4686–4694.

Zhang B, Dhital S, Gidley MJ. **2013a**. Synergistic and antagonistic effects of α-Amylase and amyloglucosidase on starch digestion. *Biomacromolecules* **14**: 1945–54.

Zhang B, Li X, Liu J, Xie F, Chen L. **2013b**. Supramolecular structure of A- and B-type granules of wheat starch. *Food Hydrocolloids* **31**: 68–73.

Zhang T, Oates CG. **1999**. Relationship between a-amylase degradation and physico-chemical properties of sweet potato starches. *Food Chemistry* **65**: 157–163.

Zhang G, Sofyan M, Hamaker BR. **2008b**. Slowly Digestible State of Starch: Mechanism of Slow Digestion Property of Gelatinized Maize Starch. *Journal of Agricultural and Food Chemistry* **56**: 4695–4702.

Zhang G, Venkatachalam M, Hamaker BR. **2006b**. Structural basis for the slow digestion property of native cereal starches. *Biomacromolecules* **7**: 3259–66.

Zheng W, Peng Y, Ma J, Appels R, Sun D, Ma W. **2011**. High frequency of abnormal high molecular weight glutenin alleles in Chinese wheat landraces of the Yangtze-River region. *Journal of Cereal Science* **54**: 401–408.

Zobel HF. **1964**. X-ray analysis of starch granules. In: Whistler RL, Smith RJ, BeMiller JN, Wolfrom ML, eds. Methods in Carbohydrate Chemistry. Academic press, 109–113.

Zulkowsky K. **1876**. Verhalten der Stärke gegen Glycerin. *Berichte der deutschen chemischen Gesellschaft* **13**: 1395–1398.

9 Abbreviations

ADP-glucose	Adenosine diphosphate glucose
ANOVA	Analysis of variance
ATP	Adenosine triphosphate
BSA	Bovine serum albumin
DMSO	Dimethyl sulphoxide
DPA	Days post anthesis
DTT	Dithiothreitol
EDTA	Ethylenediaminetetraacetic acid
ESI-MS	Electrospray ionisation mass spectrometry
GBSSI	Granule bound starch synthase I
GBSSII	Granule bound starch synthase II
HGCA	Home grown cereals authority
HMW-GS	High molecular weight glutenin subunit
ISA	Isoamylase
LMW-GS	Low molecular weight glutenin subunit
MALDI-MS	Matrix assisted laser desoption ionisation mass spectrometry
MW	Molecular weight

N	Normal
NABIM	National association of British and Irish millers
NAD	Nicotinamide
NADH	Nicotinamide adenine dinucleotide (oxidised)
OPLS-DA	Nicotinamide adenine dinucleotide (reduced)
PBS-TWEEN	Phosphate buffered saline TWEEN
PCA	Principal component analysis
PFF	Peptide fragment fingerprinting
PGM	Phosphoglucomutase
PLS-DA	Partial least squares discriminant analysis
PVP	Polyvinylpyrrolidone
SBEI	Starch branching enzyme I
SBEII	Starch branching enzyme II
SBEIIa	Starch branching enzyme IIa
SBEIIb	Starch branching enzyme IIb
SDS	Sodium dodecyl sulphate
SDS-PAGE	Sodium dodecyl sulphate polyacrylamide gel electrophoresis
SEM	Scanning electron microscopy

SSI	Starch synthase I
SSII	Starch synthase II
SSIII	Starch synthase III
SSIV	Starch synthase IV
XRD	X-ray diffraction

10 Appendix

10.1.1Analysis of amyloglucosidase starch digests by Mass spectrometry

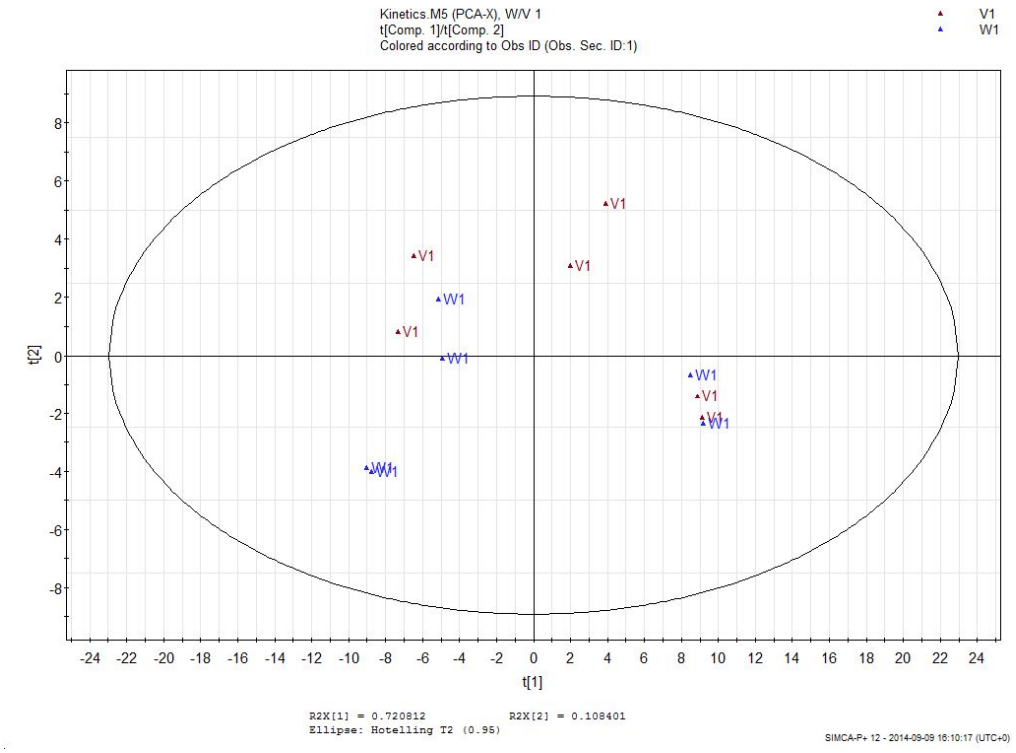

Figure 10.1. ***PCA plot of amyloglucosidase kinetics in 1mg/ml Warrior and Viscount starch****. Amyloglucosidase digested starch (1mg/ml) was analysed by MALDI-TOF. Collected spectra were centroided, and analysed by PCA. Each point represents one of two analytical replicates of one of three separate digests.*

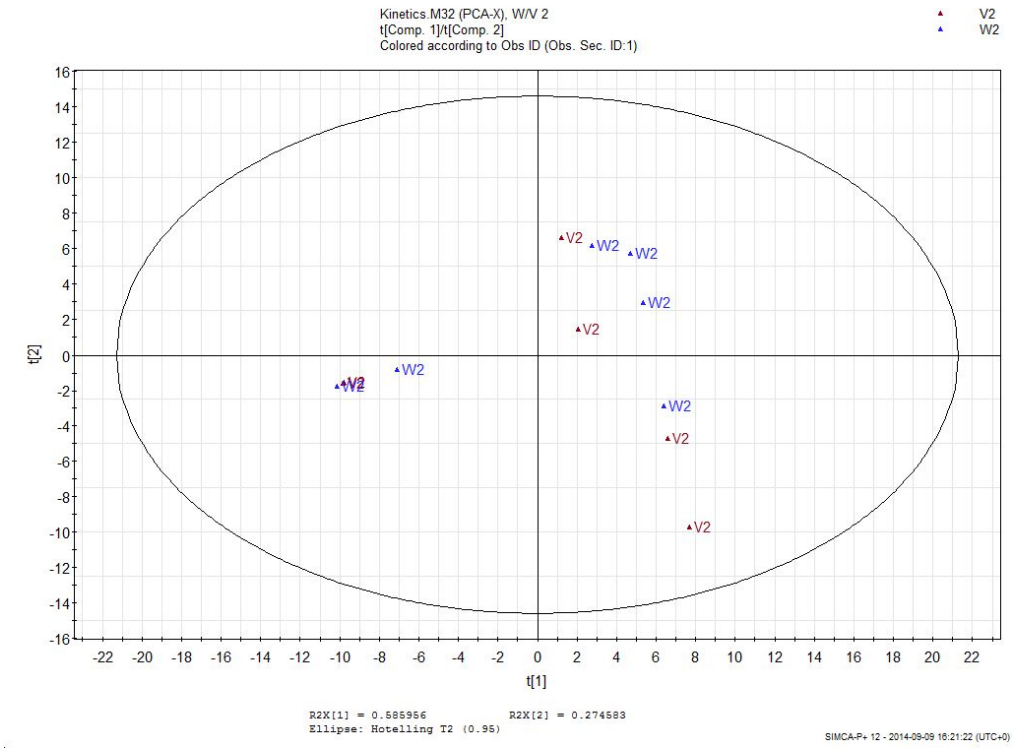

Figure 10.2. ***PCA plot of amyloglucosidase kinetics in 2.5mg/ml Warrior and Viscount starch.*** *Amyloglucosidase digested starch (2.5mg/ml) was analysed by MALDI-TOF. Collected spectra were centroided, and analysed by PCA. Each point represents one of two analytical replicates of one of three separate digests.*

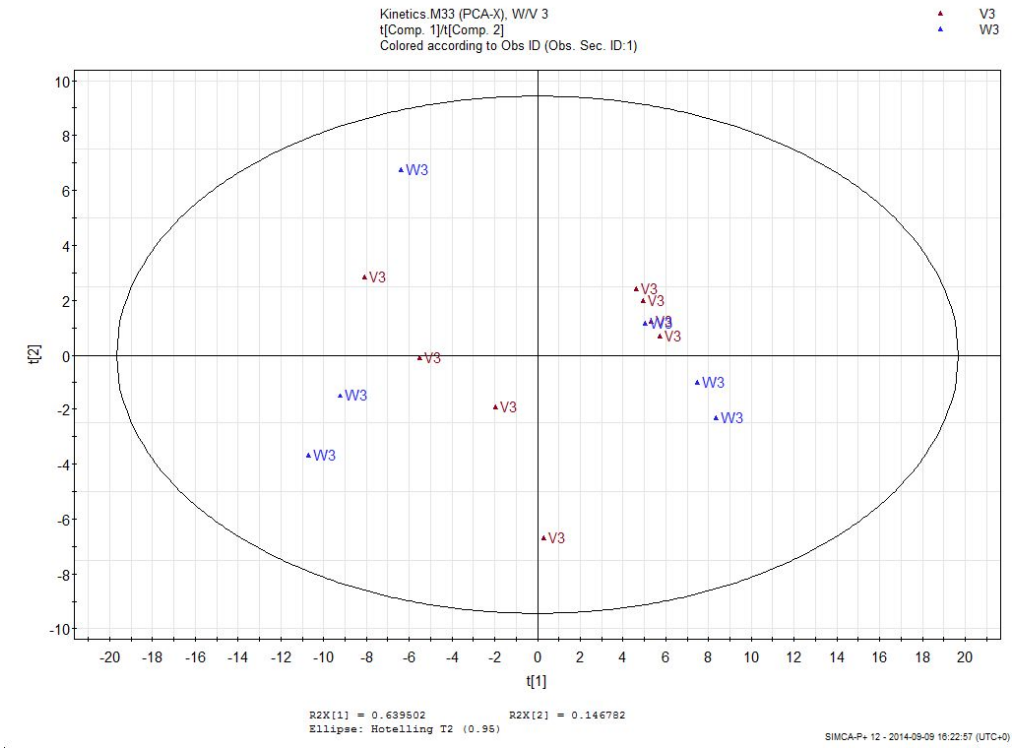

Figure 10.3. ***PCA plot of amyloglucosidase kinetics in 5mg/ml Warrior and Viscount starch****. Amyloglucosidase digested starch (5mg/ml) was analysed by MALDI-TOF. Collected spectra were centroided, and analysed by PCA. Each point represents one of two analytical replicates of one of three separate digests.*

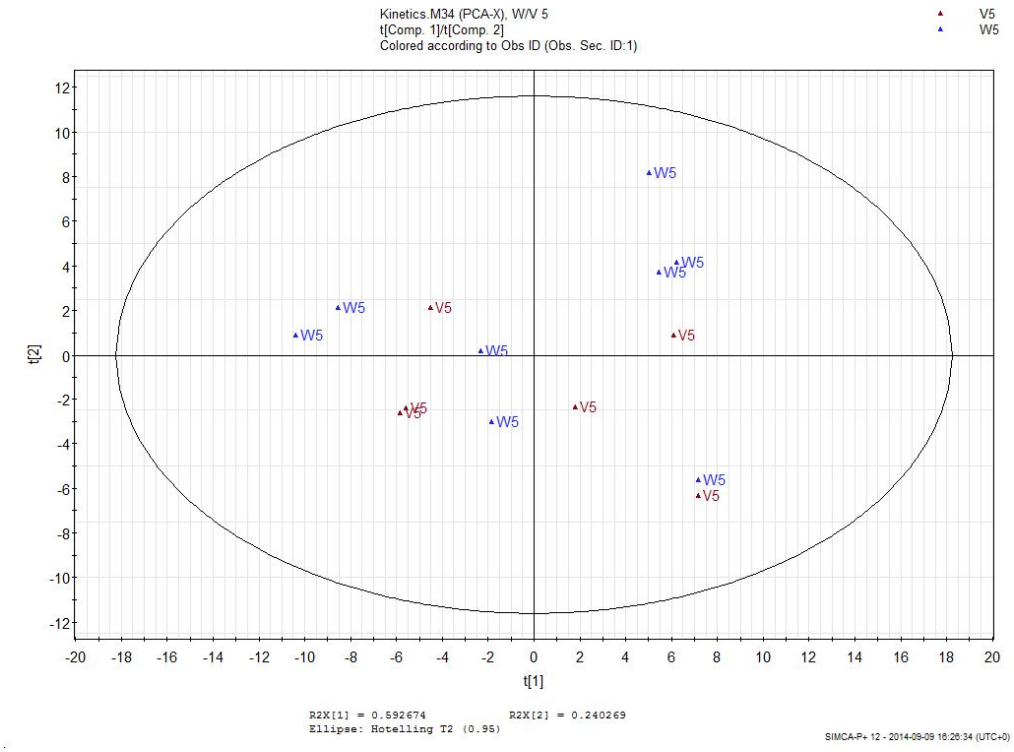

Figure 10.4. ***PCA plot of amyloglucosidase kinetics in 10mg/ml Warrior and Viscount starch.*** *Amyloglucosidase digested starch (10mg/ml) was analysed by MALDI-TOF. Collected spectra were centroided, and analysed by PCA. Each point represents one of two analytical replicates of one of three separate digests.*

10.1.2Analysis of α-amylase starch digests by Mass spectrometry

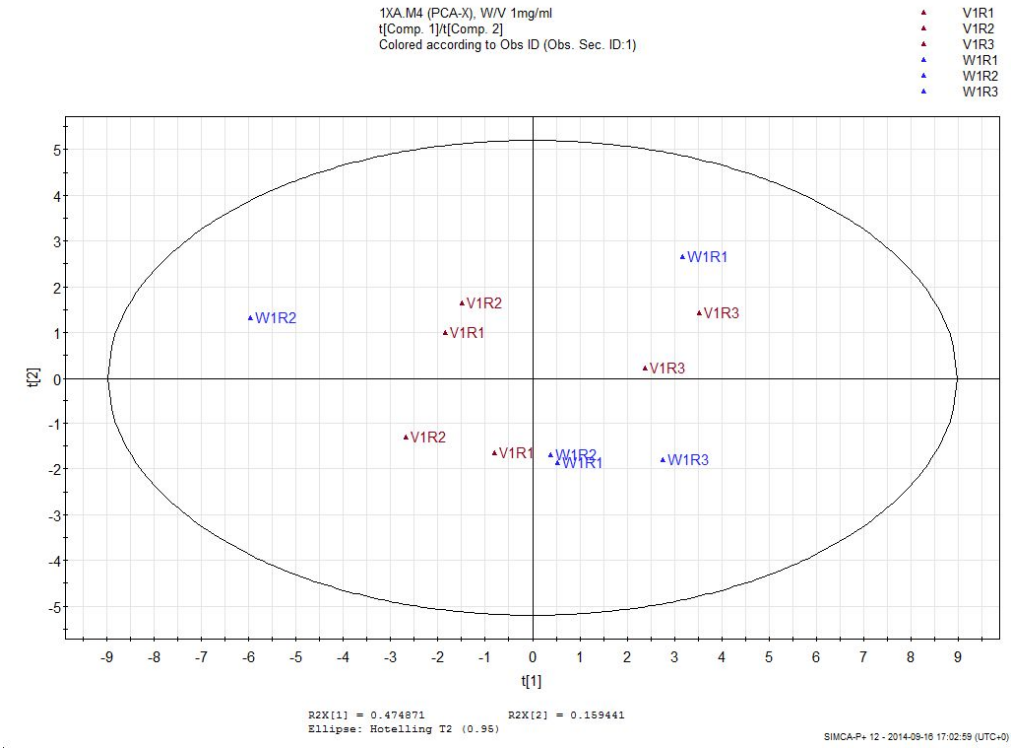

Figure 10.5. ***PCA plot of α-amylase digest in 1mg/ml Warrior and Viscount starch.*** *α-amylase digested starch (1mg/ml) was analysed by MALDI-TOF. Collected spectra were centroided, and analysed by PCA. Each point represents one of two analytical replicates of one separate digest.*

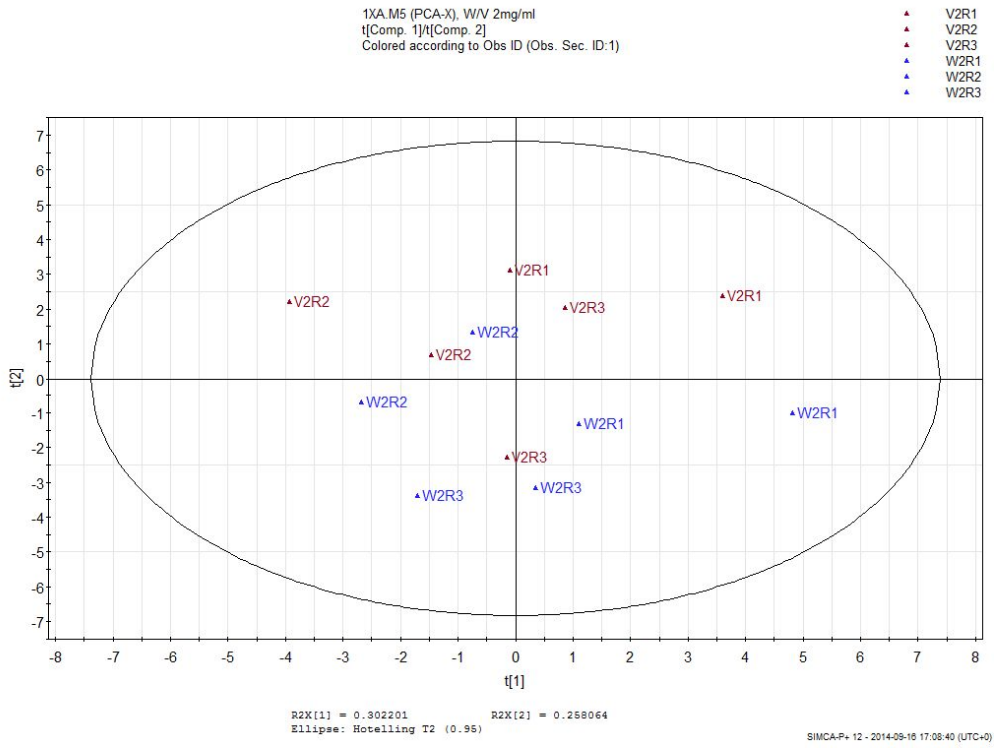

Figure 10.6. ***PCA plot of α-amylase digest in 2.5mg/ml Warrior and Viscount starch.*** *α-amylase digested starch (2.5mg/ml) was analysed by MALDI-TOF. Collected spectra were centroided, and analysed by PCA. Each point represents one of two analytical replicates of one separate digest.*

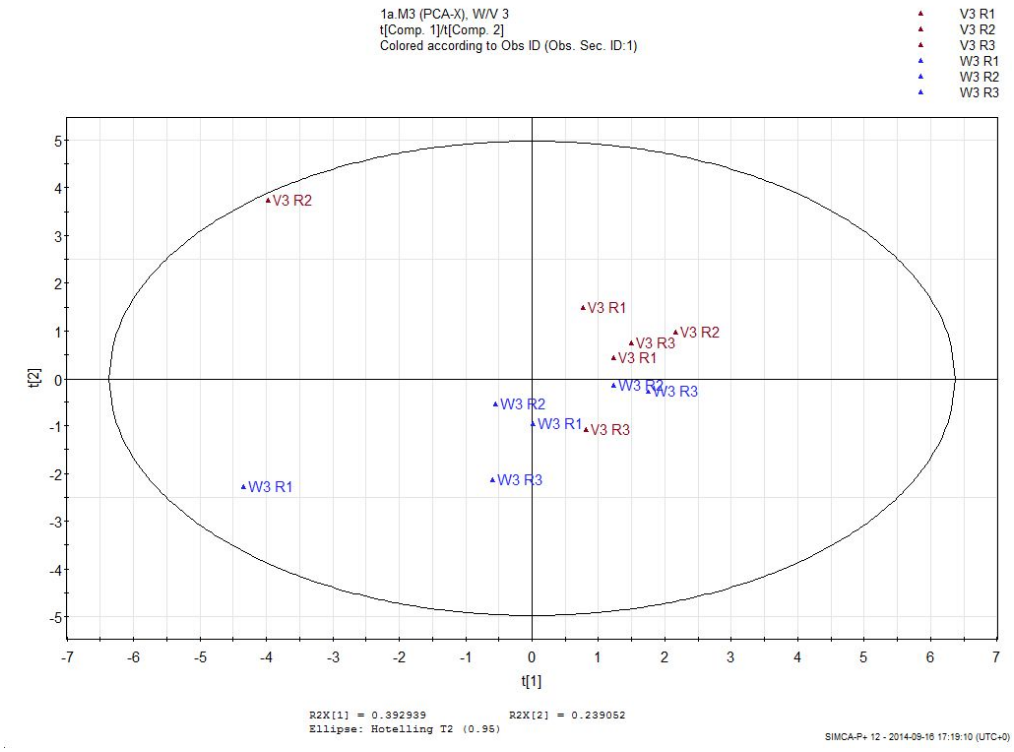

Figure 10.7. ***PCA plot of α-amylase digest in 5mg/ml Warrior and Viscount starch.*** *α-amylase digested starch (5mg/ml) was analysed by MALDI-TOF. Collected spectra were centroided, and analysed by PCA. Each point represents one of two analytical replicates of one separate digest.*

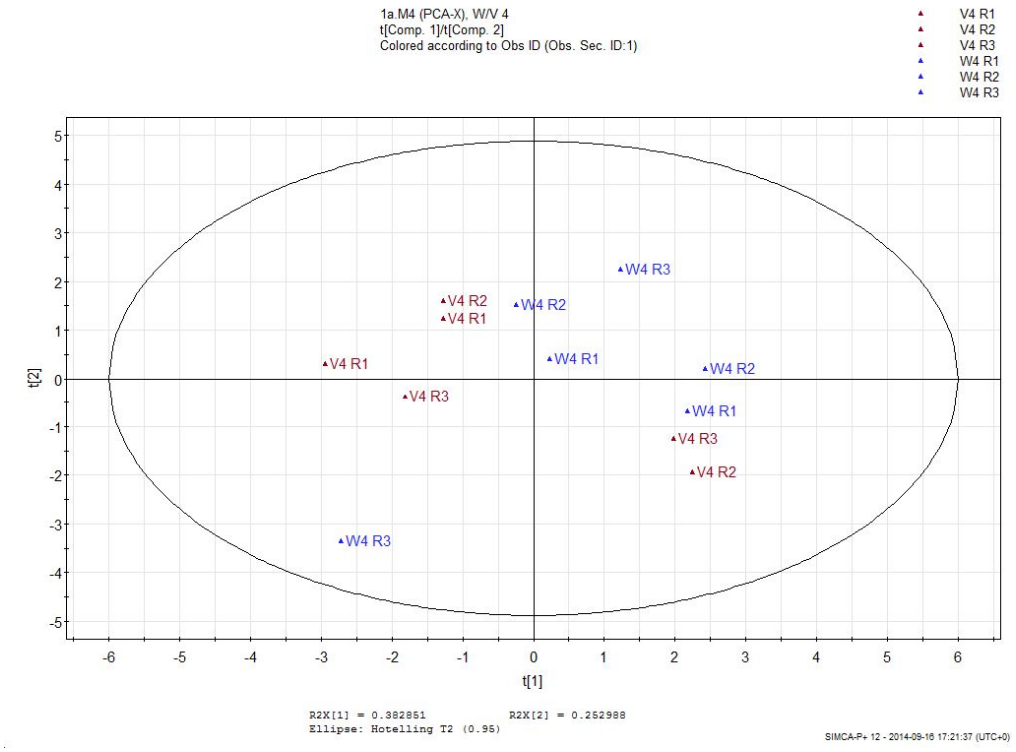

Figure 10.8. ***PCA plot of α-amylase digest in 7.5mg/ml Warrior and Viscount starch.*** *α-amylase digested starch (7.5mg/ml) was analysed by MALDI-TOF. Collected spectra were centroided, and analysed by PCA. Each point represents one of two analytical replicates of one separate digest.*